IMAGE: A MAP OF THE STARS OF THE ORION CONSTELLATION

Print ISSN: 2631-8490 Online ISSN: 2631-8504

JournalPreview

London Journal of Research in Science: Natural and Formal
Volume 23 | Issue 15 | Compilation 1.0

Great Britain Journals Press

WWW.JOURNALSPRESS.COM

Journal Content
In this Issue

Great Britain Journals Press

Spectral Dichotomy of a Matrix Pencil with Respect to a Circle, Ellipse or Parabola Not Centered at the Origin

Mouhamadou Dosso, Seydou Traore & Lassana Samassi

Université Félix

ABSTRACT

Spectral dichotomy methods of a matrix pencil which calculate projectors on the subspace associated with the eigenvalues inside or outside of any circle, any ellipse or any parabola, were proposed. These methods are an extension of those proposed in [S. Traoré and M. Dosso, European Journal of Pure and Applied Mathematics, 15 (2), (2022) 681-725] and [S. Traoré, M. Dosso and L Samassi, International Journal of Numerical Methods and Applications, 22, (2022) 87-115] to matrix pencil.Before the presentation of our methods, a reminder of the spectral dichotomy methods of a matrix with respect to any circle, any ellipse or any parabola was made. Two numerical examples of matrix pencil show the good calculation of the projectors on the subspaces associated with the part of the plane concerned by the separation made by the figures. 2020 Mathematics Subject Classifications : 65F15, 34D09, 47A46.

Keywords and Phrases: spectral dichotomy method, spectral projector, eigen subspaces, eigenvalues.

Classification: MSC: 65F15

Language: English

Great Britain Journals Press

LJP Copyright ID: 925651
Print ISSN: 2631-8490
Online ISSN: 2631-8504

London Journal of Research in Science: Natural and Formal

Volume 23 | Issue 15 | Compilation 1.0

Spectral Dichotomy of a Matrix Pencil with Respect to a Circle, Ellipse or Parabola Not Centered at the Origin

Mouhamadou Dosso[α], Seydou Traoré[σ] & Lassana Samassi[ρ]

ABSTRACT

Spectral dichotomy methods of a matrix pencil which calculate projectors on the subspace associated with the eigenvalues inside or outside of any circle, any ellipse or any parabola, were proposed. These methods are an extension of those proposed in [S. Traoré and M. Dosso, European Journal of Pure and Applied Mathematics, 15 (2), (2022) 681-725] and [S. Traoré, M. Dosso and L Samassi, International Journal of Numerical Methods and Applications, 22, (2022) 87-115] to matrix pencil.Before the presentation of our methods, a reminder of the spectral dichotomy methods of a matrix with respect to any circle, any ellipse or any parabola was made. Two numerical examples of matrix pencil show the good calculation of the projectors on the subspaces associated with the part of the plane concerned by the separation made by the figures. 2020 Mathematics Subject Classifications : 65F15, 34D09, 47A46.

Keywords and Phrases : spectral dichotomy method, spectral projector, eigensubspaces, eigenvalues.

Author α: Université Félix Houphouët-Boigny de cocody-Abidjan. Laboratoire de Mathématiques fondamentales et Applications.
UFR de Mathématiques et Informatique, 22 BP 582 Abidjan 22, Côte d'Ivoire.
σ: Université Jean Lorougnon Guédé, Daloa, Côte d'Ivoire.
ρ: Université de San-Pedro, Côte d'Ivoire.

I. INTRODUCTION

Spectral dichotomy methods were introduced by S. K. Godunov in [6] for the study of stability in the sense of Lyapunov. They consist in determining whether or not there are eigenvalues of a given matrix or a matrix pencil inside or outside a closed contour. If there are no eigenvalues in a neighborhood of the contour, these methods compute iteratevely the projector onto the invariant subspace associated to the eigenvalues of the matrix or the matrix pencil inside the contour. This computation is accompanied by the spectral norm $\|\mathbb{H}\|$ of a Hermitian positive definite matrix $\mathbb{H}$ called the dichotomy condition number. Initially developed on the imaginary axis by S. K. Godunov [6], these methods have been extended to the circle by Bulkgakov and Godunov in [2]. More efficient methods for computing the spectral projector and the dichotomy matrix in the circular case were proposed by Malyshev in [11, 12], Sadkane and Dosso in [4], Sadkane and Touhami in [17]. The methods of spectral dichotomy of a matrix or a matrix pencil with respect to the ellipse or parabola are respectively transformations of the methods with respect to the circle or imaginary axis. The methods with respect to the ellipse have been proposed by Godunov and Sadkane in [8, 9], Malyshev and sadkane in [14] and Sadkane and Touhami in [17] and those with respect to the parabola by Malyshev and sadkane in [14] and Sadkane and Touhami in [17]. Traoré et al. in [19, 20, 18] applied the dichotomy methods of a matrix with respect to the circle, the ellipse and the parabola all not centered at the origin.

London Journal of Research in Science: Natural and Formal

Let $zB - A$ be a regular matrix pencil with A and $B \in \mathbb{R}^{n\times n}(n > 1)$ with B non singular. The aim of this paper is to propose some methods of spectral dichotomy of the matrix pencil $zB - A$ with respect respectively to the circle $\mathcal{C}(\Omega, r)$ of center Ω with affix $\omega \neq 0$ and radius $r > 0$, the ellipse Ξ_{z_0} of equation

$$\left(\frac{x - x_0}{a}\right)^2 + \left(\frac{y - y_0}{b}\right)^2 = 1, \qquad a \geq b > 0 \tag{1.1}$$

and of center $z_0 = x_0 + iy_0$ different from 0 and the parabola of equation

$$2p(d - x) = (y - p\tilde{b})^2 \tag{1.2}$$

with $p > 0$.

Our work is organized as follows. In the section 2, we recall the spectral dichotomy methods of a matrix pencil with respect to the circle and the ellipse [16], all centered at the origin and with respect to the imaginary axis [16]. Algorithms developed in this section are useful for the sequel. In section 3, we propose new algorithms to compute the spectral projector and dichotomy matrix of a matrix pencil with respect to a circle, an ellipse or a parabola off centered at the origin. In this section, we use special matrix pencils to bring us back to the algorithms seen in the section 2. In section 4, we illustrate our results using graphs and tables to visualise and demonstrate the accuracy of our algorithms.

Throughout this work, we will use the following notation : the symbol $\|.\|$ denotes the 2-norm for vectors and matrices. The identity matrix (respectively the null matrix) of order k will be denoted by I_k (respectively 0_k) or just I (respectively 0) if the order is clear from the context.

II. SOME METHODS OF SPECTRAL DICHOTOMY OF A MATRIX PENCIL

Let $zB - A$ be a matrix pencil with $A,\ B \in \mathbb{R}^{n\times n}, (n > 1)$.

2.1 Method of spectral dichotomy of a matrix pencil with respect to a circle centered at the origin

Suppose that the matrix pencil $zB - A$ has no eigenvalue in a circle $\mathcal{C}(O, r),\ (r > 0)$. Then

$$\mathbb{P} = \frac{1}{2\pi}\int_0^{2\pi}\left(B - e^{-i\theta}\frac{A}{r}\right)^{-1} B d\theta \tag{2.1}$$

is a spectral projector onto the subspace corresponding to the eigenvalues of $zB - A$ inside the circle $\mathcal{C}(O, r)$.

The numerical computation of $\mathbb{P}$ is accompanied by the dichotomy condition number given by the spectral norm of the Hermitian positive definite matrix

$$\mathbb{H} = \frac{1}{2\pi}\int_0^{2\pi}\left(B - e^{-i\theta}\frac{A}{r}\right)^{-*}\mathbb{H}^0\left(B - e^{-i\theta}\frac{A}{r}\right)^{-1} d\theta \tag{2.2}$$

where $\mathbb{H}^{(0)} = \mathbb{H}^{(0)^*} > 0$ is a given arbitrary matrix.

Consider the cyclic and finite linear system [8]

$$\begin{cases} BZ_0^{(2^j)} - \dfrac{A}{r}Z_1^{(2^j)} &= I_n, \\ BZ_k^{(2^j)} - \dfrac{A}{r}Z_{k+1}^{(2^j)} &= 0, \qquad 1 \le k \le 2^j - 1. \end{cases} \tag{2.3}$$

From its solutions $Z_k^{(2^j)}$, the following theorem allows to obtain the values of $\mathbb{P}$ and $\mathbb{H}$ (see [8, 16]).

Theorem 2.1 *We have*

$$\mathbb{P} = \lim_{j \to +\infty} \mathbb{P}_j \qquad with \quad \mathbb{P}_j = Z_{2j}^{(2^j)} B \equiv Z_0^{(2^j)} B \tag{2.4}$$

and

$$\mathbb{H} = \lim_{j \to +\infty} \mathbb{H}_j \qquad with \quad \mathbb{H}_j = \sum_{k=1}^{2^j} (Z_k^{(2^j)})^* \mathbb{H}^0 (Z_k^{(2^j)}), \tag{2.5}$$

$$\mathbb{H}_j = V_j^* \mathbb{H}_{j-1} V_j + W_j^* \mathbb{H}_{j-1} W_j \tag{2.6}$$

where $V_j = BZ_{2^{j-1}}^{(2^j)} - \dfrac{A}{r}Z_1^{(2^j)}$ *and* $W_j = BZ_{2^j}^{(2^j)} - \dfrac{A}{r}Z_{2^{j-1}+1}^{(2^j)}$.

As for the computation of $Z_k^{(2^j)}$ and $\mathbb{H}_j$, they are explained in the following theorem (see [16])

Theorem 2.2 *Let*

$$Z_1^{(2)} = \Delta_0, \quad Z_2^{(2)} = \nabla_0$$

and for $j = 2, 3 \cdots$

$$Z_k^{(2^j)} = Z_k^{(2^{j-1})} \Delta_{j-1}, \quad k = 1, 2, \cdots 2^{j-1}.$$

$$Z_{k+2^{j-1}}^{(2^j)} = Z_{k+2^{j-1}}^{(2^{j-1})} \nabla_{j-1}, \quad k = 1, 2, \cdots 2^{j-1}.$$

and for $j = 2, 3 \cdots$

$$A_{j-1} + B_{j-1} = I_n \tag{2.7}$$

$$\Delta_{j-1} + \nabla_{j-1} = I_n \tag{2.8}$$

$$(2A_{j-1} - I_n)\Delta_{j-1} = A_{j-1} \tag{2.9}$$

with

$$A_{j-1} = -\frac{A}{r}Z_1^{(2^{j-1})}, \quad I_n = -Z_1^{(2^{j-1})}$$

and

$$H_j = \Delta_{j-1}^* H_{j-1} \Delta_{j-1} + (I_n - \Delta_{j-1})^* H_{j-1} (I_n - \Delta_{j-1}).$$

Following Algorithm 2.1 given in [17] summarizes the computations of the projector $\mathbb{P}$ and the dichotomy criterion $\mathbb{H}_j$.

Algorithm 2.1

Input : $A, B \in \mathbb{C}^{n\times n}$ *such the matrix pencil* $zB - A$ *is regular having no eigenvalues on the circle* $\mathcal{C}(O, r),\ (r > 0)$.

$\mathbb{H}^{(0)} = \mathbb{H}^{(0)^*} > 0$ *used for scaling.*
Output : $\mathbb{P}$ *the projector onto the subspace of* $zB - A$ *associated with the eigenvalues inside the circle* $\mathcal{C}(O, r),\ (r > 0)$.

$\mathbb{H}$ *the integral whose norm* $\|\mathbb{H}\|$ *indicates the numerical quality of the projector* $\mathbb{P}$.

1. *Initialisation and first iteration*

$$H_0 = H^0 \qquad and \quad \tilde{A} = \frac{A}{r}$$

- *Determine the solutions* X, Y *of equations*

$$X(B - \tilde{A}) = \tilde{A}, \quad Y(B - \tilde{A}) = I$$

- *Determine the solutions* Δ_0, ∇_0 *of equations*

$$(\tilde{A} + B)\Delta_0 = X, \quad (\tilde{A} + B)\nabla_0 = Y$$

- *compute* $H_1, Z_1^{(2)}, Z_2^{(2)}$*:*

$$H_1 = \Delta_0^* H_0 \Delta + \nabla_0^* H_0 \nabla_0$$
$$Z_1^2 = \Delta_0, \quad Z_2^{(2)} = \nabla_0$$

2. *Iterations for* $j = 2, 3\cdots$

- *do*

$$A_{j-1} = -\tilde{A} Z_1^{2^{j-1}}$$

$$(2A_{j-1} - I_n)\Delta_{j-1} = A_{j-1}$$

- *Compute* $H_j, Z_1^{(2^j)}, Z_{2^j}^{(2^j)}$:

$$H_j = \Delta_{j-1}^* H_{j-1} \Delta_{j-1} + (I - \Delta_{j-1})^* H_{j-1}(I_n - \Delta_{j-1})$$

$$Z_1^{(2^j)} = Z_1^{(2^{j-1})}\Delta_{j-1}, Z_{2^j}^{(2^j)} = Z_{2^{j-1}}^{(2^{j-1})}(I_n - \Delta_{j-1})$$

end for

$$\mathbb{P}_0 = Z_{2^j}^{(2^j)} \qquad and \qquad \mathbb{H} = H_j$$

2.2 Method of spectral dichotomy of a matrix pencil with respect to an ellipse centered at the origin

Suppose that the matrix pencil $zB - A$ has no eigenvalues on the ellipse Ξ_0 of equation

$$\left(\frac{x}{a}\right)^2 + \left(\frac{y}{b}\right)^2 = 1 \qquad \text{with} \quad a \geq b > 0. \tag{2.10}$$

Consider the matrix pencil of the form $\mu\mathcal{B} - \mathcal{A}$ where

$$\mathcal{B} = \begin{pmatrix} \frac{a+b}{2}B & -A \\ 0 & \frac{a+b}{2}B \end{pmatrix} \qquad \text{and} \quad \mathcal{A} = \begin{pmatrix} -\frac{a-b}{2}B & 0 \\ A & -\frac{a-b}{2}B \end{pmatrix} \tag{2.11}$$

This following proposition shows the dichotomy parameters

$$\alpha = \sup_{z \in \Xi_{z_0}} \|(zI_n - A)^{-1}\| \qquad \text{and} \quad \widetilde{\alpha} = \sup_{|\widetilde{\lambda}|=1} \|(\widetilde{\lambda}\widetilde{\mathcal{B}} - \widetilde{\mathcal{A}})^{-1}\| \tag{2.12}$$

are equal.

Proposition 2.1 *Let α and $\widetilde{\alpha}$ defined in (3.5). then*

$$\alpha = \widetilde{\alpha}. \tag{2.13}$$

Moreover, if we denote by

$$\mathcal{P}_\infty = \begin{pmatrix} \widetilde{\mathcal{P}}_{11} & \widetilde{\mathcal{P}}_{12} \\ \widetilde{\mathcal{P}}_{21} & \widetilde{\mathcal{P}}_{22} \end{pmatrix}, \quad \text{with} \quad \widetilde{\mathcal{P}}_{ij} \in \mathbb{C}^{n\times n}, \quad i,j \in 1,2. \tag{2.14}$$

the projector onto the invariant subspace of the matrix pencil $\mu\mathcal{B} - \mathcal{A}$ associated with the eigenvalues inside $\mathcal{C}(O,r)$ and $\mathbb{P}_\infty \in \mathbb{C}^{n\times n}$ the projector onto the invariant subspace of the matrix pencil $zB - A$ associated with the eigenvalues inside Ξ_0.

The following proposition characterizes the relation between $\mathbb{P}_\infty$ and $\mathcal{P}_\infty$.

Proposition 2.2 *We have*

$$\mathbb{P}_\infty = \widetilde{\mathcal{P}}_{11} + \widetilde{\mathcal{P}}_{22}. \tag{2.15}$$

Following Algorithm 2.2 given in [17] summarizes the computations of the projector $\mathbb{P}_\infty$ and the dichotomy criterion $\mathbb{H}$.

Algorithm 2.2 .

- *Input variables: The matrices A and B, the parameters a, b such that the matrix pencil $zB - A$ has no eigenvalues on the ellipse Γ_0 of equation with $a \geq b > 0$.*
- *Output variables: $\mathbb{P}_\infty$ and $\mathbb{H}$*

  $\mathbb{P}_\infty$ being the projector on the right invariant space of $zB - A$ corresponding to the eigenvalues outside the ellipse Γ_0 and $\mathbb{H}$ the dichotomy criterion.

1. *Set*

$$\mathcal{B} = \begin{pmatrix} \frac{a+b}{2}B & -A \\ 0 & \frac{a+b}{2}B \end{pmatrix} \quad and \quad \mathcal{A} = \begin{pmatrix} -\frac{a-b}{2}B & 0 \\ A & -\frac{a-b}{2}B \end{pmatrix} \tag{2.16}$$

2. *Apply algorithm 2.1 to* $\lambda\mathcal{B} - \mathcal{A}$

3. *We obtain* $\mathbb{P}_\infty$ *and* $\mathbb{H}$.

2.3 Method of spectral dichotomy of a matrix pencil with respect to an imaginary axis

Suppose that the matrix pencil $zB - A$ has no eigenvalues on the imaginary axis. Consider the matrix pencil $\lambda\mathcal{B} - \mathcal{A}$ where $\mathcal{A} = A + B$ and $\mathcal{B} = A - B$. This following proposition shows the relation between the dichotomy parameters

$$\widetilde{\alpha} = \sup_{|\lambda|=1} \|\lambda\mathcal{B} - \mathcal{A})^{-1}\| \qquad \text{and} \quad \alpha = \sup_{\Re z=0} \|(zB - A)^{-1}\| \tag{2.17}$$

Proposition 2.3 *[17] Assume that* $\|A\| \leq 1$ *and let* α *and* $\widetilde{\alpha}$ *be the two parameters defined in (2.17)*

$$\frac{1}{2}\alpha \leq \widetilde{\alpha} \leq C(\alpha + 1) \tag{2.18}$$

with $C = \max(\|B\|, 1)$

Following Algorithm 2.3 given in [16, 17] summarizes the computations of the projector $\mathbb{P}_0$ and the dichotomy criterion $\mathbb{H}$.

Algorithm 2.3 *:*

- *Input variables :* A *and* B *such that the matrix pencil* $zB - A$ *has no eigenvalues on the imaginary axis.*
- *Output variables :* $\mathbb{P}_0$ *and* $\mathbb{H}$.
  $\mathbb{P}_0$ *being the projector on the invariant subspace of* $zB - A$ *corresponding to the eigenvalues of negative real parts and* $\mathbb{H}$ *the dichotomy criterion.*

1. *Determine the matrices* $\mathcal{A} = A + B$ *and* $\mathcal{B} = A - B$.

2. *Apply Algorithm 2.1 to* $\lambda\mathcal{B} - \mathcal{A}$.

3. $\mathbb{P}_0 = \mathcal{P}$.

III. SPECTRAL DICHOTOMY METHODS OF A MATRIX PENCIL WITH RESPECT TO AN OFF-CENTER CIRCLE, ELLIPSE OR PARABOLA

Let $zB - A$ be a matrix pencil with $A,\ B \in \mathbb{R}^{n\times n}(n > 1)$ such that B is not singular.

3.1 Spectral dichotomy method of a matrix pencil with respect to a circle not c entered at the origin

If the matrix pencil $zB - A$ has no eigenvalues on the circle $\mathcal{C}(\Omega, r); (r > 0)$, then the spectral projector on the invariant subspace corresponding to the eigenvalues on the disc $|z-b| < r$ is the matrix $\mathbb{P}_0$ defined by :

$$\begin{aligned}
\mathbb{P}_0 &= \frac{1}{2i\pi}\int_{\mathcal{C}(\Omega,r)}(zB-A)^{-1}Bdz \\
&= \frac{1}{2i\pi}\int_{|z-b|=r}(zB-A)^{-1}Bdz \\
&= \frac{1}{2i\pi}\int_0^{2\pi}\left((b+re^{i\theta})B-A\right)^{-1}Bire^{i\theta}d\theta \\
&= \frac{1}{2\pi}\int_0^{2\pi}\left(B+\frac{bB-A}{r}e^{-i\theta}\right)^{-1}Bd\theta \\
&= \frac{1}{2\pi}\int_0^{2\pi}\left(B-\frac{\mathcal{A}}{r}e^{-i\theta}\right)^{-1}Bd\theta
\end{aligned}$$

where $\mathcal{A} = A - bB$.

The computation of the spectral projector $\mathbb{P}$ is accompanied by that of a Hermitian matrix $\mathbb{H}$ defined by:

$$\mathbb{H} = H(r) = \frac{1}{2\pi}\int_0^{2\pi}\left(B-\frac{e^{-i\theta}\mathcal{A}}{r}\right)^{-*}H^{(0)}\left(B-\frac{e^{-i\theta}\mathcal{A}}{r}\right)^{-1}\quad d\theta, \tag{3.1}$$

where $H^{(0)} = (H^{(0)})^* > 0$ is a positive definite Hermitian matrix used for setting purposes the scale.
We have the following algorithm that compute the projector $\mathbb{P}_0$ onto the invariant subspace of $zB - A$ corresponding to the eigenvalues inside the circle $\mathcal{C}(\Omega(b), r)$ and the Hermitian and definite positive matrix $\mathbb{H}$ associated.

Algorithm 3.1 .

- *Input variables : The matrices A and B, the parameters b and r such that the matrix pencil $zB - A$ has no eigenvalues on the circle $\mathcal{C}(\Omega, r)$.*
- *Output variables : $\mathbb{P}_0$ and $\mathbb{H}$.*
  $\mathbb{P}_0$ being the projector on the invariant space of $zB - A$ corresponding to the eigenvalues inside the circle $\mathcal{C}(\Omega(b), r)$ and $\mathbb{H}$ the matrix integral whose norm indicates the quality of the projector $\mathbb{P}_0$.

1. *Determine the matrix $\mathcal{A} = A - bB$.*

2. *Compute the projector $\mathbb{P}_0$ and the matrix $\mathbb{H}$ by applying Algorithm 2.1 to the matrix $\mathcal{A}$ and to the circle $\mathcal{C}(O, r)$ with center O and radius r.*

3.2 Spectral dichotomy method of a matrix pencil with respect to an ellipse not centered at the origin

Consider the ellipse

$$\Xi_{z_0} = \{z = x + iy \in \mathbb{C} \quad | \quad (x - x_0) + i(y - y_0) \in \Xi_0\} \tag{3.2}$$

of equation (1.1).

Suppose that the matrix pencil $zB - A$ has no eigenvalues on the ellipse Ξ_{z_0}. Consider the matrices of order $2n$ defined in the following way:

$$\widetilde{\mathcal{B}} = \begin{bmatrix} \frac{a+b}{2}B & -A_0 \\ 0 & \frac{a+b}{2}B \end{bmatrix} \quad \text{and} \quad \widetilde{\mathcal{A}} = \begin{bmatrix} -\frac{a-b}{2}B & 0 \\ A_0 & -\frac{a-b}{2}B \end{bmatrix} \tag{3.3}$$

where $A_0 = A - z_0 B$.

The eigenvalues $\widetilde{\lambda}$ of the matrix pencil $(\widetilde{\lambda}\widetilde{\mathcal{B}} - \widetilde{\mathcal{A}})$ and $\widetilde{z}$ of the matrix pencil $\widetilde{z}B - A_0$ are linked by the relation (3.4).

$$\widetilde{z} = \frac{(a+b)\widetilde{\lambda}^2 + (a-b)}{2\widetilde{\lambda}} \tag{3.4}$$

Consider the qualities of the spectral dichotomy with respect to the ellipse Ξ_{z_0} and the unit circle $\mathcal{C}(0,1)$ respectively defined by

$$\alpha = \sup_{z \in \Xi_{z_0}} \|(zB - A)^{-1} \quad \text{and} \quad \widetilde{\alpha} = \sup_{|\widetilde{\lambda}|=1} \|(\widetilde{\lambda}\widetilde{\mathcal{B}} - \widetilde{\mathcal{A}})^{-1}\| \tag{3.5}$$

Proposition 3.1 *Let α and $\widetilde{\alpha}$ be the quantities defined in (3.5). then*

$$\alpha = \widetilde{\alpha} \tag{3.6}$$

Proof

From (3.4), we have

$$\widetilde{z} = \frac{(a+b)\widetilde{\lambda}^2 + (a-b)}{2\widetilde{\lambda}}.$$

Which leads to

$$\frac{a+b}{2}B\widetilde{\lambda}^2 - A_0\widetilde{\lambda} + \frac{a-b}{2}B = \widetilde{\lambda}(\widetilde{z}B - A_0)$$

We have

$$(\mu^2\widetilde{\mathcal{B}} - \widetilde{\mathcal{A}})^{-1} = \begin{pmatrix} (\frac{a+b}{2}\mu^2 + \frac{a-b}{2})B & -\mu^2 A_0 \\ -A_0 & (\frac{a+b}{2}\mu^2 + \frac{a-b}{2})B \end{pmatrix}^{-1}$$

$$= \begin{pmatrix} \widetilde{z}\mu B & -\mu^2 A_0 \\ -A_0 & \widetilde{z}\mu B \end{pmatrix}^{-1}$$

$$
\begin{aligned}
&= \begin{pmatrix} I_n & 0 \\ 0 & \mu^{-1} I_n \end{pmatrix} \begin{pmatrix} \widetilde{z}B & -A_0 \\ -A_0 & \widetilde{z}B \end{pmatrix}^{-1} \begin{pmatrix} \mu^{-1} I_n & 0 \\ 0 & I_n \end{pmatrix} \\
&= \begin{pmatrix} I_n & 0 \\ 0 & \mu^{-1} I_n \end{pmatrix} \times \\
&\frac{1}{2} \begin{bmatrix} (\widetilde{z}B - A_0)^{-1} + (\widetilde{z}B + A_0)^{-1} & (\widetilde{z}B - A_0)^{-1} - (\widetilde{z}B + A_0)^{-1} \\ (\widetilde{z}B - A_0)^{-1} - (\widetilde{z}B + A_0)^{-1} & (\widetilde{z}B - A_0)^{-1} + (\widetilde{z}B + A_0)^{-1} \end{bmatrix} \\
&\times \begin{pmatrix} \mu^{-1} I_n & 0 \\ 0 & I_n \end{pmatrix} \\
&= \underbrace{\begin{pmatrix} I_n & 0 \\ 0 & \mu^{-1} I_n \end{pmatrix} \begin{pmatrix} \frac{I_n}{\sqrt{2}} & -\frac{I_n}{\sqrt{2}} \\ \frac{I_n}{\sqrt{2}} & \frac{I_n}{\sqrt{2}} \end{pmatrix}}_{K_1} \times \begin{bmatrix} (\widetilde{z}B - A_0)^{-1} & 0 \\ 0 & (\widetilde{z}B + A_0)^{-1} \end{bmatrix} \times \\
&\underbrace{\begin{pmatrix} \frac{I_n}{\sqrt{2}} & \frac{I_n}{\sqrt{2}} \\ -\frac{I_n}{\sqrt{2}} & \frac{I_n}{\sqrt{2}} \end{pmatrix} \begin{pmatrix} \mu^{-1} I_n & 0 \\ 0 & I_n \end{pmatrix}}_{K_2}
\end{aligned}
$$

We notice that the product $K_1 K_2 = \mu^{-1}$. Therefore, with a double inequality, we deduce:

$$\sup_{z \in \Xi_0} \|(\widetilde{z}B - A_0)^{-1}\| = \sup_{|\widetilde{\lambda}|=1} \|(\widetilde{\lambda}\widetilde{\mathcal{B}} - \widetilde{\mathcal{A}})^{-1}\|$$

We also know that $\widetilde{z}B - A_0 = zB - A$, so we can conclude that

$$\sup_{z \in \Xi_{z_0}} \|(zB - A)^{-1}\| = \sup_{|\widetilde{\lambda}|=1} \|(\widetilde{\lambda}\widetilde{\mathcal{B}} - \widetilde{\mathcal{A}})^{-1}\|$$

whence the equality (3.6). □

Moreover, if we denote by

$$\mathcal{P}_\infty = \begin{pmatrix} \widetilde{\mathcal{P}}_{11} & \widetilde{\mathcal{P}}_{12} \\ \widetilde{\mathcal{P}}_{21} & \widetilde{\mathcal{P}}_{22} \end{pmatrix} \qquad \text{with} \quad \mathcal{P}_{ij} \in \mathbb{C}^{n \times n}, i, j = 1, 2.$$

the projector associated with the eigenvalues of the matrix pencil $\lambda\mathcal{B} - \mathcal{A}$ outside the unit circle $\mathcal{C}(0, 1)$ and $\mathbb{P}_\infty$ the projector associated with the eigenvalues of the matrix pencil $zB - A$ inside Ξ_{z_0}.

The following proposition characterizes the link between $\mathbb{P}_\infty$ and $\mathcal{P}_\infty$.

Proposition 3.2 *we have*

$$\mathbb{P}_\infty = \widetilde{\mathcal{P}}_{11} + \widetilde{\mathcal{P}}_{22}$$

$$\begin{bmatrix} \frac{a-b}{2}B & 0 \\ -A_0 & \frac{a-b}{2}B \end{bmatrix} \begin{bmatrix} \widetilde{X} & \widetilde{X}_1 \\ I_n & I_n \end{bmatrix}$$
$$+ \begin{bmatrix} \frac{a+b}{2}B & -A_0 \\ 0 & \frac{a+b}{2}B \end{bmatrix} \begin{bmatrix} \widetilde{X} & \widetilde{X}_1 \\ I_n & I_n \end{bmatrix} \begin{bmatrix} \widetilde{X}^2 & 0 \\ 0 & \widetilde{X}_1^2 \end{bmatrix}$$

$$= \begin{bmatrix} \frac{a-b}{2}\widetilde{X} & \frac{a-b}{2}\widetilde{X}_1 \\ -A_0\widetilde{X} + \frac{a-b}{2}I_n & -A_0\widetilde{X}_1 + \frac{a-b}{2}I_n \end{bmatrix} + \begin{bmatrix} (\frac{a+b}{2}\widetilde{X} - A_0)\widetilde{X}^2 & (\frac{a+b}{2}\widetilde{X}_1 - A_0)\widetilde{X}_1^2 \\ \frac{a+b}{2}\widetilde{X}^2 & \frac{a+b}{2}\widetilde{X}_1^2 \end{bmatrix}$$

$$= \begin{bmatrix} \frac{a-b}{2}\widetilde{X} + (\frac{a+b}{2}\widetilde{X} - A_0)\widetilde{X}^2 & \frac{a-b}{2}\widetilde{X}_1 + (\frac{a+b}{2}\widetilde{X}_1 - A_0)\widetilde{X}_1^2 \\ -A_0\widetilde{X} + \frac{a-b}{2}I_n + \frac{a+b}{2}\widetilde{X}^2 & -A_0\widetilde{X}_1 + \frac{a-b}{2}I_n + \frac{a+b}{2}\widetilde{X}_1^2 \end{bmatrix}$$

$$= \begin{bmatrix} (\frac{a+b}{2}\widetilde{X}^2 - A_0\widetilde{X} + \frac{a-b}{2})\widetilde{X} & (\frac{a+b}{2}\widetilde{X}_1^2 - A_0\widetilde{X}_1 + \frac{a-b}{2})\widetilde{X}_1 \\ \frac{a+b}{2}\widetilde{X}^2 - A_0\widetilde{X} + \frac{a-b}{2}I_n & \frac{a+b}{2}\widetilde{X}_1^2 - A_0\widetilde{X}_1 + \frac{a-b}{2}I_n \end{bmatrix}$$

$$= \begin{bmatrix} 0 & 0 \\ 0 & 0 \end{bmatrix}$$

Which leads to

$$\begin{bmatrix} \frac{a+b}{2}I_n & -A_0 \\ 0 & \frac{a+b}{2}I_n \end{bmatrix}^{-1} \times \begin{bmatrix} \frac{a-b}{2}I_n & 0 \\ A_0 & \frac{a-b}{2}I_n \end{bmatrix} = \begin{bmatrix} \widetilde{X} & \widetilde{X}_1 \\ I_n & I_n \end{bmatrix} \times \begin{bmatrix} \widetilde{X}^2 & 0 \\ 0 & \widetilde{X}_1^2 \end{bmatrix} \times \begin{bmatrix} \widetilde{X} & \widetilde{X}_1 \\ I_n & I_n \end{bmatrix}^{-1}$$

Let $\mathcal{P}_\infty$ be the projector on the unit circle associated with the eigenvalues of the matrix pencil $\lambda\widetilde{\mathcal{B}} - \widetilde{B}$ outside the circle.

$$\mathcal{P}_\infty = \begin{pmatrix} \widetilde{X} & \widetilde{X}_1 \\ I_n & I_n \end{pmatrix} \begin{bmatrix} Q \begin{bmatrix} I_k & 0 \\ 0 & 0 \end{bmatrix} Q^{-1} & 0 \\ 0 & 0 \end{bmatrix} \begin{pmatrix} \widetilde{X} & \widetilde{X}_1 \\ I_n & I_n \end{pmatrix}^{-1}$$

where k is the order of the matrix J_∞. Note that the matrix $X - X_1$ is nonsingular if and only if the matrix pencil $zI_n - A$ does not have $\pm\sqrt{a^2 - b^2}$ as own values. We can assume this without losing the

generalities (the continuity arguments). Thereby

$$\mathcal{P}_\infty = \begin{pmatrix} \widetilde{X} & \widetilde{X}_1 \\ I_n & I_n \end{pmatrix} \begin{bmatrix} Q \begin{pmatrix} I_k & 0 \\ 0 & 0 \end{pmatrix} Q^{-1} & 0 \\ 0 & 0 \end{bmatrix} \begin{pmatrix} I_n & -\widetilde{X}_1 \\ -I_n & \widetilde{X} \end{pmatrix} \begin{pmatrix} \widetilde{X} - \widetilde{X}_1 & 0 \\ 0 & \widetilde{X} - \widetilde{X}_1 \end{pmatrix}^{-1}$$

$$= \begin{pmatrix} Q & 0 \\ 0 & Q \end{pmatrix} \begin{bmatrix} J_\infty & 0 & 0 & 0 \\ 0 & 0 & 0 & 0 \\ I_k & 0 & 0 & 0 \\ 0 & 0 & 0 & 0 \end{bmatrix} \begin{bmatrix} I_k & 0 & -\frac{a-b}{a+b} J_\infty^{-1} & 0 \\ 0 & 0 & 0 & 0 \\ 0 & 0 & 0 & 0 \\ 0 & 0 & 0 & 0 \end{bmatrix} \begin{pmatrix} Q & 0 \\ 0 & Q \end{pmatrix}^{-1}$$

$$\times \begin{pmatrix} \widetilde{X} - \widetilde{X}_1 & 0 \\ 0 & \widetilde{X} - \widetilde{X}_1 \end{pmatrix}$$

$$= \begin{bmatrix} Q \begin{pmatrix} J_\infty & 0 \\ 0 & 0 \end{pmatrix} Q^{-1} & Q \begin{pmatrix} -\frac{a-b}{a+b} I_k & 0 \\ 0 & 0 \end{pmatrix} Q^{-1} \\ Q \begin{pmatrix} I_k & 0 \\ 0 & 0 \end{pmatrix} Q^{-1} & Q \begin{pmatrix} -\frac{a-b}{a+b} J_\infty^{-1} & 0 \\ 0 & 0 \end{pmatrix} Q^{-1} \end{bmatrix} \begin{pmatrix} \widetilde{X} - \widetilde{X}_1 & 0 \\ 0 & \widetilde{X} - \widetilde{X}_1 \end{pmatrix}^{-1}$$

$$\equiv \begin{pmatrix} \widetilde{\mathcal{P}}_{11} & \widetilde{\mathcal{P}}_{12} \\ \widetilde{\mathcal{P}}_{21} & \widetilde{\mathcal{P}}_{22} \end{pmatrix}.$$

with

$$\widetilde{\mathcal{P}}_{11} = Q \begin{bmatrix} J_\infty (J_\infty - \frac{a-b}{a+b} J_\infty^{-1})^{-1} & 0 \\ 0 & 0 \end{bmatrix} Q^{-1}$$

$$\widetilde{\mathcal{P}}_{12} = Q \begin{bmatrix} -\frac{a-b}{a+b} (J_\infty - \frac{a-b}{a+b} J_\infty^{-1})^{-1} & 0 \\ 0 & 0 \end{bmatrix} Q^{-1}$$

$$\widetilde{\mathcal{P}}_{21} = Q \begin{bmatrix} (J_\infty - \frac{a-b}{a+b} J_\infty^{-1})^{-1} & 0 \\ 0 & 0 \end{bmatrix} Q^{-1}$$

$$\widetilde{\mathcal{P}}_{22} = Q \begin{bmatrix} -\frac{a-b}{a+b} J_\infty^{-1} (J_\infty - \frac{a-b}{a+b} J_\infty^{-1})^{-1} & 0 \\ 0 & 0 \end{bmatrix} Q^{-1}$$

and we get $\widetilde{\mathcal{P}}_{11} + \widetilde{\mathcal{P}}_{22} = Q \begin{pmatrix} I_k & 0 \\ 0 & 0 \end{pmatrix} Q^{-1} = \mathbb{P}_\infty$ □

Let $\mathbb{H}$ the dichotomy criterion

$$\mathbb{H} = \frac{1}{4} \int_0^2 \left[(\frac{a+b}{2} e^{i\frac{\theta}{2}} + \frac{a-b}{2} e^{-i\frac{\theta}{2}}) B - A_0 \right]^{-*} \left[(\frac{a+b}{2} e^{i\frac{\theta}{2}} + \frac{a-b}{2} e^{-i\frac{\theta}{2}}) B - A_0 \right]^{-1} d\theta$$

Algorithm 3.2 .

- *Input variables: The matrices A and B, the parameters a, b and z_0 such that the matrix pencil $zB - A$ has no eigenvalues on the ellipse Ξ_0 of equation with $a \geq b > 0$.*

- *Output variables: $\mathbb{P}_\infty$ and $\mathbb{H}$.*
  $\mathbb{P}_\infty$ being the projector on the right invariant space of $zB - A$ corresponding to the eigenvalues outside the ellipse Ξ_{z_0} and $\mathbb{H}$ the criterion of dichotomy.

1. *Determine $A_0 = A - z_0 B$*
2. *Set*
$$\mathcal{B} = \begin{pmatrix} \frac{a+b}{2}B & -A_0 \\ 0 & \frac{a+b}{2}B \end{pmatrix} \quad \text{and} \quad \mathcal{A} = \begin{pmatrix} -\frac{a-b}{2}B & 0 \\ A_0 & \frac{a-b}{2}B \end{pmatrix} \tag{3.8}$$
2. *Apply Algorithm 2.2 to $\lambda\mathcal{B} - \mathcal{A}$*
3. *We obtain $\mathbb{P}_\infty$ et $\mathbb{H}$.*

3.3 Spectral dichotomy to a matrix pencil with respect to a parabola not centered at the origin

Let $zB - A$ be a regular matrix pencil of order n having no eigenvalues on the parabola Γ of equation

$$2p(d - x) = (y - p\tilde{b})^2 \tag{3.9}$$

with $p > 0$.

Let consider the following change of variable $\widetilde{x} = x + \frac{p}{2} - d$, we obtain

$$2p(\frac{p}{2} - \widetilde{x}) = (y - p\tilde{b})^2 \tag{3.10}$$

Consider the set

$$\widetilde{\Gamma}_d = \left\{ z = x + iy | \quad x + \left(\frac{p}{2} - d\right) + i(y - p\tilde{b}) \in \Gamma \right\}$$

described by the following equation (3.10).
We consider the following matrices of order $2n$

$$\widetilde{\mathcal{A}}_d = \begin{bmatrix} -\sqrt{\frac{p}{2}}B & A_{d\tilde{b}} \\ I_n & -\sqrt{\frac{p}{2}}I_n \end{bmatrix} \quad \text{with} \quad A_{db} = A + \left(\frac{p}{2} - d - ip\tilde{b}\right) B. \tag{3.11}$$

and

$$\mathcal{B} = \begin{bmatrix} B & 0 \\ 0 & I_n \end{bmatrix} \tag{3.12}$$

The respective eigenvalues $\widetilde{\lambda}_d$ and $z_{d\tilde{b}}$ of the matrices pencils $\lambda\mathcal{B} - \widetilde{\mathcal{A}}_d$ And $z_{d\tilde{b}}B - A_{d\tilde{b}}$ verifies the following relation

$$z_{d\tilde{b}} = \left(\sqrt{\frac{p}{2}} + \widetilde{\lambda}_d\right)^2.$$

$$\begin{aligned} z_{d\tilde{b}}B - A_{db} &= z_{d\tilde{b}}B - \left(A - \left(\frac{p}{2} - d - ip\tilde{b}\right)B\right) \\ &= z_{d\tilde{b}}B - A - \left(\frac{p}{2} - d - ip\tilde{b}\right)B \\ &= \left(z_{d\tilde{b}} - \left(\frac{p}{2} - d - ip\tilde{b}\right)\right)B - A \\ &= zB - A \end{aligned}$$

where z is the eigenvalue of the matrix pencil $zB - A$. Therefore,

$$z = \left(\sqrt{\frac{p}{2}} + \widetilde{\lambda}_d\right)^2 - \left(\frac{p}{2} - d - ip\tilde{b}\right) \tag{3.13}$$

We also assume that $\|A_{d\tilde{b}}\| = 1$. Otherwise (if $\|A_{d\tilde{b}}\| \neq 1$), we can take

$$A^1_{d\tilde{b}} = \frac{1}{\|A_{db}\|}A_{d\tilde{b}} \qquad \text{et} \qquad \widetilde{p}^1_{db} = \frac{1}{\|A_{d\tilde{b}}\|}.$$

Let consider numerics parameters $\alpha_{\widetilde{\mathcal{A}}_d}$ et $\alpha_{A_{d\tilde{b}}}$ defined by

$$\alpha_{\widetilde{\mathcal{A}}_d} = \sup_{\Re(\widetilde{\lambda}_d)=0} \|(\widetilde{\lambda}_d\mathcal{B} - \widetilde{\mathcal{A}}_d)^{-1}\| \text{ and } \alpha_{A_{d\tilde{b}}} = \sup_{z\in\widetilde{\Gamma}_d} \|(zB - A)^{-1}\| \tag{3.14}$$

The following proposition gives a relation between the parameters $\alpha_{\widetilde{\mathcal{A}}_d}$ et $\alpha_{A_{d\tilde{b}}}$.

Proposition 3.3 *Assume that* $\max(\|A\|, \|B\|) \leq 1$ *and let* $\alpha_{\widetilde{\mathcal{A}}_d}$ *and* $\alpha_{A_{d\tilde{b}}}$ *be the two parameters defined in* (3.18). *Suppose that*

$$\|A_{d\tilde{b}}\| = 1 \qquad \textit{and} \qquad \left|\frac{p}{2} - d - ip\tilde{b}\right| < \frac{1}{\alpha_{A_{d\tilde{b}}}} \tag{3.15}$$

then

$$\alpha_{A_{d\tilde{b}}} \leq \alpha_{\widetilde{\mathcal{A}}_d} \leq C\left(\alpha_{A_{d\tilde{b}}} + \sqrt{\alpha_{A_{d\tilde{b}}}}\left(\sqrt{1 + \alpha_{A_{d\tilde{b}}}} + 1\right)\right). \tag{3.16}$$

with $C = \max(\|B^{-1}\|, 1)$.

Proof

Let the matrix

$$\left(\widetilde{\lambda}_d\mathcal{B} - \widetilde{\mathcal{A}}_d\right) = \begin{bmatrix} (\widetilde{\lambda}_d + \sqrt{\frac{p}{2}})B & -A_{d\tilde{b}} \\ -I_n & (\widetilde{\lambda}_d + \sqrt{\frac{p}{2}})I_n \end{bmatrix}$$

We have

$$\begin{bmatrix} (\widetilde{\lambda}_d + \sqrt{\frac{p}{2}})I_n & A_{d\tilde{b}} \\ I_n & (\widetilde{\lambda}_d + \sqrt{\frac{p}{2}})B \end{bmatrix} \times \begin{bmatrix} (\widetilde{\lambda}_d + \sqrt{\frac{p}{2}})B & -A_{d\tilde{b}} \\ -I_n & (\widetilde{\lambda}_d + \sqrt{\frac{p}{2}})I_n \end{bmatrix} =$$
$$\begin{bmatrix} (\widetilde{\lambda}_d + \sqrt{\frac{p}{2}})^2B - A_{d\tilde{b}} & 0 \\ 0 & (\widetilde{\lambda}_d + \sqrt{\frac{p}{2}})^2B - A_{d\tilde{b}} \end{bmatrix}$$

London Journal of Research in Science: Natural and Formal

thus

$$(\widetilde{\lambda}_d\mathcal{B}-\widetilde{\mathcal{A}}_d)^{-1}=\begin{bmatrix}(\widetilde{\lambda}_d+\sqrt{\frac{p}{2}})^2B-A_{db} & 0\\ 0 & (\widetilde{\lambda}_d+\sqrt{\frac{p}{2}})^2B-A_{d\tilde{b}}\end{bmatrix}^{-1}\times \begin{bmatrix}(\widetilde{\lambda}_d+\sqrt{\frac{p}{2}})B & A_{d\tilde{b}}\\ I_n & (\widetilde{\lambda}_d+\sqrt{\frac{p}{2}})I_n\end{bmatrix}$$

$$=\begin{bmatrix}(\widetilde{\lambda}_d+\sqrt{\frac{p}{2}})^2B-(A+(\frac{p}{2}-d-ip\tilde{b})B) & 0\\ 0 & (\widetilde{\lambda}_d+\sqrt{\frac{p}{2}})^2B-(A+(\frac{p}{2}-d-ip\tilde{b})B)\end{bmatrix}^{-1}\times \begin{bmatrix}(\widetilde{\lambda}_d+\sqrt{\frac{p}{2}})B & (A+(\frac{p}{2}-d-ip\tilde{b})B)\\ I_n & (\widetilde{\lambda}_d+\sqrt{\frac{p}{2}})I_n\end{bmatrix}$$

$$=\begin{bmatrix}((\widetilde{\lambda}_d+\sqrt{\frac{p}{2}})^2-\frac{p}{2}+d-ip\tilde{b})B-A & 0\\ 0 & ((\widetilde{\lambda}_d+\sqrt{\frac{p}{2}})^2-\frac{p}{2}+d-ip\tilde{b})B-A\end{bmatrix}^{-1}\times \begin{bmatrix}(\widetilde{\lambda}_d+\sqrt{\frac{p}{2}})I_n & A+(\frac{p}{2}-d-ip\tilde{b})B)\\ I_n & (\widetilde{\lambda}_d+\sqrt{\frac{p}{2}})I_n\end{bmatrix}$$

$$=\begin{bmatrix}(zB-A)^{-1} & 0\\ 0 & (zB-A)^{-1}\end{bmatrix}\times\begin{bmatrix}\sqrt{z+\frac{p}{2}-d-ip\tilde{b}}I_n & A+(\frac{p}{2}-d-ip\tilde{b})B\\ I_n & \sqrt{z+\frac{p}{2}-d-ip\tilde{b}}I_n\end{bmatrix}$$

$$=\begin{bmatrix}\sqrt{z+\frac{p}{2}-d-ip\tilde{b}}(zB-A)^{-1} & (zB-A)^{-1}(A+(\frac{p}{2}-d-ip\tilde{b})B)\\ (zB-A)^{-1} & \sqrt{z+\frac{p}{2}-d-ip\tilde{b}}(zB-A)^{-1}\end{bmatrix}$$

Knowing that the norm of $(\widetilde{\lambda}_dI_{2n}-\widetilde{\mathcal{A}}_d)^{-1}$ is greater than or equal to the norm of each of its block components taken individually, we can deduce that

$$\alpha_{\widetilde{\mathcal{A}}_d}=\sup_{\Re(\widetilde{\lambda}_d)=0}\|(\widetilde{\lambda}_d\mathcal{B}-\widetilde{\mathcal{A}}_d)^{-1}\|\geq\sup_{z\in\widetilde{\Gamma}_d}\|(zB-A)^{-1}\|=\alpha_{A_{d\tilde{b}}}$$

and also

$$\left\|(\widetilde{\lambda}_d\mathcal{B}-\widetilde{\mathcal{A}}_d)^{-1}\right\| \leq \left\|\begin{pmatrix} \sqrt{z+\frac{p}{2}-d-ip\tilde{b}}I_n & A+(\frac{p}{2}-d-ip\tilde{b})B \\ I_n & \sqrt{z+\frac{p}{2}-d-ip\tilde{b}}I_n \end{pmatrix}\right\| \|(zB-A)^{-1}\|$$

$$\leq \left\|\begin{pmatrix} \|\sqrt{z+\frac{p}{2}-d-ip\tilde{b}}I_n\| & \|A+(\frac{p}{2}-d-ip\tilde{b})B\| \\ \|I_n\| & \|\sqrt{z+\frac{p}{2}-d-ip\tilde{b}}I_n\| \end{pmatrix}\right\| \|(zB-A)^{-1}\|$$

$$\leq \left\|\begin{pmatrix} \sqrt{|z|}+\sqrt{|\frac{p}{2}-d-ip\tilde{b}|} & 1 \\ 1 & \sqrt{|z|}+\sqrt{|\frac{p}{2}-d-ip\tilde{b}|} \end{pmatrix}\right\| \|(zB-A)^{-1}\|$$

$$\leq \left(\sqrt{|z|}+\sqrt{|\frac{p}{2}-d-ip\tilde{b}|}+1\right)\|(zB-A)^{-1}\|$$

- if $|z| \leq \dfrac{\alpha_{A_{d\tilde{b}}}+1}{\alpha_{A_{d\tilde{b}}}}$ then

$$\begin{aligned}\|(\lambda\mathcal{B}-\widetilde{\mathcal{A}}_d)^{-1}\| &\leq \alpha_{A_{d\tilde{b}}}(\sqrt{|z|}+\sqrt{|\frac{p}{2}-d-ip\tilde{b}|}+1) \\ &\leq \alpha_{A_{d\tilde{b}}} \quad \sqrt{\frac{\alpha_{A_{d\tilde{b}}}+1}{\alpha_{A_{d\tilde{b}}}}}+\frac{1}{\sqrt{\alpha_{d\tilde{b}}}}+1\Big) \\ &\leq \alpha_{A_{d\tilde{b}}}+\sqrt{\alpha_{d\tilde{b}}}(\sqrt{\alpha_{d\tilde{b}}+1}+1)\end{aligned}$$

- Assume that $|z| > \dfrac{\alpha_{A_{d\tilde{b}}}+1}{\alpha_{A_{d\tilde{b}}}}$, we get

$$\begin{aligned}(zB-A)(zB-A)^{-1} &= I_n \\ (zB)(zB-A)^{-1}-A(zB-A)^{-1} &= I_n \\ (zB)(zB-A)^{-1} &= I_n+A(zB-A)^{-1}I_n \\ (zB-A)^{-1} &= (zB)^{-1}(I_n+A(zB-A)^{-1})\end{aligned}$$

As a result

$$\left\|(\widetilde{\lambda}_d\mathcal{B}-\widetilde{\mathcal{A}}_d)^{-1}\right\| \leq \left\|(zB)^{-1}(I_n+A(zB-A)^{-1})\right\| \times \left\|1+\sqrt{|z|}+\sqrt{\left|\frac{p}{2}-d-ip\tilde{b}\right|}\right\|$$

$$\leq \left\|B^{-1}\right\|\left(\left\|A(zB-A)^{-1}\right\|+1\right)\frac{1+\sqrt{|z|}+\sqrt{\left|\frac{p}{2}-d-ip\tilde{b}\right|}}{|z|}$$

$$\leq C\left(\|A\|\left\|(zB-A)^{-1}\right\|+1\right)\frac{1+\sqrt{|z|}+\sqrt{\left|\frac{p}{2}-d-ip\tilde{b}\right|}}{|z|}$$

$$\leq C\left(\alpha_{A_{d\tilde{b}}}+1\right)\left(\frac{1}{\sqrt{|z|}}+\frac{1}{|z|}+\frac{\sqrt{|\frac{p}{2}-d-ip\tilde{b}|}}{|z|}\right)$$

$$\leq C\left(\alpha_{A_{d\tilde{b}}}+1\right)\quad\frac{\sqrt{\alpha_{A_{d\tilde{b}}}}}{\sqrt{\alpha_{A_{d\tilde{b}}}+1}}+\frac{\alpha_{A_{d\tilde{b}}}}{\alpha_{A_{d\tilde{b}}}+1}+\frac{\sqrt{\alpha_{A_{d\tilde{b}}}}}{\alpha_{A_{d\tilde{b}}+1}}\Bigg)$$

$$\leq C\left(\sqrt{\alpha_{d\tilde{b}}+1}\sqrt{\alpha_{d\tilde{b}}}+\alpha_{d\tilde{b}}+\sqrt{\alpha_{d\tilde{b}}}\right)$$

$$\leq C\left(\alpha_{A_{d\tilde{b}}}+\sqrt{\alpha_{A_{d\tilde{b}}}}\left(\sqrt{\alpha_{A_{d\tilde{b}}+1}}+1\right)\right)$$

Finally

$$\alpha_{A_{d\tilde{b}}} \leq \alpha_{\mathcal{A}_{d\tilde{b}}} \leq C\left(\alpha_{A_{d\tilde{b}}}+\sqrt{\alpha_{A_{d\tilde{b}}}}\left(\sqrt{\alpha_{A_{d\tilde{b}}+1}}+1\right)\right).$$

Moreover, if we denote by

$$\widetilde{\mathcal{P}}_+=\begin{pmatrix}\widetilde{\mathcal{P}}_{11}^{(d)} & \widetilde{\mathcal{P}}_{12}^{(d)}\\ \widetilde{\mathcal{P}}_{21}^{(d)} & \widetilde{\mathcal{P}}_{22}^{(d)}\end{pmatrix} \qquad \text{avec} \qquad \widetilde{\mathcal{P}}_{ij}^{(d)}\in\mathbb{C}^{n\times n}, \qquad i,j=1,2. \tag{3.17}$$

the projector onto the subspace of $\widetilde{\mathcal{A}}_d$ associated with the eigenvalues in the left complex half-plane and $\widetilde{\mathbb{P}}_\infty \in \mathbb{C}^{n\times n}$ the projector onto the suspace of $zB-A_{d\tilde{b}}$ associated with the eigenvalues inside the parabola $\widetilde{\Gamma_d}$, then the following proposition characterizes the link between $\widetilde{\mathbb{P}}_\infty$ and $\widetilde{\mathcal{P}}_+$

Proposition 3.4 *We have*

$$\widetilde{\mathbb{P}}_\infty = 2\widetilde{\mathcal{P}}_{11}^{(d)} = 2\widetilde{\mathcal{P}}_{22}^{(d)} = 4\widetilde{\mathcal{P}}_{12}^{(d)}\widetilde{\mathcal{P}}_{21}^{(d)} \tag{3.18}$$

Moreover

$$\widetilde{\mathbb{P}}_\infty A = 4(\widetilde{\mathcal{P}}_{12}^{(d)})^2-(p-2d-2ipb)B\widetilde{\mathcal{P}}_{11}^{(d)} \tag{3.19}$$

Proof

Let $\widetilde{X_d}$ be a solution of the matrix equation

$$\left(\tilde{X_d} + \sqrt{\frac{p}{2}} I_n\right)^2 = A_{d\tilde{b}}. \tag{3.20}$$

Let $\tilde{X}_1$ be another solution of the same matrix equation (3.20). We have

$$\begin{aligned}
&\left(\tilde{X_d} + \sqrt{\frac{p}{2}} I_n\right)^2 = \left(\tilde{X}_1 + \sqrt{\frac{p}{2}} I_n\right)^2 \\
&\Leftrightarrow \left(\tilde{X_d} + \sqrt{\frac{p}{2}} I_n\right) = \left(\tilde{X}_1 + \sqrt{\frac{p}{2}} I_n\right) \qquad \text{where} \qquad \left(\tilde{X_d} + \sqrt{\frac{p}{2}} I_n\right) = -\left(\tilde{X}_1 + \sqrt{\frac{p}{2}} I_n\right) \\
&\Leftrightarrow \tilde{X_d} = \tilde{X}_1 \qquad \text{where} \quad \tilde{X}_1 = -\tilde{X_d} - 2\sqrt{\frac{p}{2}} I_n
\end{aligned}$$

Finally the other solution $\tilde{X}_1$ is written in the form $\tilde{X}_1 = -\tilde{X} - 2\sqrt{\frac{p}{2}} I_n$. We get [19]

$$\tilde{\mathcal{A}_d} = \begin{bmatrix} \tilde{X_d} + \sqrt{\frac{p}{2}} I_n & -\tilde{X_d} - \sqrt{\frac{p}{2}} I_n \\ I_n & I_n \end{bmatrix} \times \begin{bmatrix} \tilde{X_d} & 0 \\ 0 & -\tilde{X_d} - 2\sqrt{\frac{p}{2}} I_n \end{bmatrix} \times \begin{bmatrix} \frac{1}{2}(\tilde{X_d} + \sqrt{\frac{p}{2}} I_n)^{-1} & \frac{1}{2} I_n \\ -\frac{1}{2}(\tilde{X_d} + \sqrt{\frac{p}{2}} I_n)^{-1} & \frac{1}{2} I_n \end{bmatrix}$$

Soit $\tilde{X_d} = Q_{d\tilde{b}} \begin{bmatrix} M_+ & 0 \\ 0 & M_- \end{bmatrix} Q_{d\tilde{b}}^{-1}$ the canonical jordan form of the matrix $\tilde{X_d}$ with M_+ and M_- the Jordan blocks associated respectively with the eigenvalues of $\tilde{X_d}$ located in the right half-plane and the left half-plane.

By replacing $\tilde{X_d}$ by its decomposition in the matrix $\tilde{\mathcal{A}_d}$, we get

$$\widetilde{\mathcal{A}_d} = \widetilde{\mathcal{Q}}_{d\tilde{b}} \mathcal{M} (\widetilde{\mathcal{Q}}_{d\tilde{b}})^{-1}$$

with

$$\widetilde{\mathcal{Q}_{d\tilde{b}}} = \begin{bmatrix} Q_{d\tilde{b}} & 0 \\ 0 & Q_{d\tilde{b}} \end{bmatrix} \begin{bmatrix} \begin{pmatrix} M_+ & 0 \\ 0 & M_- \end{pmatrix} + \sqrt{\frac{p}{2}} I_n & -\begin{bmatrix} M_+ & 0 \\ 0 & M_- \end{bmatrix} - \sqrt{\frac{p}{2}} I_n \\ I_n & I_n \end{bmatrix}$$

and

$$\mathcal{M} = \begin{bmatrix} \begin{bmatrix} M_+ & 0 \\ 0 & M_- \end{bmatrix} & 0 \\ 0 & \begin{bmatrix} M_+ & 0 \\ 0 & M_- \end{bmatrix} - 2\sqrt{\frac{p}{2}} I_n \end{bmatrix}$$

We can therefore compute the associated projector

$$\begin{aligned}
\widetilde{\mathcal{P}}_+ &= (\widetilde{\mathcal{Q}}_{d\tilde{b}}) \begin{bmatrix} I_k & 0 \\ 0 & 0 \end{bmatrix} (\widetilde{\mathcal{Q}}_{d\tilde{b}})^{-1} \\
&= \begin{bmatrix} Q_{d\tilde{b}} & 0 \\ 0 & Q_{d\tilde{b}} \end{bmatrix} \begin{bmatrix} \begin{bmatrix} M_+ & 0 \\ 0 & M_- \end{bmatrix} + \sqrt{\frac{p}{2}} I_n & -\begin{bmatrix} M_+ & 0 \\ 0 & M_- \end{bmatrix} - \sqrt{\frac{p}{2}} I_n \\ I_n & I_n \end{bmatrix} \times \begin{bmatrix} \begin{bmatrix} I_k & 0 \\ 0 & 0 \end{bmatrix} & \begin{bmatrix} 0 & 0 \\ 0 & 0 \end{bmatrix} \\ \begin{bmatrix} 0 & 0 \\ 0 & 0 \end{bmatrix} & \begin{bmatrix} 0 & 0 \\ 0 & 0 \end{bmatrix} \end{bmatrix} \\
&\times \begin{bmatrix} \frac{1}{2} \left(\begin{bmatrix} M_+ & 0 \\ 0 & M_- \end{bmatrix} + \sqrt{\frac{p}{2}} I_n \right)^{-1} & \frac{1}{2} I_n \\ -\frac{1}{2} \left(\begin{bmatrix} M_+ & 0 \\ 0 & M_- \end{bmatrix} - \sqrt{\frac{p}{2}} I_n \right)^{-1} & \frac{1}{2} I_n \end{bmatrix} \begin{bmatrix} Q_{d\tilde{b}}^{-1} & 0 \\ 0 & Q_{d\tilde{b}}^{-1} \end{bmatrix} \\
&= \begin{bmatrix} Q_{d\tilde{b}} & 0 \\ 0 & Q_{d\tilde{b}} \end{bmatrix} \begin{bmatrix} \begin{bmatrix} M_+ + \sqrt{\frac{p}{2}} I_k & 0 \\ 0 & 0 \end{bmatrix} & \begin{bmatrix} 0 & 0 \\ 0 & 0 \end{bmatrix} \\ \begin{bmatrix} I_k & 0 \\ 0 & 0 \end{bmatrix} & \begin{bmatrix} 0 & 0 \\ 0 & 0 \end{bmatrix} \end{bmatrix} \\
&\times \begin{bmatrix} \frac{1}{2} \begin{bmatrix} (M_+ + \sqrt{\frac{p}{2}} I_k)^{-1} & 0 \\ 0 & (M_- + \sqrt{\frac{p}{2}} I_{n-k})^{-1} \end{bmatrix} & \frac{1}{2} \begin{bmatrix} I_k & 0 \\ 0 & I_{n-k} \end{bmatrix} \\ -\frac{1}{2} \begin{bmatrix} (M_+ + \sqrt{\frac{p}{2}} I_k)^{-1} & 0 \\ 0 & (M_- + \sqrt{\frac{p}{2}} I_{n-k})^{-1} \end{bmatrix} & \frac{1}{2} \begin{bmatrix} I_k & 0 \\ 0 & I_{n-k} \end{bmatrix} \end{bmatrix} \begin{bmatrix} Q_{d\tilde{b}}^{-1} & 0 \\ 0 & Q_{d\tilde{b}}^{-1} \end{bmatrix} \\
&= \begin{bmatrix} Q_{d\tilde{b}} & 0 \\ 0 & Q_{d\tilde{b}} \end{bmatrix} \begin{bmatrix} \frac{1}{2} \begin{bmatrix} I_k & 0 \\ 0 & 0 \end{bmatrix} & \frac{1}{2} \begin{bmatrix} M_+ + \sqrt{\frac{p}{2}} I_k & 0 \\ 0 & 0 \end{bmatrix} \\ \frac{1}{2} \begin{bmatrix} (M_+ + \sqrt{\frac{p}{2}} I_k)^{-1} & 0 \\ 0 & 0 \end{bmatrix} & \frac{1}{2} \begin{bmatrix} I_k & 0 \\ 0 & 0 \end{bmatrix} \end{bmatrix} \begin{bmatrix} Q_{d\tilde{b}}^{-1} & 0 \\ 0 & Q_{d\tilde{b}}^{-1} \end{bmatrix} \\
&= \begin{bmatrix} Q_{d\tilde{b}} \begin{bmatrix} \frac{1}{2} I_k & 0 \\ 0 & 0 \end{bmatrix} Q_{d\tilde{b}}^{-1} & Q_{db} \begin{bmatrix} \frac{1}{2} (M_+ + \sqrt{\frac{p}{2}} I_k) & 0 \\ 0 & 0 \end{bmatrix} Q_{d\tilde{b}}^{-1} \\ Q_{d\tilde{b}} \begin{bmatrix} \frac{1}{2} (M_+ + \sqrt{\frac{p}{2}} I_k)^{-1} & 0 \\ 0 & 0 \end{bmatrix} Q_{d\tilde{b}}^{-1} & Q_{d\tilde{b}} \begin{bmatrix} \frac{1}{2} I_k & 0 \\ 0 & 0 \end{bmatrix} Q_{d\tilde{b}}^{-1} \end{bmatrix} \\
&= \begin{bmatrix} \widetilde{\mathcal{P}}_{11}^{(d)} & \widetilde{\mathcal{P}}_{12}^{(d)} \\ \widetilde{\mathcal{P}}_{21}^{(d)} & \widetilde{\mathcal{P}}_{22}^{(d)} \end{bmatrix}
\end{aligned}$$

It follows that

$$\widetilde{\mathcal{P}}_{11}^{(d)} = Q_d \begin{bmatrix} \frac{1}{2}I_k & 0 \\ 0 & 0 \end{bmatrix} Q_{d\tilde{b}}^{-1} = \frac{1}{2}\widetilde{\mathbb{P}}_\infty$$

$$\widetilde{\mathcal{P}}_{12}^{(d)} = \frac{1}{2}Q_{d\tilde{b}} \begin{bmatrix} M_+ + \sqrt{\frac{p}{2}}I_k & 0 \\ 0 & 0 \end{bmatrix} Q_{d\tilde{b}}^{-1}$$

$$\widetilde{\mathcal{P}}_{21}^{(d)} = \frac{1}{2}Q_{db} \begin{bmatrix} (M_+ + \sqrt{\frac{p}{2}}I_k)^{-1} & 0 \\ 0 & 0 \end{bmatrix} Q_{d\tilde{b}}^{-1}$$

$$\widetilde{\mathcal{P}}_{22}^{(d)} = Q_{d\tilde{b}} \begin{bmatrix} \frac{1}{2}I_k & 0 \\ 0 & 0 \end{bmatrix} Q_{d\tilde{b}}^{-1} = \frac{1}{2}\widetilde{\mathbb{P}}_\infty$$

with $\widetilde{X_d} = Q_{d\tilde{b}} \begin{bmatrix} M_+ & 0 \\ 0 & M_- \end{bmatrix} Q_{d\tilde{b}}^{-1}$ we have

$$\begin{aligned} A &= A_{d\tilde{b}} - \left(\frac{p}{2} - d - ipb\right) B \\ &= Q_{d\tilde{b}} \begin{bmatrix} \left(M_+ + \sqrt{\frac{p}{2}}I_k\right)^2 - \left(\frac{p}{2} - d - ip\tilde{b}\right) B_1 & -\left(\frac{p}{2} - d - ip\tilde{b}\right) B_2 \\ -\left(\frac{p}{2} - d - ip\tilde{b}\right) B_3 & \left(M_- + \sqrt{\frac{p}{2}}I_{n-k}\right)^2 - \left(\frac{p}{2} - d - ip\tilde{b}\right) B_4 \end{bmatrix} Qj_{d\tilde{b}}^{-1} \end{aligned}$$

where $B = \begin{pmatrix} B_1 & B_2 \\ B_3 & B_4 \end{pmatrix}$ and

$$\begin{aligned} \widetilde{\mathbb{P}}_\infty A &= Q_{d\tilde{b}} \begin{bmatrix} I_k & 0 \\ 0 & 0 \end{bmatrix} \begin{bmatrix} \left(M_+ + \sqrt{\frac{p}{2}}I_k\right)^2 - \left(\frac{p}{2} - d - ip\tilde{b}\right) B_1 & -\left(\frac{p}{2} - d - ip\tilde{b}\right) B_2 \\ -\left(\frac{p}{2} - d - ip\tilde{b}\right) B_3 & \left(M_- + \sqrt{\frac{p}{2}}I_{n-k}\right)^2 - \left(\frac{p}{2} - d - ip\tilde{b}\right) B_4 \end{bmatrix} Q_{d\tilde{b}}^{-1} \\ &= Q_{db} \begin{bmatrix} \left(M_+ + \sqrt{\frac{p}{2}}I_k\right)^2 - (\frac{p}{2} - d - ip\tilde{b})B_1 & 0 \\ 0 & 0 \end{bmatrix} Q_{d\tilde{b}}^{-1} \\ &= 4(\widetilde{\mathcal{P}}_{12}^{(d)})^2 - (p - 2d - 2ip\tilde{b})B\widetilde{\mathcal{P}}_{11}^{(d\tilde{b})} \end{aligned}$$

so (3.18) et (3.19). □

Remark 3.1 *We note that:*

- *If the parameter* $d = \frac{p}{2}$, *hence the equalities (3.19) are reduced to* $\widetilde{\mathbb{P}}_\infty A = 4(\widetilde{\mathcal{P}}_{12}^{(d)})^2 + 2ipbB\widetilde{\mathcal{P}}_{11}^{(d)}$.
- *If the parameter* $b = 0$, *hence the equalities(3.19) are reduced to* $\widetilde{\mathbb{P}}_\infty A = 4(\widetilde{\mathcal{P}}_{12}^{(d)})^2 - (p - 2d)B\widetilde{\mathcal{P}}_{11}^{(d)}$.
- *If the parameters* $b = 0, d = \frac{p}{2}$, *hence the equalities (3.19) are reduced to* $\widetilde{\mathbb{P}}_\infty A = 4(\widetilde{\mathcal{P}}_{12}^{(d)})^2$.

Algorithm 3.3 (DichoP)

- *Input variables : A and B such that the matrix pencil $zB - A$ has no eigenvalues on the parabola with equation $2p\left(\frac{p}{2} - \tilde{x}\right)^2 = (y - pb)^2$ with $p > 0$*

- *Output variables: $\mathbb{P}$ and $\mathbb{H}$*

  $\mathbb{P}$ being the projector on the right subspace of $zB - A$ associated with the eigenvalues outside the parabola and the matrix $\mathbb{H}$ whose norm gives the dichotomy criterion.

1. - *If $d = \frac{p}{2}$ and $b = 0$, set*

$$\mathcal{A} = \begin{pmatrix} -\sqrt{\frac{p}{2}}B & A \\ I_n & -\sqrt{\frac{p}{2}}I_n \end{pmatrix} \quad \text{and} \quad \mathcal{B} = \begin{pmatrix} B & 0 \\ 0 & I_n \end{pmatrix}$$

   - *elseif $d = \frac{p}{2}$ and $b \neq 0$, set*

$$\mathcal{A} = \begin{pmatrix} -\sqrt{\frac{p}{2}}B & A - ipbB \\ I_n & -\sqrt{\frac{p}{2}}I_n \end{pmatrix} \quad \text{and} \quad \mathcal{B} = \begin{pmatrix} B & 0 \\ 0 & I_n \end{pmatrix}$$

   - *elseif $d \neq \frac{p}{2}$ and $b = 0$, set*

$$\mathcal{A} = \begin{pmatrix} -\sqrt{\frac{p}{2}}B & A + (\frac{p}{2} - d)B \\ I_n & -\sqrt{\frac{p}{2}}I_n \end{pmatrix} \quad \text{and} \quad \mathcal{B} = \begin{pmatrix} B & 0 \\ 0 & I_n \end{pmatrix}$$

   - *else $d \neq \frac{p}{2}$ and $b \neq 0$, set*

$$\mathcal{A} = \begin{pmatrix} -\sqrt{\frac{p}{2}}B & A + (\frac{p}{2} - d - ip\tilde{b})B \\ I_n & -\sqrt{\frac{p}{2}}I_n \end{pmatrix} \quad \text{and} \quad \mathcal{B} = \begin{pmatrix} B & 0 \\ 0 & I_n \end{pmatrix}$$

2. *Using Algorithm 2.3 to $\lambda\mathcal{B} - \mathcal{A}$, compute the Projector $\mathcal{P}$ onto the right eigenspace of $\mathcal{A}$ associated with the eigenvalues on the right half-plane of the complex plane and the matrix $\mathbb{H}_{d\tilde{b}}$;*

3. *If $\|\mathbb{H}\|$ is not large, determine the projectors $\mathbb{P}$ by*

$$\mathbb{P} = 2\widetilde{\mathcal{P}}_1$$

IV. NUMERICAL TESTS

Example 4.1 *We consider the matrix pencil $zB - A$ of order 20 defined by [18]*

$$A = \begin{cases} a_{2i,2i} = -\frac{1}{3} & if \quad 1 \leq i \leq 10 \\ a_{2i-1,2i+1} = 1 & if \quad 1 \leq i \leq 9 \\ a_{2i+1,2i-1} = \frac{1}{3} & if \quad 1 \leq i \leq 9 \\ a_{2i,2i+1} = 3 & if \quad 1 \leq i \leq 9, \\ a_{i,j} = 0 & otherwise \end{cases} \quad \text{and} \quad B = \begin{cases} b_{2i-1,2i-1} = -\frac{1}{4} & if \quad 1 \leq i \leq 10 \\ b_{2i,2i+2} = -1 & if \quad 1 \leq i \leq 9 \\ b_{2i+2,2i} = 5 & if \quad 1 \leq i \leq 9 \\ b_{2i,2i-1} = 2 & if \quad 1 \leq i \leq 9, \\ b_{i,j} = 0 & otherwise \end{cases} \tag{4.1}$$

London Journal of Research in Science: Natural and Formal

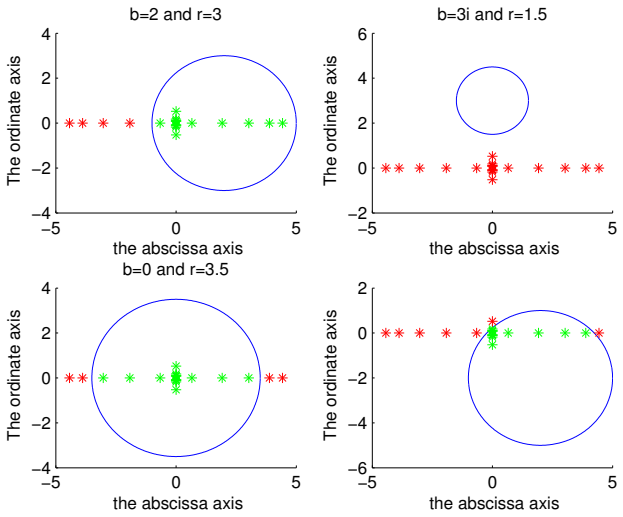

Figure 1: Partition of the spectrum of the matrix pencil$zB - A$ by the off-center circle with center with affix $z0$.

Table 1: Traces, norms and quality of the spectral projector $\mathbb{P}_0$ by applying Algorithm 3.1 for four values of the couple (b, r)

(b, r)	$tr(\mathbb{P}_0)$	$\|\mathbb{P}_0\|$	$\|\mathbb{P}_0^2 - \mathbb{P}_0\|$	$\|\mathbb{P}_0 W - W\mathbb{P}_0\|$	$\|\mathbb{H}_0\|$
$(2, 3)$	16	$1.9428\ 10^{04}$	$4.4207\ 10^{-10}$	$4.9178\ 10^{-7}$	$6.5654\ 10^{10}$
$(3i, 1.5)$	0	0	0	0	$4.2800\ 10^{08}$
$(0, 3.5)$	16	$1.9089\ 10^{4}$	$1.5983\ 10^{-11}$	$4.6416\ 10^{-6}$	$6.6210\ 10^{10}$
$(2 - 2i, 3)$	13	$2.1814\ 10^{4}$	$5.3396\ 10^{-9}$	$3.3987\ 10^{-7}$	$8.8018\ 10^{10}$

Table 2: Traces, norms and quality of the spectral projector$\mathbb{P}_\infty$by applying Algorithm 3.2 for values $a, b, z0$

.

$(a, b, z0)$	$tr(\mathbb{P}_\infty)$	$\|\mathbb{P}_\infty\|$	$\|\mathbb{P}_\infty^2 - \mathbb{P}_\infty\|$	$\|\mathbb{P}_\infty W - W\mathbb{P}_\infty\|$	$\|\mathbb{H}_\infty\|$
$(6, \sqrt{(3)}, 1)$	20	1	$7.7410\ 10^{-14}$	$2.8899\ 10^{-12}$	$1.3900\ 10^{8}$
$(2, \sqrt{(2)}, i)$	11	$2.3358\ 10^{4}$	$1.5964\ 10^{-7}$	$1.0407\ 10^{-6}$	$5.0865\ 10^{10}$
$(4, 1, 1 - i)$	5	$1.6850\ 10^{4}$	$5.4046\ 10^{-7}$	$2.8924\ 10^{-6}$	$3.9620\ 10^{11}$
$(3, 1.2, 2 + 2i)$	0	$3.0725\ 10^{-8}$	$3.0725\ 10^{-8}$	$1.4260\ 10^{-7}$	$1.9655\,10^{9}$

Table 3: Traces, norms and quality of the spectral projector$\mathbb{P}$ by applying Algorithm 3.3 for four values p, b and d.

(p, b, d)	$tr(\mathbb{P})$	$\|\mathbb{P}\|$	$\|\mathbb{P}^2 - \mathbb{P}\|$	$\|\mathbb{P}W - W\mathbb{P}\|$	$\|\mathbb{H}\|$
$(2, 0, 10)$	20	1	$4.8955\ 10^{-13}$	$1.0086\ 10^{-12}$	$4.2198\ 10^{6}$
$(1.5, 3, 1)$	16	$2.7889\ 10^{-8}$	$2.7889\ 10^{-8}$	$2.0312\ 10^{-8}$	$1.7304\ 10^{10}$
$(1, 4, 1)$	0	$3.5172\ 10^{-9}$	$3.5172\ 10^{-9}$	$2.6957\ 10^{-8}$	$3.5087\ 10^{8}$
$(3, 2, 3)$	3	$1.8947\ 10^{4}$	$1.4058\ 10^{-7}$	$1.3711\ 10^{-7}$	$9.0937\,10^{11}$

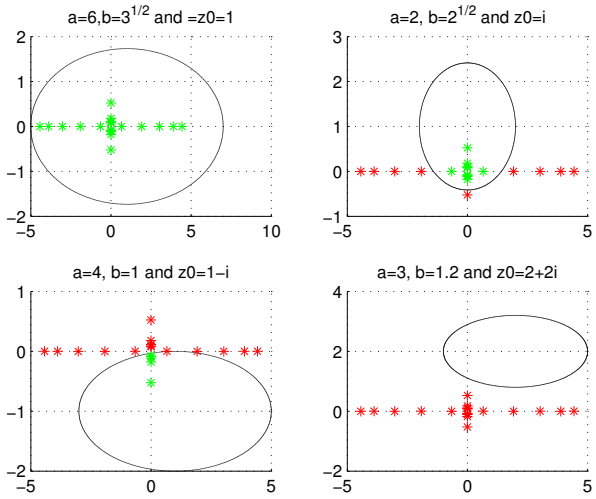

Figure 2: Partition of the spectrum of the matrix pencil $zB - A$ by the off-center ellipse with center with affix $z0$ and parameters a and b.

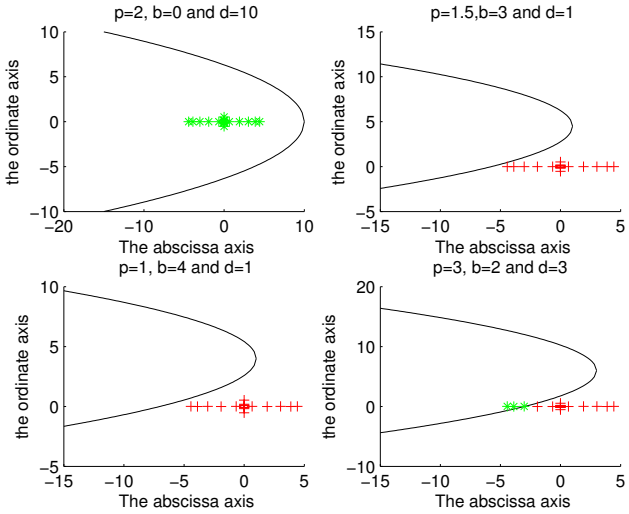

Figure 3: Partition of the spectrum of the matrix pencil $zB-A$ by the parabola of equation $2p(d-x) = y^2$.

The graphs above effectively show a dichotomy of the spectrum of the matrix pencil by the various curves which are the circle, the ellipse and the parabola all not centered at the origin. To corroborate our algorithms, we give in tables, the values of the norms of the projector $\mathbb{P}$ and of the norm of the dichotomy matrix $\mathbb{H}$.

We note that the values taken by the norms of the projector $\mathbb{P}$ and of its dichotomy criterion $\mathbb{H}$ are high . This is due to the fact that the matrices A and B are badly conditioned ($\kappa(A) = 2.836310^3$ et $\kappa(B) = 3.253410^4$ where $\kappa(A) = \|A\|.\|A^-1\|$).

Example 4.2 *Consider the matrices*

$$A = \begin{bmatrix} 0.49 & 0.89 & 0.33 & 0.32 & 1.09 & -0.01 \\ 1.03 & -1.15 & -0.75 & 0.31 & 1.11 & 1.53 \\ 0.73 & -1.07 & 1.37 & -0.86 & -0.86 & -0.77 \\ -0.30 & -0.81 & -1.71 & -0.03 & 0.08 & 0.37 \\ 0.29 & -2.94 & -0.10 & -0.16 & -1.21 & -0.23 \\ -0.79 & 1.44 & -0.24 & 0.63 & -1.11 & 1.12 \end{bmatrix}, \quad B = \begin{bmatrix} 5 & 1.5 & 0 & 0 & 1 & 0 \\ 0 & 4 & 1 & 1 & 0 & 1 \\ 0 & 1 & 3 & 1 & 0 & 0 \\ 1 & 0 & 0 & 2 & 1 & 1 \\ 1 & 1 & 0 & 0 & 2 & 1 \\ 1 & 0 & 0 & 0 & 0 & 1 \end{bmatrix} \tag{4.2}$$

with matrix B a no singular matrix.

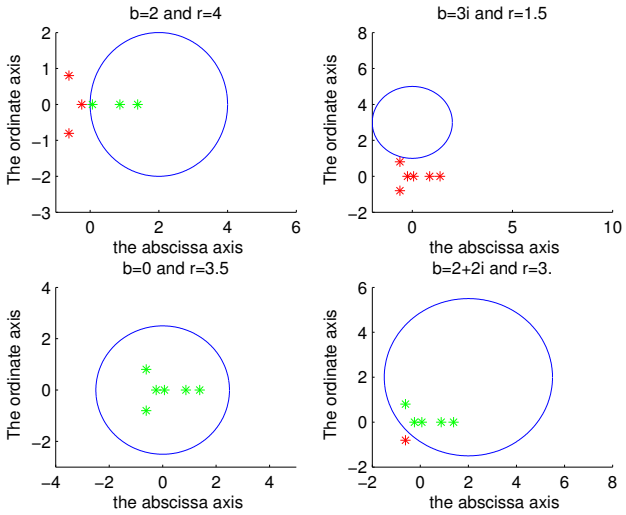

Figure 4: Partition of the spectrum of the matrix pencil$zB - A$ by the off-center circle with center with affix $z0$.

Table 4: Traces, norms and quality of the spectral projector $\mathbb{P}_0$ by applying Algorithm 3.1 for four values of the couple (b, r)

(b, r)	$tr(\mathbb{P}_0)$	$\|\mathbb{P}_0\|$	$\|\mathbb{P}_0^2 - \mathbb{P}_0\|$	$\|\mathbb{P}_0 W - W\mathbb{P}_0\|$	$\|\mathbb{H}_0\|$
$(2, 4)$	6	1	$3.1317\ 10^{-16}$	$4.4730\ 10^{-16}$	1.3256
$(3i, 1.5)$	0	0	0	0	0.4696
$(0, 3.5)$	6	1	$3.4282\ 10^{-16}$	$7.9911\ 10^{-16}$	1.2442
$(2 + 2i, 3)$	4	1.8397	$5.8237\ 10^{-16}$	$4.3141\ 10^{-15}$	68.5791

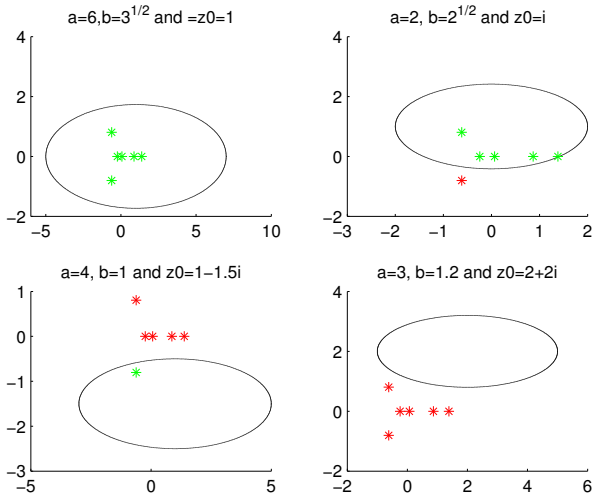

Figure 5: Partition of the spectrum of the matrix pencil$zB - A$ by the off-center ellipse with center with affix $z0$ and parameters a and b.

Table 5: Traces, norms and quality of the spectral projector$\mathbb{P}_\infty$by applying Algorithm 3.2 for values $a, b, z0$.

$(a, b, z0)$	$tr(\mathbb{P}_\infty)$	$\|\mathbb{P}_\infty\|$	$\|\mathbb{P}_\infty^2 - \mathbb{P}_\infty\|$	$\|\mathbb{P}_\infty W - W\mathbb{P}_\infty\|$	$\|\mathbb{H}_\infty\|$
$(6, \sqrt{(3)}, 1)$	6	1	$6.6926\ 10^{-16}$	$8.9554\ 10^{-16}$	0.1147
$(2, \sqrt{(2)}, i)$	5	1.7637	$8.2272\ 10^{-16}$	$8.3327\ 10^{-15}$	17.3309
$(4, 1, 1 - 1.5i)$	1	1.7637	$1.1051\ 10^{-15}$	$8.9629e - 15\ 10^{-15}$	0.3607
$(3, 1.2, 2 + 2i)$	0	$1.8846\ 10^{-15}$	$1.8846\ 10^{-15}$	$3.9832\ 10^{-15}$	0.3056

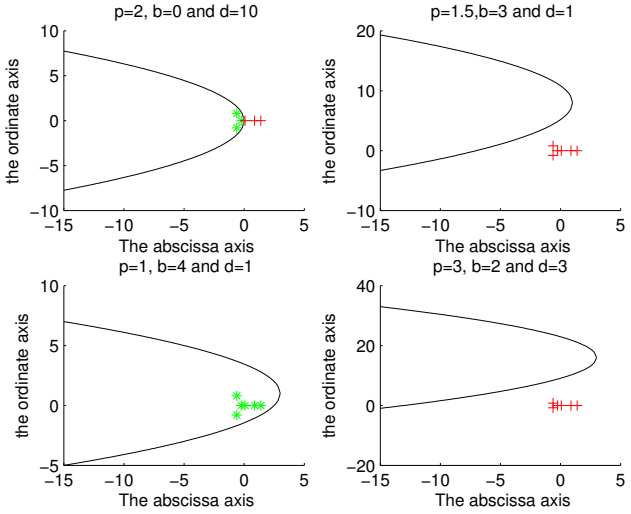

Figure 6: Partition of the spectrum of the matrix pencil$zB - A$ by the parabola of equation $2p(d - x) = y^2$.

Table 6: Traces, norms and quality of the spectral projector $\mathbb{P}$ by applying Algorithm 3.3 for four values p, b and d.

(p, b, d)	$tr(\mathbb{P})$	$\|\mathbb{P}\|$	$\|\mathbb{P}^2 - \mathbb{P}\|$	$\|\mathbb{P}W - W\mathbb{P}\|$	$\|\mathbb{H}\|$
$(2, 0, 10)$	6	1	$4.5305e-16\ 10^{-16}$	$3.9732\ 10^{-16}$	1.4152
$(1.5, 3, 1)$	0	$5.0943\ 10^{-15}$	$5.0943\ 10^{-15}$	$4.8198\ 10^{-15}$	1.3944
$(1, 4, 1)$	0	0	$2.6692\ 10^{-15}$	$6.6636\ 10^{-15}$	1.2688
$(3, 2, 3)$	0	$5.5735\ 10^{-15}$	$5.5735\ 10^{-15}$	$8.3372\ 10^{-15}$	8.7003

The graphs above effectively show a dichotomy of the spectrum of the matrix pencil by the various curves which are the circle, the ellipse and the parabola all not centered at the origin. To corroborate our algorithms, we give in tables, the values of the norms of the projector $\mathbb{P}$ and of the norm of the dichotomy matrix $\mathbb{H}$.

We can notice that the values of the norm of $\mathbb{H}$ are small. This proves the very good quality of the dichotomy carried out

V. CONCLUSION

After a few reminders on methods of spectral dichotomy of a pencil matrix with respect to a circle, an ellipse or a parabola all not centered at the origin and/or not symmetrical with respect to the abscissa axis, we presented, by making changes of variables, methods of spectral dichotomy of a pencil matrix with respect to an off-center circle, an off-center ellipse or any parabola. In the spectral dichotomy method of a pencil matrix $zB - A$ with respect to

- a circle $\mathcal{C}(\Omega, r)$, $(r > 0)$ not originally centered, by considering the change of variable $\mathcal{A} = A - bB$, we obtain projector $\mathbb{P}_0$ on the invariant space of the pencil matrix corresponding to the eigenvalues inside the circle and a Matrix $\mathbb{H}$ whose the norm indicates the quality of the projector, by applying the spectral dichotomy method of the pencil matrix $zB - \mathcal{A}$ with respect to the circle $\mathcal{C}(O, r)$ centered at the origin.
- an ellipse Ξ_{z_0} centered at a point $z_0 \neq 0$, by considering the change of variable $A_0 = A - z_0 B$, we obtain the projector $\mathbb{P}_\infty$ on the right invariant space of $zB - A$ corresponding to the eigenvalues outside the ellipse Ξ_{z_0} and a Matrix $\mathbb{H}$ whose the norm indicates the quality of the projector, by applying the spectral dichotomy method of a pencil matrix $zB - A_0$ with respect to the ellipse Ξ_0 centered at the origin.
- any parabola Γ of equation $2p(d - x) = (y - p\tilde{b})^2$ with $p > 0$, by considering the change of variable $A_{db} = A + \left(\frac{p}{2} - d - ip\tilde{b}\right) B$, we obtain $\mathbb{P}$ on the right subspace of $zB - A$ associated with the eigenvalues outside the parabola and a Matrix $\mathbb{H}$ whose the norm indicates the quality of the projector, by applying the spectral dichotomy method of a pencil matrix $zB - A_{db}$ with respect to the parabola $2p\left(\frac{p}{2} - x\right) = y^2$ studied by Malyshev and Sadkane.

Numerical tests on two examples of matrices pencils show that the presented methods compute well the projectors if there are no eigenvalues on or in a close neighborhood of the figures.

REFERENCES

1. A Ya Bulgakov. Generalization of a matrix Lyapunov equation. (Russian) Sibirsk. Mat. Zh., 30(4)(1989)30_39.
2. A. Ya. Bulgakov and S. K. Godunov, Circular Dichotomy of the Spectrum of a Matrix, Siberian math. J., (29)(1988)734-744.

3. M.Dosso, Sur quelques algorithms d'analyse de stabilité forte de matrices symplectiques, PHD Thesis, Université de Bretagne Occidentale. Ecole Doctorale SMIS, Laboratoire de Mathématiques, UFR Sciences et Techniques, (2006).
4. M. Dosso, & M. Sadkane, On the strong stability of symplectic matrices, Numerical Linear Algebra with Applications, 20(2013) 234-249.
5. M. Dosso, N. Coulibaly and L. Samassi, Strong stability of symplectic matrices using a spectral dicotomy method, far East Journal of Applied Mathematics. Vol. 79, (2)(2013) 73-110.
6. S.K. Godunov, The problem of dichotomy of the spectrum of a matrix, Sib. Mat. Zh., 26, (5)(1986) 25-37.
7. S. K. Godunov, spectrum dichotomy and stability criterion for sectorial operators, Siberian Mathematical Journal, Vol. 36, (6)(1995) 1328-1335.
8. S. K. Godunov and M. Sadkane, Some new algorithms for the spectral dichotomy methods, Linear Algebra and its Applications, 358(2001) 173-194.
9. S. K. Godunov and M. Sadkane, Elliptic Dichotomy of a Matrix Spectrum, linear algebra and its Applications, 248 (1996) 205-232.
10. S. K. Godunov and M. Sadkane, Spectral analysis of symplectic matrices with application to the theory of parametric resonance, SIAM Journal on Matrix Analysis and Applications, vol. 28, (4)(2006) 1083-1096.
11. A N Malyshev. Calculation of invariant subspaces of a regular linear matrix pencil. (Russian) Sibirsk. Mat. Zh., 30(4)(1989)76_86.
12. A N Malyshev, Guaranted Accuracy in Spectral Problems of Linear Algebra. Siberian Adv. Math. J.I,II.2 (1992) 144-197.
13. A. N. Malyshev, Parallel algorithm for solving some spectral problems of linear algebra, Linear Algebra Appl. (1993)188_189:489_520.
14. A.N. Malyshev, M. Sadkane, On parabolic and elliptic spectral dichotomy. SIAM J. Matrix Anal. Appl.18(2)(1997) 265-278.
15. Yu. M. Nechepurenko, Integral Criteria for the Quality of the Dichotomy of a Matrix Spectrum by a Closed Contour, Mathematical Notes, vol. 78, (5)(2005)669_676. Translated from Matematicheskie Zametki, vol. 78, (5)(2005)718_726.
16. M. Sadkane and A. Touhami, On modi_cation to the spectral dichotomy algorithm. Numerical functional Analysis and optimization, 34(7)(2013)791-817.
17. M. Sadkane and A. Touhami, Algorithm 918:spedicho: A MATLAB program for the spectral dichotomy of regular matris pencils, ACM trans. Math. Softw. 38, 3, Article 21 (April 2012).
18. M. Traoré, Méthodes de dichotomie spectrale d'une matrice par rapport à quelques _gures, PHD Thesis, Université Felix Houphoüet-Boigny , Laboratoire de Mathématiques et Applications, UFR Mathématiques et Informatiques, (2023).
19. S. Traoré and M. Dosso, Spectral dichotomy methods of a matrix with respect to the general equation of the parabola, European Journal of Pure and Applied Mathematics. Vol 15, (2)(2022)681-725.
20. S. Traoré, M. Dosso and L. Samassi, Method of spectral dichotomy of a matrix with respect to a circle or an ellipse not centered at the origin, International Journal of Numerical Methods and Applications. Vol 22, (2022) 87-115.

Mapping of Groundwater Potential Zones for Gudumadanahalli Village using Remote Sensing and GIS

Girish P, K.J. Suresha, B.S. Shilpa, Poojashree B P & P. C. Srinivasa

University of Mysuru

ABSTRACT

Drought is a serious problem in Karnataka, which is predominantly a 60 to 70% dry farming state. The development of any micro, mini, sub, or watershed area using a different approach is only the key solution, and it is no longer a secret. The village of Gudumadanahalli is separated into sections depending on the origin and flow direction of water drains / streams. Water harvesting and drainage line treatment buildings were discovered using a study of topo-sheet and LANDSAT images of the region, as well as other parameters such as soil type, slope type, land use / cover, waste lands, hydro-morphology, forest cover, command area, and so on. Prioritization is important in identifying groundwater potential that requires immediate attention so that it can be developed with available resources. An attempt has been made to prioritise the study area based on several criteria, with the total weightage of marks given in the table. Data for these criteria were generated using remote sensing, GIS, and other resources. The study also demonstrates that when remote sensing and GIS are used in tandem, they provide ample scope for the integration of spatial and non-spatial data, which can be successfully used to prioritise any of the watersheds in a more scientific and unbiased manner.

Keywords: NA

Classification: LCC: QC879.5

Great Britain Journals Press

LJP Copyright ID: 925652
Print ISSN: 2631-8490
Online ISSN: 2631-8504

London Journal of Research in Science: Natural and Formal

Volume 23 | Issue 15 | Compilation 1.0

Mapping of Groundwater Potential Zones for Gudumadanahalli Village using Remote Sensing and GIS

Girish P[α], K.J.Suresha[σ], B.S.Shilpa[ρ], Poojashree B P[ↀ] & P. C. Srinivasa[¥]

ABSTRACT

Drought is a serious problem in Karnataka, which is predominantly a 60 to 70% dry farming state. The development of any micro, mini, sub, or watershed area using a different approach is only the key solution, and it is no longer a secret. The village of Gudumadanahalli is separated into sections depending on the origin and flow direction of water drains / streams. Water harvesting and drainage line treatment buildings were discovered using a study of topo-sheet and LANDSAT images of the region, as well as other parameters such as soil type, slope type, land use / cover, waste lands, hydro-morphology, forest cover, command area, and so on. Prioritization is important in identifying groundwater potential that requires immediate attention so that it can be developed with available resources. An attempt has been made to prioritise the study area based on several criteria, with the total weightage of marks given in the table. Data for these criteria were generated using remote sensing, GIS, and other resources. The study also demonstrates that when remote sensing and GIS are used in tandem, they provide ample scope for the integration of spatial and non-spatial data, which can be successfully used to prioritise any of the watersheds in a more scientific and unbiased manner.

Author α: Department of civil engineering Vidyavardhaka college of Engineering, Mysuru.
σ: Department of studies. Earth science, University of Mysuru, Manasagangotri, Mysuru.
ρ: Department of Civil engineering Vidyavardhaka college of Engineering, Mysore.
ↀ: Research Scholar, Department of Marine Geology, Mangalore University.
¥:: Department of Civil Engineering, govt. engineering college, Kushal nagar.

I. INTRODUCTION

Groundwater is a highly valued natural resource that promotes human health while also being cost-effective for development and ecological variety. Groundwater is a type of water that fills all of the gaps in a geological section. Water-bearing formations in the earth's crust serve as transmission routes as well as reservoirs for storing water. In India, 80 to 90 percent of the rural population and about 30 to 40 percent of the urban population rely on groundwater for domestic needs (A.A. Akinlalu *et al. 2017,* Krishnamurthy et al., 1996, Suresha and Taj.,2019, Suresha and Jayashree 2019. Groundwater is a geological formation that exists under the Earth's surface in the pore spaces and cracks of rocks and sediments. The extent of exploitation is essentially determined by the creation of porosity. High relief and steep slopes promote drainage, but topographic depressions improve infiltration. When compared to a low density region, a higher drainage density area increases surface runoff. Surface water bodies include streams, tanks, check dams, and ponds. This serves as the study area's recharging ground water potential zone (Murugesan et al.,2012, Ramya et al., 2019 and Suresha et al 2014).

Certain key characteristics of groundwater, including temperature huge and non-predictability, very good limited vulnerability, lower development expense, and drought dependability, have exposed its

London Journal of Research in Science: Natural and Formal

impertinence as the single trustworthy provide of water for any weather conditions. 2005, Todd and Mays Heath, R. (2004) Freeze, R., and Cherry, J. (1987) B. M. Hussien, A. S. Fayyadh 1996 William, M., Thomas, E., and Franke, O. (1999)), it is able to be tapped when necessary and is less affected by cartotropic processes (Manap et al 2013 According to the crucial Central Groundwater Department, roughly 85 percent of rural, 50 percent urban, and 65 percent irrigated water demands are met with the help of groundwater throughout the country. Thus, groundwater depletion is a critical issue due to population growth, increasing demand, and limited availability in the last 35 to 40 years across a big portion of India, particularly in the states of Karnataka, Tamil Nadu, Andhra Pradesh, Punjab, Rajasthan, and many others. Unscientific research of floor water growing water pressure situation has resulted from some of the importance of developing groundwater based largely on availability want. This disquieting state of affairs requires a fee and time powerful techniques for proper evaluation of groundwater belongings and management making plans.

Remote sensing (RS) is an emerging technology. It is a very advanced instrument for handling, discovering, analysing, and managing essential groundwater resources (Krishnamurthy and Venkatesesa, 1996, Sabins, 1997; Sander, 1997; Teevw, 1999; Singh and Prakash, 2003; Sikdar et al., 2004, Kusky and Gad, 2006; Sultan et al., 2008; Dinesh kumar et al., 2007). GIS has evolved into a standard and necessary instrument for controlling geographic information in the discovery, development, and management of the earth's resources. ArcGIS software works with data on geographical patterns or features, as well as their properties. It is a higher level computer coded map that allows for the storing, selected dedicated modification, display, and output of geographic information. Remote sensing and geographic information system integration has shown to be efficient, quick, and cost effective. This approach generates useful data on geology, geomorphology, lineaments, and slope, as well as a systematic integration of these data for groundwater potential zone study.

II. STUDY AREA

The present work has been carried out for the village of Gudumadanahalli Fig.1 is located in Mysore taluk of Mysore district in Karnataka, India. It is situated 3 Kms away from Mysore, which is both district & sub-district headquarters of Gudumadanahalli village. As per 2009 stats, Hosahundi is the gram panchayat of Gudumadanahalli village (Fig.1 and 2). The total area of village is 179.71 hectares. Gudumadanahalli has a total population of 850 people. Among this, Net shown area of 179.71 ha, Total Un-irrigated land of 118.35 ha and Total irrigated area of 27.24 ha (Table 3.1). As per 2019 stats, Gudumadanahalli village comes under Varuna assembly & Chamarajanagar parliamentary constituency. have another problem. There, drinking water sources have dried up, as water table has depleted by a great extent. Many villages nested at the foot of the Western sides. On one side of the village, greenery abounds. But inside the village, land that has turned dry, plants and trees which have withered due to strong sunshine, dried wells and bore wells have made the people to hanker for water that has vanished. Study is a progressively converting into an urban area. As result of rapid urbanization the demand of water is increasing day by day. Main objectives of the study are as follows:

- Identify the underground water potential zones and problematic areas for underground water harvesting.
- Mapping of freshwater potential zone using spatial and non-spatial methods.
- Supply and securing of clean and sufficient drinking water for the population.

Fig. 1: Boundary of study area

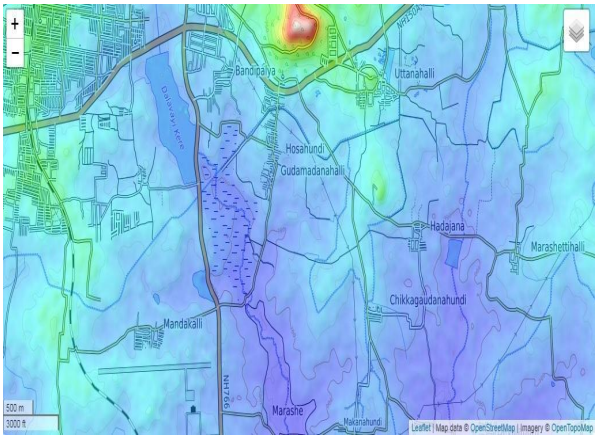

Fig. 2: Toposheet of study area

III. METHODOLOGY

The current research field is comprised of four primary components. It entails gathering data from satellites, analysing topo sheets, creating maps, and making extensive use of supplementary data. PAN and LISS collect satellite data from a specific source. Topo sheet data are utilised as the basis map, which serves as the backdrop for a map. It comes from the Geological Survey of India. Thematic maps are used to collect information about the current research region, such as soil type, slope of the area, rainfall data, geology, and geomorphology. These maps are submitted to supervised classification, and the characteristics for the ARC map are generated. Generated these thematic maps are overlaid using weighted overlay analysis in spatial analyst tools to obtain the final groundwater prospect map of study area.

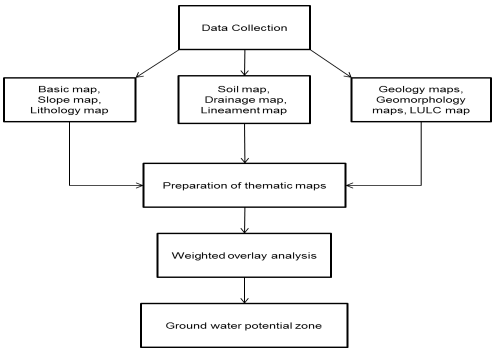

Figure 3: Methodology

IV. PRIORITIZATION OF SUB WATERSHED

Some of the restricted resources, if not adequate to handle the research field in a timely manner Prioritization of watersheds is important in identifying any micro watershed or specific region that requires immediate attention or action plan that can be taken of development with available resources. This also makes it easier to address the problematic areas and find appropriate solutions. Because it involves an integrated approach, the resources-based approach is found to be realistic of watershed prioritization. An attempt was made to prioritization of Gudumadanahalli village was done based on several criteria like soil, rainfall, slope, wasteland, irrigated area. Based on this analysis, we found the scores in table thus the study also proves that remote sensing and GIS when synergistically used provide ample scope for the integration of spatial and non-spatial data can

successful adopted to prioritization the Gudumadanahalli village in more scientific and unbiased manner.

V. RESULTS

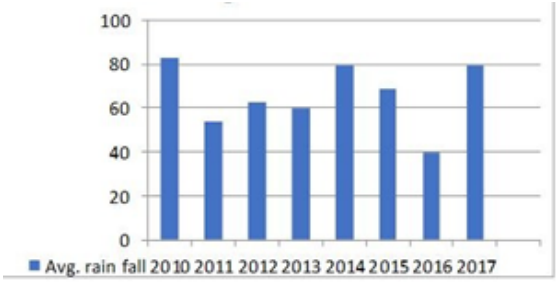

Fig. 4: Rainfall data of Gudumadanahalli

The average rainfall in Mysore Taluk is 776.7 to 780 mm. The district has 53 wet days on average, with the southwest monsoon accounting for almost half of the annual rainfall (Fig. 4). Rainfall tends to decrease from west to east. The coefficient of variation ranges from roughly 30% in the west to over 35% in the east, indicating that rainfall is more constant in the west than in the east. Pre-monsoon rainfall is more reliable than post-monsoon rainfall. The southwest monsoon was normal from 1994 to 1999, but excessive in 2012, and the northwest monsoon is significantly better compared to being excessive to normal in recent years. Annually, there are more normal to exceptional rainfall years than deficient years. While the district had excessive rainfall in 2014 and 2016, Rainfall was typical in 2010, 2011, and 2012, with the exception of 2006 and up to the present. In April, the average minimum and maximum temperatures range from 34 to 21.4°C to 16.4 to 28.5°C in January. The relative humidity ranges from 21 and 84 percent.

5.1 Lithology Map

The current research investigation identifies two kinds of rocks: Chamundi granite and tonaltic gneiss. Tonaltic gneiss dominates the region of approximately 34051 m2 (Fig. 6 and 5). Granite intrusion is frequent in the 750 Ma ancient landscape, according to Janardhan et al. (1978). (Srikantappa et al.,1992). Pink granite bodies abound from Chamundi hill onward. The rocks are pink and grey granite geologically, depending on the materials present. When compared to the surrounding peninsular Gneissic rocks of Sargur-kabbal durga, these youngest igneous rocks (0.8 billion years old) are the result of recent volcanic activity (3 billion years old) (Gazetteer., 1988, Srikantappa and Prakash Narasima., 1992). The entire tract areas around is essential made upto of a tract of pinkish granite. It is an igneous rock made with combination of plagioclase feldspar with quartz. The different types of rocks (Gneiss), Fig.5. and its area have been depicted in the Table 3.

Table 3: Lithology of the study area

Sl. No	Type of rock	Area (m2)
1	Chamundi Granite	850
	Migmatities and Granodiorite – Tonalitic gneiss	34051

Fig.5: Tonalitic Gneiss

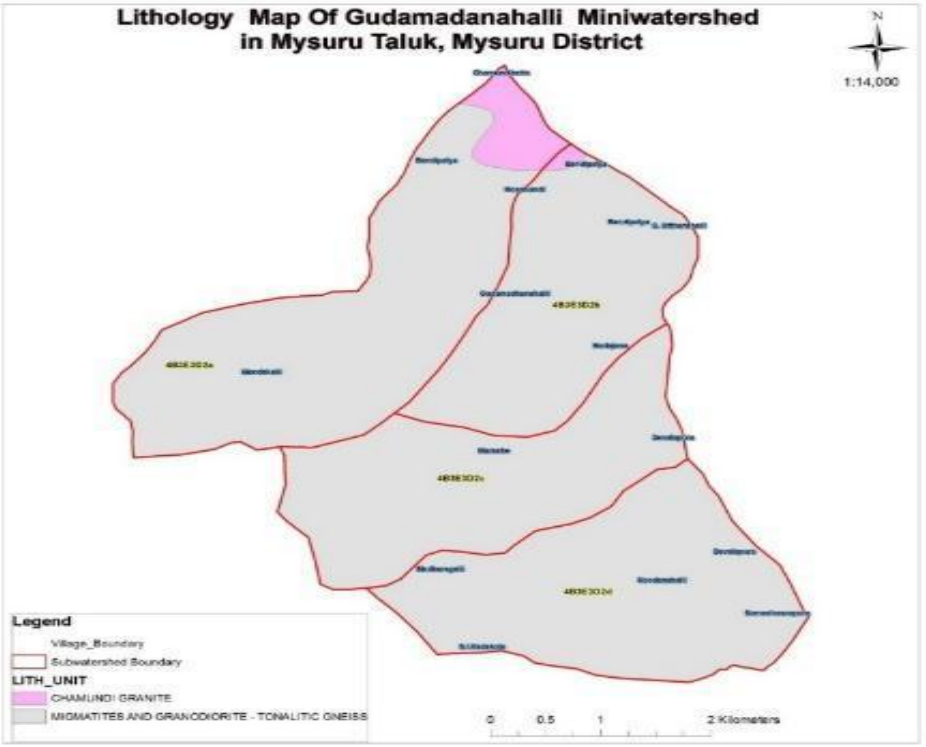

Figure 6: Lithology map of Gudumadanahalli

5.2 Lineament map

A lineament is a landscape feature that is a linear manifestation of an underlying geological structure, such as a fault. A lineament is typically depicted as a fault-aligned valley on geological or topographic maps, and it is visible on aerial or satellite pictures, as seen in Fig.1. Lineaments are the primary conduits of freshwater in impermeable rocks all around the world. Indeed, the fracture planes form the useful void volume, which corresponds to the potential space that water can occupy in such a medium. The aperture, positioning, interconnection, and direction of fracture planes all have an effect on the occurrence and flow of underground water supplies in broken aquifers. As a result, zones with open, regular, and jointed fractures can be favorable for water occurrences. The majority of the lineaments in the region follow the pattern of stream courses. Lineaments are concerned with high porosity and hydraulic conductivity zones (Subba Rao and Prathap, 1999; Subba Rao et al., 2001and Pojashree et al., 2021) Normalized transmissivity is elevated near the lineaments, and there is an outstanding association between higher fracture densities and higher well yields (Magowe and Carr, 1999). In general, the thickness of weathered/fractured rock is supposed to be greater along the lineaments, and hence the lineaments are thought to have a control on the supply of underground water (Fig.75). The fractures and lineaments are important in rocks where secondary permeability and porosity dominate. Some fracture lines / linear features are observed in study area. Lineaments are fracture lines / linear features formed by tectonic action that represent a general surface manifestation of underground fractures with inherent porosity and permeability characteristics of the underlying

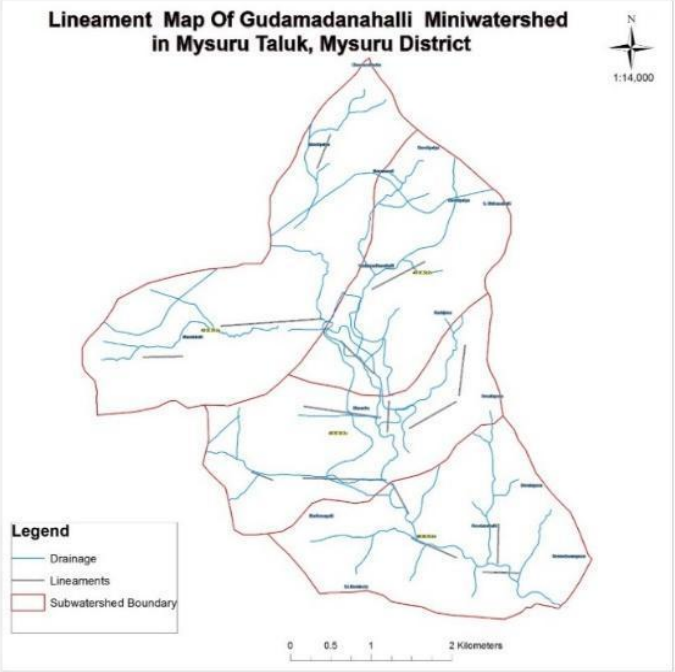

Fig. 7: Lineament of Gudumadanahalli materials

5.3. Soil Map

Soil map In Gudumadhanahalli, Mysuru taluk, soil consisting of different types based on soil profile available (Fig.8& 9) and considering one gram panchayats, the soil analysis made for the profile analysis. Soil maps (Fig.8) were originally produced by field surveys and Mapping using software techniques such as aerial photography and satellite-based. Image analysis and Global Positioning Systems (GPS), for ground truth verification and collection of soil samples for analysis of engineering parameters for the resources development Fig.9 and 10. Soil map is a map is a geographical representation showing diversity of soil types and soil properties like soil textures, soil pH in the area of interest. Varied soils have different reflectance, resulting in a distinct colour. These colours are examined and compared to existing charts. The loamy skeletal soil found near the riverbanks dominates the majority of the study region. Soil ranking is linked to infiltration capability, which is determined by soil thickness and grain size (permeability). Fine-grained soils have lower permeability than coarse-grained soils. Meanwhile, clay is categorised as poor because to its poor drainage, sluggish permeability, severe erodibility, and low hydraulic conductivity. The geological research of the area has been divided into five groups, each with its own geographic extent, as shown in Table 4.

Table 4: Lithology of the study area

Sl. No	Type of soil	Area (m^2)
1	Clayey skeletal	2644.11
2	Loamy skeletal	14587.94
3	Habitation mask	1968.00
4	Water body mask	280.00
5	Fine soil	15421.00

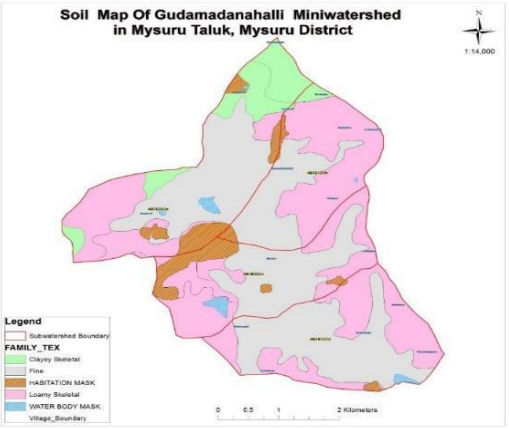

Figure 8: Soil map of Gudumadanahalli

Fig. 9: Loamy skeletal

Fig. 10: Fine soil

5.4 Geomorphology

The geomorphology of a region was determined by the structural development of the geological formation. It reflects varied landforms and structural characteristics. The map is generated using a visual interpretation of Landsat TM and IRS LISS - III data on a 14000 scale, as well as the research area's geo-hydrology characteristics. Various geomorphological units have been delineated using photo geology features such as tone, texture, form, size, and association. Denudation hills, pediplains, and water body masks are the geomorphologic features. The figure depicts a geomorphology map. 11. A pediplain is a large and generally flat rock surface created by the connecting of many pediments, and is considered the final step of landform evolution caused by erosion processes. The categories of the geomorphological study of the area are depicted in the Table 6.

Denudation hill:-Covers an area of about 842 m^2. A group of massive hills with resistant rock bodies, with medium to high relief. These are characterised by high topography and high surface runoff zones where the rate of infiltration is low or negligible with poor groundwater prospects.

Table 6: Geomorphology of the study area

Sl. No	Description	Area (m^2)
1	Denudational hills	842.00
2	Pediplain	33779.00
3	Water body	280.00

5.4.1 Pediplain

A pediment, as the name indicates, is a feature that frequently occurs at the base of a mountain. Pediments resemble gently undulating plains with a gentle slope. The pediment is a low-sloped terrestrial erosional foot slope surface that lacks significant relief in all directions. Any lineaments or cracks may allow for some movement of groundwater potential. The pediments form because of weathering in dry and semi-arid environments, representing the last stage of cyclic erosion. A pediment is developed because of a combination of activities such as stream erosion, weathering, sheet wash, and lateral planting. When sediment accumulates across a vast area as a consequence of a continuous process of pedimentation, this is referred to as a Pediplain. Pediplain is seen on large portion of basin with an aerial extent of 33779 m^2 m^2. Most of the study area is constituted by pediplain and groundwater potential is very good to moderate in this region.Water mask:-Surface water bodies like river, ponds, etc., can act as recharge zones, enhancing the groundwater potential in the neighbourhood.

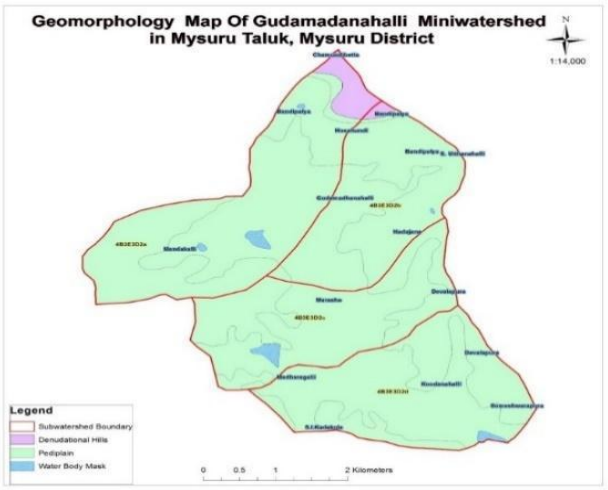

Figure 11: Geomorphology map of Gudumadanahalli

5.5 LU / LC map

Land Use and Land Cover (LULC) data files describe plant, water, natural surface, and cultural elements on land surfaces. Remote sensing (LISS IV) gives good information on the geographical distribution of plant types and land use data (Fig.12), which is important in the development of groundwater resources. It regulates numerous hydrogeological processes in the water cycle, including infiltration, evapotranspiration, and surface runoff. Surface cover roughens the surface, reducing discharge and increasing infiltration. The volume, timing, and recharging of the groundwater system are also affected by LULC. Croplands and forests, both in terms of land use, are ideal locations for groundwater investigation. Infiltration will be greater and discharge will be less in forest regions. Meanwhile, in urban areas or built-up terrain, the rate of infiltration is low due to reduced recharging of the groundwater regime caused by aquifer inhibition. A revised categorization of the study area reveals that agricultural land accounts for the majority of land use, occupying an area of 3134 m2. (Table .7).

Table 7: LULC of the study

SL.No	Type of Land	Area in m²
1	Agriculture Land	31364
2	Built up land	2025
3	Forest	872
4	Waste lands	360
Water bodies	Water bodies	280

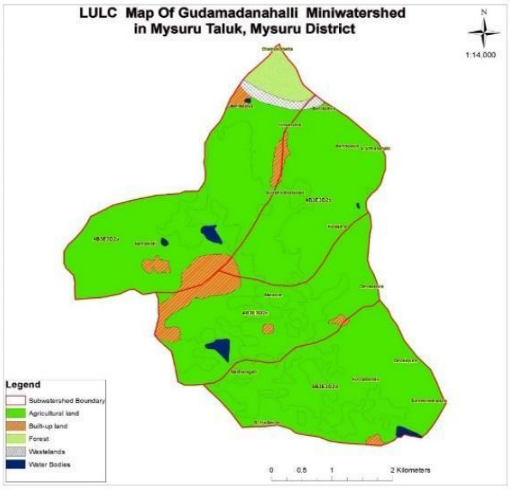

Fig. 12: LULC map of Gudumadanahalli

5.6 Slope map

Slope is the elevation variation of a surface and the primary determinant of superficial water flow since it influences the gravity impact on water movement. To create the slope map, first extract the elevation contours at 20 m intervals from the topographic sheet (Fig.13). Table 8 shows how the research region was developed using contours generated from SOI Topographical data.

Table 8: Slope gradient and category

Sl. No	Slope Gradient	Slope Category	Area (m²)
1	35 – 50	Steep	583.90
2	10 – 15	Strong	310.26
3	5 – 10	Moderate	541.63
4	3 – 5	Gentle	1805.00
5	1 – 3	Very gentle	20542.09
6	0 – 1	Nearly level	11117.00

Figure 13: Slope Map of Gudumadanahalli

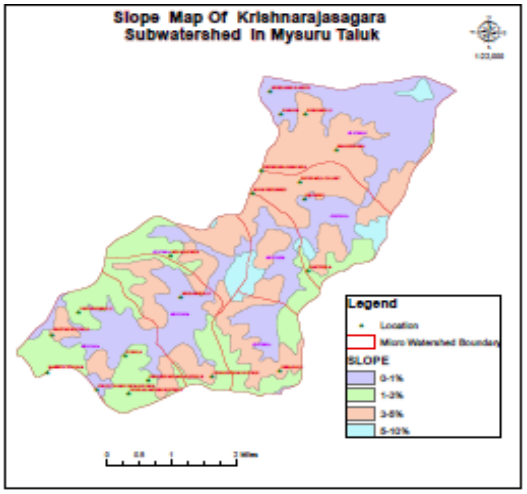

5.74 Drainage map

The drainage map depicts the geographical region where precipitation drains off into creeks, streams, rivers, lakes, and reservoirs. It is a terrain feature that may be recognised on a map by drawing a line along the greatest height between two points. Larger drainage basins flow into smaller drainage basins, which are commonly referred to as watersheds. The stream order was determined using the Strahler technique Fig 14 tables no.9 and 10.

Table 9: Drainage density of the study area

Sl. No	Zones	Km/ K m^2 m^2
1	Sub-watershed 1	1 -1.5
2	Sub-watershed 2	2.5 – 6
3	Sub-watershed 3	1.8 – 2.2
4	Sub-watershed 4	2.2 – 2.9

Table 10: Drainage density category

Sl. No	Km/ K m^2 m^2	Drainage density category
1	0 – 1.2	Very low
2	1.2 – 2.4	Low
3	2.4 – 3.6	Moderate
4	3.6 – 4.8	High
5	4.8 – 6	Very high

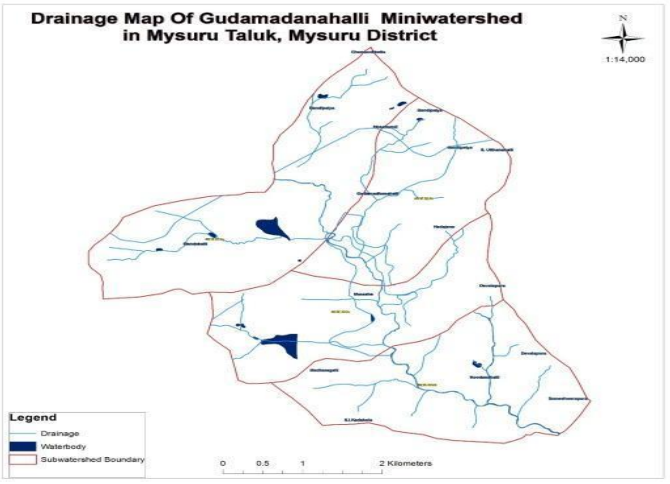

Fig. 14: Drainage map of Gudamadanahalli

5.5 Groundwater prospect map

Groundwater potential zones were defined and categorised as moderate, moderate to poor, poor to nil, and very good to good in Fig.13: Groundwater potential map of GudumadanahalliFig.13 by

integrating all maps (soil, geomorphology, lithology, LULC, slope, drainage, and lineament). The 14184 m2 research area was identified as order potential zone in a few spots with slopes ranging from 1-3 percent to 3-5 percent and 5-10 percent. The 15421-m2 research area was assessed as an excellent good prospective zone with a slope of 0-1 percent. Table 8 displays the many probable zone ranges discovered (Fig.15)

Table 11: Watershed area of the study area

Sl. No	Particulars	Area in
1	Sub-watershed 1	11063.51
2	Sub-watershed 2	7139.38
3	Sub-watershed 3	7889.04
4	Sub-watershed 4	8809.40
5	Total Area	34901.34

Table 12: Groundwater prospect area and classification

Sl. No	Potential zone	Area (m^2)	% Area
1	Moderate	14184.02	40.64
2	Moderate to Poor	838.72	2.40
3	Poor to Nil	302.27	0.87
4	Very good to Good	15421.00	44.18
5	Water Body mask	280.00	0.80

Table 13: Rank and weight for different parameter of groundwater potential zone

Parameter	Classes	Groundwater prospect	Weight	Rank
Geomorphology	Pediplain	Very good		5
	Water body	Good	30	4
	Denudational hills	Moderate		3
Slope classes	Nearly level (0 -1)	Very good		5
	Very gentle (1 -3)	Good		4
	Gentle (3 - 5)	Moderate	20	3
	Moderate (5 -10)	Poor		2
	Strong (10 - 15)	Very poor		1
	Steep (35 - 40)	Very poor		1
Drainage density (Km/ K m ^2)	0 – 1.2	Very poor		1
	1.2 – 2.4	Poor		2
	2.4 – 3.6	Moderate	15	3
	3.6 – 4.8	Good		4
	4.8 - 6	Very good		5
Land use/ Land cover	Agricultural land	Very good		5
	Water bodies	Good		4
	Forest	Moderate	15	3
	Built-up area	Poor		2
	Waste land	Very poor		1
Geology	Migmatites and Granodiorite - Tonalitic gneiss	Very good	5	5
	Chamundi Granite	Poor		1

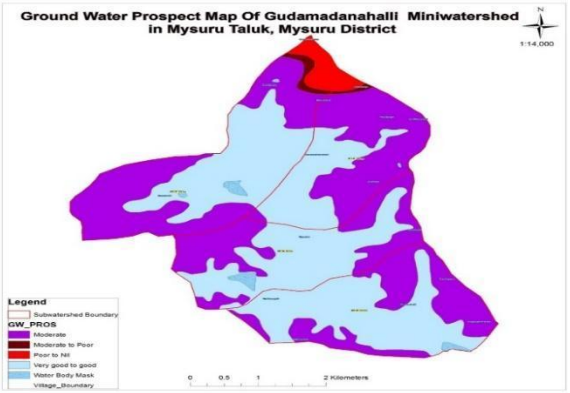

Figure 15: Prospect Map of Gudumadanahalli mini watershed

VI. CONCLUSIONS

The following points might be stated as closing remarks based on the findings of the current study:

From remotely sensed data, thematic maps of the study area such as soil, geomorphology, lithology, lineaments, landforms, and slopes were created. The groundwater prospect map obtained comprises moderate and excellent to good potential zones comprising 14184.02 m2 and 15421 m2 respectively. The modest potential zone consists of an area with a slope of 1-3 percent. The background is made up of loamy-skeletal earth. The area with excellent to decent potential has a 0-1 percent potential, which is practically flat. The beautiful soil serves as the backdrop. Loamy-skeletal soil and fine soil have infiltration rates ranging from 1.2 mm/hr to 3.8 mm/hr. Surface runoff is slower in flat and gently slopped areas, giving rainfall more time to percolate. Check dams and vegetative checks can be built in regions with a slope of 3-5 percent to improve rainwater percolation and boost the region's groundwater recharge capacity.

REFERENCE

1. A.A. Akinlalu *et al.* Application of multi-criteria decision analysis in prediction of groundwater resources potential: a case of Oke-Ana, Ilesa Area Southwestern, Nigeria Nria G J. Astron. Geophys(2017)
2. Krishnamurthy, J.; Venkatesa Kumar, N.; Jayaraman, V., & Manivel, M. (1996). An approach to demarcate groundwater potential zones through remote sensing and a geographical information system. International Journal of Remote Sensing, 17(10): 1867–1884.
3. Suresha KJ and Humera Taj -2019 Groundwater Investigation of Upper Kabini Watershed Using Remote Sensing and GIS Technique, HD Kote Taluk, Mysuru District. J Remote Sens GIS, an open access journal ISSN: 2469-4134 Volume 8 • Issue 2 • 1000265 pp 1-7
4. Suresha KJ and Jayashree TL Demarcation of Groundwater Potential Zones in Devalapura Sub Watershed Mysuru District Using Remote Sensing and GIS . J Remote Sens GIS, an open access journal ISSN: 2469-4134 Volume 8 • Issue 3 • 267 ISSN: 2469-4134 PP 1-6
5. Senanayake, I. P., Dissanayake, D., Mayadunna, B. B. and Weerasekera, W. L. (2015). An approach to delineate groundwater recharge potential sites in Ambalantota, Sri Lanka using GIS techniques. Geoscience Frontiers, 1-10.
6. Suresh KJ (2014) Groundwater Potential Zone Mapping, Using Remote Sensing and GIS Application for Ayyarahalli Sub Watershed, Mysore, District IJETR 2: 114-119.
7. Ramya, R1, Nanthakumaran, A1 and Senanayake, Identification of artificial groundwater recharge zones in vavuniya District using Remote Sensing and GIS artificial groundwater recharge zones agrieast 2019 vol.13(1): 44-55

8. CGWB (2000) Ground water quality in urban environment of India. Central Ground Water Board, Faridabad. 3.
9. CGWB (2001) Hydrogeological framework and groundwater development prospects in Jabalpur City, M.P. Central Ground Water Board, North Central Region, Bhopal.
10. Todd, D. and Mays, L. (2005) Groundwater Hydrology. 3rd Edition, John Wiley and Sons, Inc., Hoboken, 652 p.
11. Heath, R. (2004) Basic Groundwater Hydrology, US Geological Survey Water Supply. Paper 2220, 91 p.
12. [Freeze, R. and Cherry, J. (1987) Groundwater. Prentice-Hall International, London, 524
13. B. M. Hussien, A. S. Fayyadh 1196 [13] Weight, W. (2004) Manual of Applied Hydrogeology. McGraw-Hill, New York, 553 p. [14]
14. William, M., Thomas, E. and Franke, O. (1999) Sustainability of Ground-Water Resources, US Geological Survey Circular 1186, Denver, US Government Printing Office, Free on application to the US Geological Survey Branch of Information Services, Box25286 Denver, 80225-0286 Library of Congress Cataloging-in-Publications Data.
15. Krishnamurthy J, Mani A, Jayaraman V, Manivel M (2000) Groundwater resources development in hard rock terrain-an approach using remote sensing and GIS techniques. Int J App Earth Obser Geoinform 2: 204-215.
16. Janardhan AS, Srikantappa H, Ramachandra HM (1978) Sargur schist complex an Archaean high grade terrain in south India. In Developments in Precambrian Geology 1: 127-149. 12.
17. Prakash Narasimha KN, Kobayashi S, Shoji T, Sasaki M, Sethumadhav MS (2009) XRD, EPMA AND FTIR studies on Garnet from Bettadabidu, Sargur area, Karnataka, India. J Appl Geochem 1: 1-11
18. HalehNampak, BiswajeetPradhan, Mohammad AbdManap, Mendeley -2014 Application of GIS based data driven evidential belief function model to predict groundwater potential zonation . Journal of hydrology Volume 513, Pages 283-300
19. Teevw RM (1999) Groundwater exploration using remote sensing and a low cost GIS. Hydrogeol J 3(3):21–30
20. P.K. Dineshkumar *et al.* Application of remote sensing and GIS for the demarcation of groundwater potential zones of a river basin In Kerala, southwest coast of India International Journal of Remote Sensing (2007)
21. Chandra S, Singh PK, Tiwari AK, Panigrahy B, Kumar A (2015) Evaluation of hydrogeological factor and their relationship with seasonal water table fluctu DtLon in Dhanbad district, Jharkhand, India. ISH J Hydraul Eng 21: 193-206. 2.

This page is intentionally left blank

A New Method of the Coupling Coordination Degree for Quantifying Sustainable Development from the Cosine of the High-Dimensional Spatial Angle Perspective

Dehui Bian, Rumeng Zhang Shan Liu, Ran Liu, Guoshuang Li & Yiming Qi

Beijing Normal University

ABSTRACT

The coupling coordination degree (CCD) is considered to be an important yardstick for guiding practice toward sustainable development. It helps quantitatively investigate the interactions between two or more subsystems within a complex system. However, the existing CCD models have inherent shortcomings. Currently, no consensus has been reached on CCD models. In line with this background, this research proposes a new CCD model from the perspective of the cosine of the high-dimensional spatial angle and develops a novel Excel© tool named Ex-CCD. Taking the coupling coordination analysis between economic-social development, resource consumption, and environmental pollution in China during 2000–2016 as an example, a case demonstration is conducted, and the results show that the model proposed in this research can more accurately describe the coupling coordination state of a system. This new model provides a significant theoretical and practical basis as well as a novel perspective for further coupling coordination research.

Keywords: coupling coordination analysis; high-dimensional spatial angle; applied mathematical modelling; complex system analysis; sustainable development.

Classification: LCC: HD75-76.8

Language: English

Great Britain Journals Press

LJP Copyright ID: 925653
Print ISSN: 2631-8490
Online ISSN: 2631-8504

London Journal of Research in Science: Natural and Formal

Volume 23 | Issue 15 | Compilation 1.0

A New Method of the Coupling Coordination Degree for Quantifying Sustainable Development from the Cosine of the High-Dimensional Spatial Angle Perspective

Dehui Bian[α,¥], Rumeng Zhang[σ,ρ,¥], Shan Liu[ↀ], Ran Liu[§], Guoshuang Li[σ] & Yiming Qi[§]

ABSTRACT

The coupling coordination degree (CCD) is considered to be an important yardstick for guiding practice toward sustainable development. It helps quantitatively investigate the interactions between two or more subsystems within a complex system. However, the existing CCD models have inherent shortcomings. Currently, no consensus has been reached on CCD models. In line with this background, this research proposes a new CCD model from the perspective of the cosine of the high-dimensional spatial angle and develops a novel Excel© tool named Ex-CCD. Taking the coupling coordination analysis between economic-social development, resource consumption, and environmental pollution in China during 2000–2016 as an example, a case demonstration is conducted, and the results show that the model proposed in this research can more accurately describe the coupling coordination state of a system. This new model provides a significant theoretical and practical basis as well as a novel perspective for further coupling coordination research.

Keywords: coupling coordination analysis; high-dimensional spatial angle; applied mathematical modelling; complex system analysis; sustainable development.

Author α: State Key Laboratory of Water Environment Simulation, School of Environment, Beijing Normal University, Beijing, 100875, China.
σ: Jingyue Branch of Bureau of Ecology and Environment of Changchun, Changchun, 130117, China.
ρ: Songliao Water Resources Commission, Ministry of Water Resources, Changchun, 130021, China.
ↀ: Environmental, Social and Governance (ESG) Group, Refinitiv, London Stock Exchange Group, Beijing, 100738, China.
§: Independent Researcher.
¥: These authors contributed equally.

I. INTRODUCTION

1.1 Research background and significance

According to the Global Sustainable Development Report 2019, *The Future is Now: Science for Achieving Sustainable Development*, with the continuous increase of population, the intensification of human activities and the economy development, the resources and environment globally are under unprecedented pressure (United Nations, 2019). The shortage of resources and the continuous deterioration of the environment caused by the global population increase and economic-social

London Journal of Research in Science: Natural and Formal

development seriously threaten the realization of sustainable development goals (SDGs). Moreover, due to the continuous acceleration of urbanization (according to a report released by the United Nations in 2018 (United Nations, 2018), *World Urbanization Prospects: The 2018 Revision*, the urban population accounted for more than 55% of the world's total population, and this proportion will increase significantly in the future), the contradictions among population, economy, resources, and environment in some areas may become more prominent (Shen et al., 2020). Taking a specific example, Jakarta, the capital of Indonesia, the excessive increase in population and rapid economic-social development in recent years have caused Jakarta to suffer from river pollution, air pollution, insufficient resources, traffic paralysis and other urban problems for a long time (Delinom et al., 2009), even causing Indonesia to decide to move its capital from Jakarta to East Kalimantan Province (Delinom et al., 2009; Nugroho, 2019). Given that resources and the environment continue to provide important guarantees and support for population growth and socioeconomic development, it is imperative to understand the interaction and coordination relationship between the population (including anthropogenic activities), economy, resources, and environment (Li and Yi, 2020; Xiao et al., 2020), which can provide an important guarantee for achieving SDGs (Huan et al., 2021; Li et al., 2021a). The interaction and coordination relationship of the different subsystems is a key issue to realize sustainable development (Li and Yi, 2020). Accordingly, as a measurement, the coupling coordination degree (CCD) was introduced and has become a widely used approach to help understand and analyze the interactions between the different elements in the system in the process of system operation, development and evolution (Shi et al., 2020; Sun et al., 2022). In recent years, CCD research has gradually become a hot spot in the field of sustainable development.

Coupling was originally a physical concept (Etherington et al., 2016). "Coupling" refers to a phenomenon in which multiple systems with multiple connections closely cooperate and rely on each other. "Coupling degree" is a measure of the coupling state (Yang et al., 2017), which refers to the phenomenon that two or more systems or motion forms influence each other through various interactions (Wang et al., 2011). Subsequently, it was widely used in many fields outside of physics. The coupling degree model is only a representation of the strength of interaction between systems and cannot effectively reflect the level of coordinated development. That is, when the development level of both systems is low, a higher degree of coupling can be obtained, but this coupling is not an ideal state. To avoid this deficiency, the coordination degree model is introduced (Fan et al., 2019). The coordination degree is a quantitative indicator to measure the status or level of the development of the elements in a system (Li et al., 2014). This implies that the coupling coordination degree considers not only the interaction degree but also the coordination level of the elements in a system (Li et al., 2012). The interactions of the two subsystems are intricate: they support and hinder each other with time. Coupling coordination refers to the status where subsystems interact and have effects on each other (Liu et al., 2018; Sofowote et al., 2010), and it is proper to analyze the interactions between the subsystems. Coupling coordination reflects how the subsystems interact with each other and how the system evolves from disorder to harmony (Ding et al., 2015). Many studies are dedicated to revealing the complex interactions between different subsystems using the coupling coordination model and its extensions (Zhang and Li, 2020; Zhao et al., 2016; Zhou et al., 2017).

Judging from the existing research status, the understanding of the concepts of coupling degree, coordination degree, and coupling coordination degree are all widely accepted in academia. However, there is still no consensus on the corresponding calculation models. According to the different understandings and cognitions, scholars have made many modifications and improvements based on the original coupling coordination degree model. For example, Feng and his colleagues (Feng et al.,

2021) adopted a modified coupling coordination degree model to investigate the coupling coordination relationship between urbanization and eco-environment. With the help of a modified coupling coordination degree model, Cai and other researchers (Cai et al., 2021) conducted a study on the coupling coordination degree on China's urbanization and agricultural ecological environment at the provincial level. However, due to the inherent shortcomings of the original coupling coordination degree model, none of the modified models overcame the shortcomings.

Therefore, it is imperative to reproduce the calculation model of the coupling coordination degree from a novel perspective. To facilitate the application and promotion of the model, it is necessary to propose a user-friendly calculation tool, which preferably has both a calculation function and a result visualization function, so that the users can understand the calculation results at a glance.

1.2. Literature review and research gap

1.2.1. Summary of the previous literature

In terms of the coupling coordination degree (CCD) modeling approaches proposed in the previous literature, various methods have emerged (Sun et al., 2022; Zhang et al., 2020). These methods are very similar, but there are subtle differences. A detailed summary of the existing CCD evaluation models was conducted in this research, and typical CCD evaluation models were divided into 8 categories (Table 1).

Table 1: Summary of the typical CCD evaluation models presented in previous research

CCD modeling approaches in the previous literature		The number of elements (n)	Details of elements	References
$CD^{(Coup)} = \sqrt[n]{\frac{\prod_{i=1}^{n} x_i}{(\frac{\sum_{i=1}^{n} x_i}{n})^n}}$ $CD^{(Coord)} = \sum_{i=1}^{n} w_i \times x_i$ $CCD = \sqrt{CD^{(Coup)} \times CD^{(Coord)}}$	Model 1	2	Coastal ecology and coastal development level	(Zhang et al., 2019a)
		2	Air environment and tourism	(Geng et al., 2021)
		2	Carbon emission and eco-environment	(Chen et al., 2020a)
		2	Urbanization rate and rural hollowing index	(Zhang et al., 2019b)
		3	Economy, society and environment	(Li and Yi, 2020)
		2	Urbanization and ecosystem health	(Li et al., 2021a)
		4	Society, economy, environment, means of implementation and cooperation	(Huan et al., 2021)
		2	Urbanization and geological hazards	(Zhang and Li, 2020)
		2	Economic growth and urban climate change	(Liu et al., 2020a)
		2	Supply and demand of ecosystem services	(Xin et al., 2021)
$CD^{(Coup)} = (\frac{\prod_{i=1}^{n} x_i}{(\frac{\sum_{i=1}^{n} x_i}{n})^n})^n$	Model 2	2	Urbanization and air quality	(Fan et al., 2020)
		2	Forestry management efficiency and forest ecological security	(Chen et al., 2020b)

$CD^{(Coord)}$ and $CCD^{\star}$		2	Economic development and ecological environment	(Shi et al., 2020)
		2	Ecological and economic development	(Meng et al., 2021)
		3	Food, economy and ecology	(Liu et al., 2020b)
		3	Production, living and ecology	(Zhou et al., 2017)
$CD^{(Coup)} = n\times\sqrt[n]{\frac{\prod_{i=1}^{n} x_i}{(\sum_{i=1}^{n} x_i)^{n}}}$ $CD^{(Coord)}$ and $CCD^{\star}$	Model 3	3	Land areas of production, living and ecological spaces	(Li et al., 2021b)
		3	Upstream, midstream and downstream of the wind power industry chain	(Dong and Li, 2021)
		2	Urbanization and ecosystem service	(Xiao et al., 2020)
		2	Urbanization and eco-environment	(Feng et al., 2021)
$CD^{(Coup)} = \frac{\sqrt[n]{\prod_{i=1}^{n} x_i}}{\frac{\sum_{i=1}^{n} x_i}{n}}$ $CD^{(Coord)}$ and $CCD^{\star}$	Model 4	3	Water, energy and food systems	(Han et al., 2020)
		2	Urbanization and ecological risk of PAHs	(Han et al., 2021)
$CD^{(Coup)} = \sqrt[n]{\frac{\prod_{i=1}^{n} x_i}{\frac{\sum_{i=1}^{n} x_i}{n}}}$ $CD^{(Coord)}$ and $CCD^{\star}$	Model 5	4	Social development, economic development, resource utilization, and environment system	(Sun et al., 2022)
$CD^{(Coup)} = \sqrt[n]{\prod_{i=1}^{n} x_i}$ $CD^{(Coord)}$ and $CCD^{\star}$	Model 6	3	Economy, society and the environment	(Xu and Hu, 2020)
$CD^{(Coup)} = \left(\frac{(\prod_{i=1}^{n} x_i)^{\frac{1}{n}}}{\frac{\sum_{i=1}^{n} x_i}{n}}\right)^{2}$ $CD^{(Coord)}$ and $CCD^{\star}$	Model 7	2	Urbanization and the atmospheric environment	(Liu et al., 2018)
$CD^{(Coup)} = \sqrt[n]{\frac{\prod_{i=1}^{n} x_i}{(\sum_{i=1}^{n} x_i)^{n}}}$ $CD^{(Coord)}$ and $CCD^{\star}$	Model 8	2	Urbanization and the agro-ecological environment	(Cai et al., 2021)

Notes: $CD^{(Coup)}$, $CD^{(Coord)}$, CCD *denote the coupling degree, the coordination degree and the coupling coordination degree, respectively.* n *is the number of elements used to calculate* $CD^{(Coup)}$, $CD^{(Coord)}$, CCD. i *represents the ith element,* $i\in[1,n]$. x_i *is the value of the ith element.* w_i *is the weight of the ith element, which generally refers to "1/n".*

* *The calculation methods of* $CD^{(Coord)}$ *and* CCD *are the same as Model 1.*

Model 1 in Table 1 is the original and most commonly adopted CCD evaluation model. According to Model 1, the $CD^{(Coup)}$ is calculated by the multiple and the average results of the elements, $CD^{(Coord)}$

refers to the sum of the multiple results of the weights (generally referred to as "1/n", where n is the element number) and the element values, and the CCD is the square root of the multiple results of $CD^{(Coup)}$ and $CD^{(Coord)}$ (a detailed algorithm decomposition of Model 1 is displayed in Section 1.2.2.). With the help of this model, the coupling coordination relationships between the different elements within a certain system have been extensively studied. For example, Geng and his colleagues (Geng et al., 2021) revealed the interactions of China's air environment and tourism. Liu and other researchers (Liu et al., 2020b) studied the relationships among economic growth and urban climate change.

Because of different interpretations, some other CCD evaluation models have been proposed (Table 1 Models 2-8). From the perspective of the development process of the CCD models, Models 2-8 are proposed by researchers on the basis of Model 1. Therefore, Models 2-8 are quite similar to Model 1. It is worth noting that almost all the researchers fully agree with the calculation of $CD^{(Coord)}$ and CCD. The controversy among researchers is mainly focused on the calculation method of $CD^{(Coup)}$, which is the core difference among Models 1-8. Another point worth highlighting is that in Models 2-8, the $CD^{(Coup)}$s are all calculated on the results of the multiple results and the average results of the elements. All the above analyses show that, in essence, the differences between Models 1-8 are not large.

1.2.2. Algorithm decomposition of the original CCD model

Algorithm decomposition is the basis of model understanding and a necessary prerequisite for model upgrading. As mentioned above, all the CCD models proposed in the previous literature are similar in essence. Therefore, in this research, a detailed algorithm decomposition was conducted on the initial CCD model, Model 1. Considering the fact that the major controversy among researchers is focused on the calculation of the $CD^{(Coup)}$, we mainly analyze the algorithms of the calculation of $CD^{(Coup)}$. For ease of understanding, we graphically display the algorithm of $CD^{(Coup)}$ in Model 1 (Fig. 1).

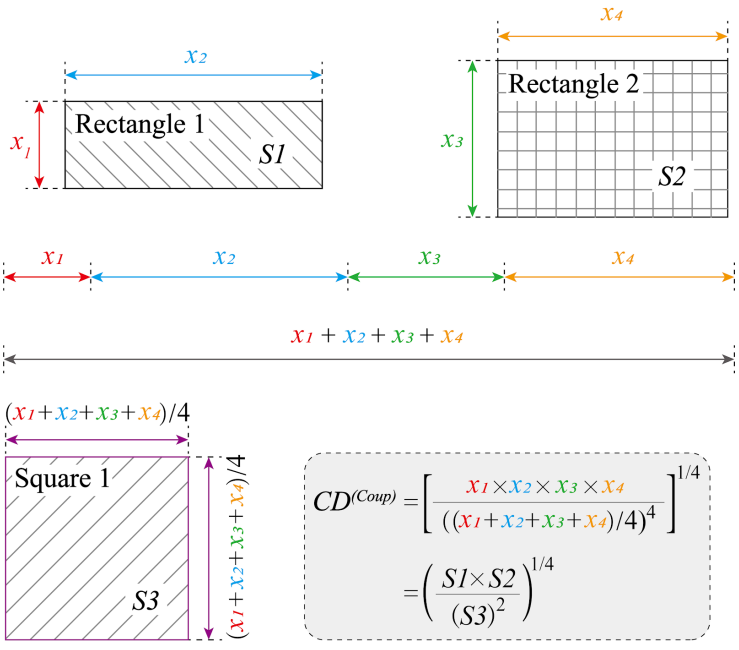

Fig. 1: Graphical algorithm decomposition of the calculation of $CD^{(Coup)}$ in Model 1

Notes: To be more specific, four elements are used to calculate $CD^{(Coup)}$, $CD^{(Coord)}$, CCD. x_1, x_2, x_3, *and* x_4 are the values of these four elements. *S1* and *S2* represent the areas of Rectangle 1 and Rectangle 2, respectively, and *S3* is the area of Square 1. Thus, $CD^{(Coup)}$ can be re-expressed as shown in Fig. 1.

In Fig. 1., x_1, x_2, x_3, *and* x_4 are the widths and heights of Rectangle 1 and Rectangle 2, respectively. A square has been constructed, the width of which is the average of x_1, x_2, x_3, x_4. Then, the equation to calculate $CD^{(Coup)}$ can be rewritten as displayed in Fig. 1. From this equation, we find that if a value of the elements refers to 0, the result of $CD^{(Coup)}$ will be 0. To be more specific, if there are two systems with 4 elements to calculate, $CD^{(Coup)}$, the values of the elements in the two systems are (10, 7, 9, 0) and (1, 0, 1, 0), respectively, and the $CD^{(Coup)}$ results of these two systems will be both 0. Clearly, the $CD^{(Coup)}$ results of these two systems are not the same, and the results are quite inaccurate. This phenomenon is a malfunction of the model, named the "failure phenomenon".

$CD^{(Coord)}$ represents the overall development level of the different elements within the system (Li et al., 2014; Li et al., 2012). It is generally calculated by the sum of the multiple results of the weights and the element values, and the weights are generally referred to as "1/n", which is the element number (Chen et al., 2020a; Zhang et al., 2019b). CCD refers to the square root of the multiple results between $CD^{(Coup)}$ and $CD^{(Coord)}$ (Zhang and Li, 2020). $CD^{(Coord)}$ and CCD calculation methods have been widely accepted and adopted by almost all researchers.

Moreover, from the graphical algorithm decomposition of $CD^{(Coup)}$ in Fig. 1, we can find that the results of $CD^{(Coup)}$ have a strong correlation with the results of $CD^{(Coord)}$ since the average of the elements ($CD^{(Coord)}$) has been used in the $CD^{(Coup)}$ calculation process. A case study was conducted to confirm this argument. Virtual data for seven sections each with four elements are displayed in Table 2. A detailed case study for five hundred virtual regions is shown in the Supplemental Material (S1).

Table 2: Virtual data for case study

Virtual data	x_1	x_2	x_3	x_4
Section 1	0.1000	0.2000	0.3000	0.4000
Section 2	0.2000	0.3000	0.4000	0.5000
Section 3	0.3000	0.4000	0.5000	0.6000
Section 4	0.4000	0.5000	0.6000	0.7000
Section 5	0.5000	0.6000	0.7000	0.8000
Section 6	0.6000	0.7000	0.8000	0.9000
Section 7	0.7000	0.8000	0.9000	1.0000

The calculation results of $CD^{(Coup)}$, $CD^{(Coord)}$ and CCD are shown in Table 3.

Table 3: Calculation results for case study

Calculation results	Section 1	Section 2	Section 3	Section 4	Section 5	Section 6	Section 7
$CD^{(Coup)}$	0.8853	0.9456	0.9680	0.9788	0.9849	0.9887	0.9913
$CD^{(Coord)}$	0.2500	0.3500	0.4500	0.5500	0.6500	0.7500	0.8500
CCD	0.4705	0.5753	0.6600	0.7337	0.8001	0.8611	0.9179

$CD^{(Coup)}$ is a metric used to reveal the degree of coupling of the various elements within the system (Yang et al., 2017), which should be a number independent of the average of x_1, x_2, x_3, and x_4 ($CD^{(Coord)}$). However, it can be seen in Table 3 that the values of $CD^{(Coup)}$ increase significantly as the values of $CD^{(Coord)}$ increase (with a correlation coefficient of 0.8603). Such calculation results are caused by the inherent defects of the model, so it is imperative to improve the CCD model from a novel perspective.

1.2.3. Overview of the advantages and shortcomings

In summary, the existing coupling coordination models mainly have the following advantages: 1) The algorithms are very easy to learn and master by new users. In other words, the existing CCD calculation models are very easy to understand, allow new users to quickly begin using them it within a very short period of time. 2) The existing CCD models are very easy for new users to utilize. To be more specific, the calculation processes of the existing CCD calculation methods are relatively simple, and the result can be calculated through the commonly used Excel© software without using any special software or having any programming knowledge.

The main shortcomings can be summarized into the following two aspects: 1) The existing CCD calculation model has an unavoidable failure phenomenon. If one value of the elements refers to 0, the result of $CD^{(Coup)}$ and CCD will be both 0. This causes it to be impossible to accurately calculate the $CD^{(Coup)}$ and CCD of the system. 2) $CD^{(Coup)}$ should be an index independent of the average value of the elements ($CD^{(Coord)}$), revealing the coupling state of the various elements within a system (Chen et al., 2020b). However, using the existing coupling coordination models, the values of $CD^{(Coup)}$ increase significantly as the values of $CD^{(Coord)}$ increase. This kind of algorithmic confusion between $CD^{(Coup)}$ and $CD^{(Coord)}$ causes it to be difficult to give specific and effective countermeasures to improve the CCD of the system.

1.3. The main work and innovations of this research

The main work and innovations of this research are mainly reflected in the following aspects: First, this research summarizes the existing CCD algorithms and analyzes the initial CCD algorithm in detail, which has always been lacking in previous CCD studies. Second, this research proposes a novel perspective, the cosine of the high-dimensional spatial angle, to improve the existing CCD evaluation models to eliminate the inherent shortcomings. At the same time, to make the operation of the method proposed in this study more convenient, an Excel© based tool named Ex-CCD was developed. Third, to test the validity of the model proposed in this research, a case study was conducted by taking China's economic and social development, natural resource consumption and environmental pollution coupling and coordination analysis from 2000 to 2016 as an example. The objective of this research is to propose a novel CCD calculation model and provide a user-friendly operating tool.

II. METHOD AND MATERIALS

2.1. A novel model for calculating the coupling coordination degree

2.1.1. The initial matrix

We assume that CCD needs to be investigated in h regions. The original data matrix of all the elements of the regions can be expressed as shown in Formula (1).

$$A = [a_{h,i}] = \begin{bmatrix} a_{1,1} & a_{1,2} & a_{2,1} & a_{2,2} & \cdots & a_{1,n} & \cdots & a_{2,n} \\ \vdots & \vdots & a_{s,1} & a_{s,2} & \ddots & \vdots & \cdots & a_{s,n} \end{bmatrix} \quad (1)$$

where $a_{h,i}$ is the value of region h's (h=1, 2, ..., s) ith (i=1, 2, ..., n) element.

2.1.2. Initial data standardization

To eliminate the differences in the magnitudes of the values of different elements and to make the results more comparable, it is necessary to standardize the original data before the calculation process.

The min-max normalization method (Peng and Deng, 2020; Bian et al., 2022) was used in this research, as shown in Formula (2). The range of the standardized results is [0, 1].

$$a_{h,i}' = \frac{a_{h,i} - (a_{1,i},\ a_{2,i},\ \ldots,\ a_{s,i})}{(a_{1,i},\ a_{2,i},\ \ldots,\ a_{s,i}) - (a_{1,i},\ a_{2,i},\ \ldots,\ a_{s,i})} \quad (2)$$

$a_{h,i}$ is the normalized value of region h's (h=1, 2, ..., s) ith (i=1, 2, ..., n) element.

2.1.3. Weight Determination

The weighting of elements often has a nonnegligible effect on the result (Kurz-Kim, 2010; Uyan, 2014; Gorgij et al., 2017; Sun et al., 2019). Thus, the calculation of element weight is often a key procedure. Generally, weights can be divided into subjective weights and objective weights (Sun et al., 2020; Sun and Yang, 2019). In this study, researchers are allowed to choose the method of weight calculation independently and only need to enter the results of the element weight into the table of the tool developed in this research. If each element is equally important, then the weight setting can be ignored because in the tool, each element is equally important by default, and the value of each weight is 1. In this research, the element weight of element i is denoted as w_i.

2.1.4. The cosine of the high-dimensional spatial angle

We summarized the general expression form of the cosine of the high-dimensional spatial angle through specific conditions. In other words, by expressing the cosine of the spatial angle when there are one, two, or three elements (Fig. 2.), we obtain the expression of the cosine of the spatial angle when there are multiple elements.

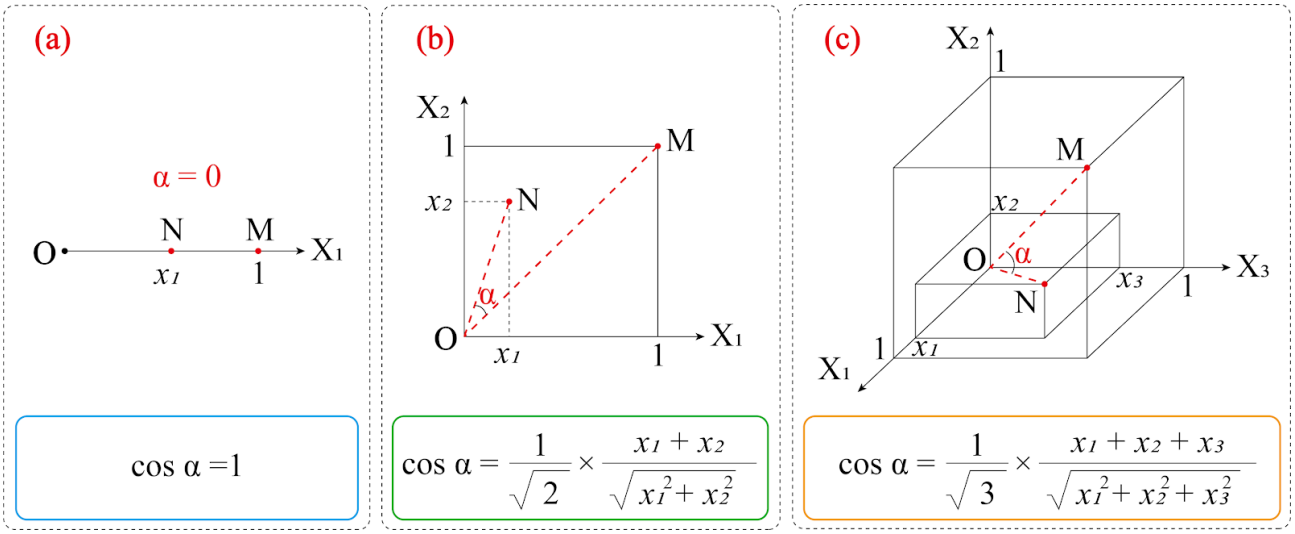

Fig. 2: Illustration of the cosine of the high-dimensional spatial angle

Notes: x_1, x_2, x_3, ... x_n (n is the number of elements) are the values of the elements X_1, X_2, X_3, ... X_n for calculating $CD^{(Coup)}$, respectively. Point M is the ideal state point of all of the elements. Point N is the actual state point of all elements. α represents the angle formed by point M, point N, and the origin, point O. It is worth noting that, according to the law of cosines, the minimum and maximum values of cosα are $1/\sqrt{n}$ and 1, respectively.

The expressions of the cosine of the spatial angle when there are one, two, or three elements are shown in Fig. 2. We can infer that when there are multiple elements, the expression of the spatial angle cosine is as shown in Formula (3).

$$cos\,\alpha = \frac{1}{\sqrt{n}} \times \frac{\sum_{i=1}^{n} x_i}{\sqrt{\sum_{i=1}^{n} (x_i)^2}} \tag{3}$$

The closer the actual state point (N) is to the ideal state point (M), the stronger the interaction between the elements of the system and the greater the degree of coupling. The maximum value of angle α is *Pi/2*, and the cosine function happens to be a monotonically decreasing function in the interval of [*0*, *Pi/2*], so the cosine value of α is selected to indicate the coupling degree between elements.

2.1.5. The modified coupling coordination degree model

Regarding the CCD model, the main controversy among researchers is the algorithm of the $CD^{(Coup)}$. Therefore, this research mainly improves the algorithm of the $CD^{(Coup)}$ through the cosine of the high-dimensional spatial angle, which provides a novel perspective for the calculation of the $CD^{(Coup)}$. The minimum and maximum values of cosα vary with the values of the elements. To eliminate the influence of the number of elements on the result distribution, it is necessary to carry out the standardization operation, as shown in Formula (2). Taking all these aspects into consideration, the calculation methods of the $CD^{(Coup)}$, $CD^{(Coord)}$, *and* CCD proposed in this study are shown in Formulas (4-6).

$$CD_h^{(Coup)} = \frac{\frac{1}{\sqrt{n}} \times \frac{\sum_{i=1}^{n} a_{h,i}' \times w_i}{\sqrt{\sum_{i=1}^{n} (a_{h,i}' \times w_i)^2}} - \frac{1}{\sqrt{n}}}{1 - \frac{1}{\sqrt{n}}} \tag{4}$$

$$CD_h^{(Coord)} = \frac{\sum_{i=1}^{n} a_{h,i}' \times w_i}{n} \tag{5}$$

$$CCD_h = \sqrt{CD_h^{(Coup)} \times CD_h^{(Coord)}} \tag{6}$$

where $CD_h^{(Coup)}$, $CD_h^{(Coord)}$, *and* CCD_h denote the coupling degree, the coordination degree and the coupling coordination degree of region h, respectively.

2.2. Model performance: a case study

To test the performance of the model proposed in this study, we chose to use the model proposed in this study to recalculate the results of the published research and compare the recalculated results with the results of the published research. The case study data comes from (Sun et al., 2022).

In Sun et al. (2022), the researchers established a detailed index system to calculate China's social development, economic development, resource utilization, and environment pollution indices from 2000 to 2016 and calculated the *CCDs* based on these indices. The values of these indices are shown in Table 4. The data in Table 4 are used as raw data to illustrate the performance of the CCD model proposed in this research.

Table 4: Indices of social development, economic development, resource utilization, and environmental pollution in China during 2000-2016 (Sun et al., 2022)

Year	Social development	Economic development	Resource utilization	Environment pollution
2000	0.11	0	0.45	0.43
2001	0.13	0.01	0.47	0.39
2002	0.16	0.03	0.57	0.47
2003	0.19	0.05	0.43	0.34
2004	0.23	0.08	0.33	0.32
2005	0.27	0.11	0.45	0.53
2006	0.3	0.16	0.39	0.52
2007	0.35	0.24	0.41	0.45
2008	0.4	0.34	0.47	0.62
2009	0.44	0.39	0.36	0.69
2010	0.5	0.49	0.54	0.56
2011	0.57	0.64	0.31	0.61
2012	0.63	0.74	0.49	0.75
2013	0.71	0.84	0.45	0.62
2014	0.78	0.93	0.45	0.64
2015	0.83	0.99	0.49	0.7
2016	0.93	1	0.63	0.8

2.3. Tool applicability

Based on the analysis of the existing literature, we found that the number of elements is generally 2-5, and the number of regions to be investigated is usually a few or dozens. To meet the needs of users for the number of elements and regions to the greatest extent, this new Excel-based tool, the Ex-CCD, was designed to conduct coupling coordination analysis of up to 500 regions from up to 15 elements. In addition, the tool developed in this research is capable of handling not only panel data but also time series data. Therefore, this tool can meet the reasonable needs of all groups of users.

2.4. Tool implementation

In this research, "user-centered design (UCD)" is accepted as the basic principle of tool design (Barnum, 2011; Acutis et al., 2022). We coded the Ex-CCD tool in the Excel© environment. UCD is an ISO standard (9241-210: 2019, https://www.iso.org/standard/77520.html), and it is a participatory-based technique. Accordingly, a group of users consisting of Ph.D. candidates, junior and senior researchers were invited to participate in the development of the tool. Designers adjusted the tool according to the feedback of the users. The most frequent feedback from users was the need for a user-friendly tool. In this regard, Excel© is a widely known environment (Berardi, 2002; IZAGIRRE et al., 2007). Excel© allows users with different backgrounds to use the toolkits included in Excel© without mastering the complex algorithms and logics behind these toolkits (Acutis et al., 2022; Jones et al., 2014). These algorithms and logics are more complex than spreadsheet-based solutions. They require coding skills and a deep understanding of the statistical theory behind each test. Moreover, the user interface of the Ex-CCD tool arranges the design of the input and output interfaces very well, and the Ex-CCD tool also includes an operating system with a certain and clear process. A user manual with detailed information can be found in the Supplemental Material (S2). In addition, we also provide a set of video tutorials to introduce the operating steps of the tool.

2.5. Tool effectiveness

To test the accuracy of the Ex-CCD tool, we directly compare the results calculated by using Excel© with those calculated by using the Ex-CCD tool to see if they are consistent. If these two kinds of calculation results are completely consistent, then the tool developed in this research is efficient and accurate. In this study, 500 virtual areas (each area with 4 elements) were used to verify the effectiveness of the Ex-CCD tool. See Supplemental Material (S3) for detailed information on the 500 virtual regions.

III. I LLUSTRATIVE RESULTS AND DISCUSSION

The main contribution of this research is to propose a new CCD calculation model originating from a novel perspective, which is the cosine of the high-dimensional spatial angle. Compared with the existing CCD calculation models, the process of implementing the method proposed in this research using Excel© is very cumbersome, and thus, an Excel-based tool for this model named Ex-CCD has been developed.

The following paragraphs describe the interface, the model performances, and the tool effectiveness analysis.

3.1. Tool interface

As an outcome of the UCD approach, Ex-CCD, the developed Excel-based tool, has a user-friendly interface (Fig. 3.). On the homepage of the tool, we give detailed information about the tool (including operation steps and tutorials).

The tool mainly includes three spreadsheets: the homepage spreadsheet, the input spreadsheet for initial element data and element weights, and the calculation and visualization spreadsheet for the results.

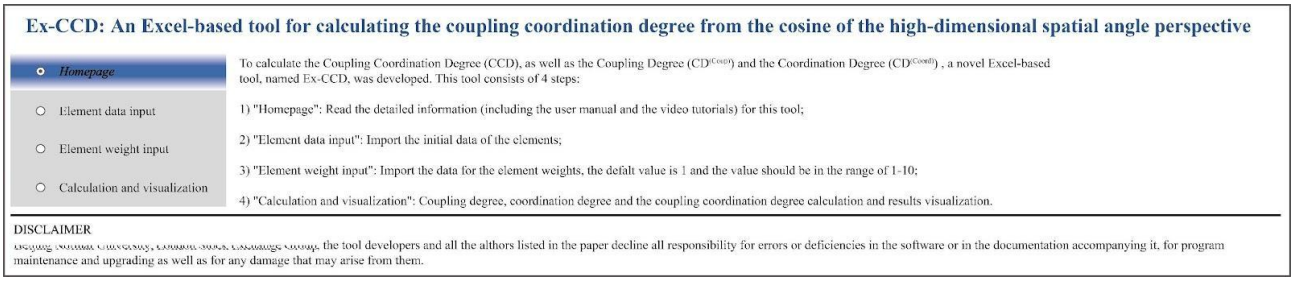

Fig. 3: The Ex-CCD tool introductory screen page

3.1.1. Input

The data input interface is shown in Fig. 4.

(a) Initial element data used for coupling coordination degree calculation

Element data / Regions	a_1	a_2	a_3	a_4	a_5	a_6	a_7	a_8	a_9	a_{10}	a_{11}	a_{12}	a_{13}	a_{14}	a_{15}
Region 1															
Region 2															
Region 3															
Region 4															
Region 5															
⋮															
Region 500															

(b) Element weight

Element weight	W_1	W_2	W_3	W_4	W_5	W_6	W_7	W_8	W_9	W_{10}	W_{11}	W_{12}	W_{13}	W_{14}	W_{15}
Values	1	1	1	1	1	1	1	1	1	1	1	1	1	1	1

Notes: The greater the weight value of an indicator, the more important the indicator is. The defalt value is 1 and the value should be in the range of 1-10.

Fig. 4: Data entry and weight setting interface

The data input interface mainly contains two parts: one part is about the input of the original data (Fig. 4. (a)), and the other part is about the input of the weights of the different elements (Fig. 4. (b)) (the default value of each weight is 1). Through the standardization process of Formula (2), the data will be distributed in the range of 0-1. To show the calculated results more clearly, we recommend setting the weight value to 1-10 (decimals can be used).

3.1.2. Output

To allow users to obtain a better operating experience, we will display the calculation results and the visualization tables of the same spreadsheet (Fig. 5).

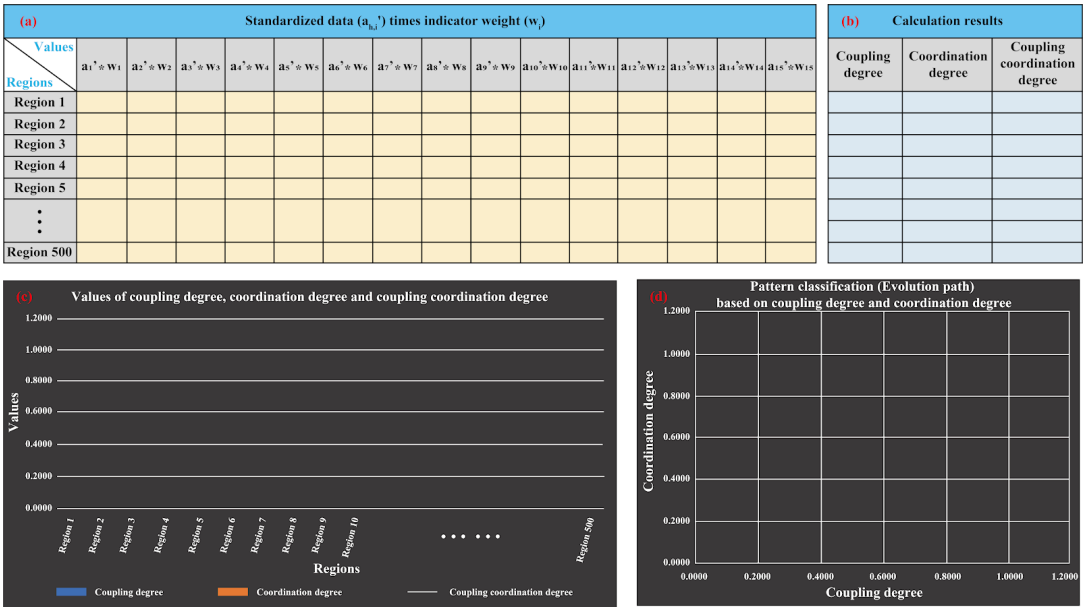

Fig. 5: Calculation results and visualization interface

The output page not only displays the final results of the $CD^{(Coup)}$, $CD^{(Coord)}$, and *CCD* of the investigated areas in the form of a table (Fig. 5. (b)) but also shows the result of multiplying the standardized data and the element weights (Fig. 5. (a)). Moreover, to obtain a more intuitive understanding, the $CD^{(Coup)}$, $CD^{(Coord)}$, and *CCD* values of the investigated areas are displayed graphically (Fig. 5. (c)). Based on $CD^{(Coup)}$ and $CD^{(Coord)}$ values the types of coupling coordination states in different regions can be divided (Fig. 5. (d)). If the data for multiple years can be obtained, the evolution path of the CCD can also be displayed.

3.2. Model performance: case study result analysis

The calculation results based on the model proposed in this research and the calculation results of Sun et al. (2022) are shown in Fig. 6. To obtain a more intuitive experience, Fig. 6 also shows the social development index, economic development index, resource utilization index, environment pollution index, and the sum of these indices. Overall, the calculation results of the model proposed in this research and the calculation results of Sun et al. (2022) generally show the similar trends. The results of both models show that the *CCD* of social development, economic development, resource utilization and environmental pollution in China from 2000 to 2016 generally showed upward trends year by year.

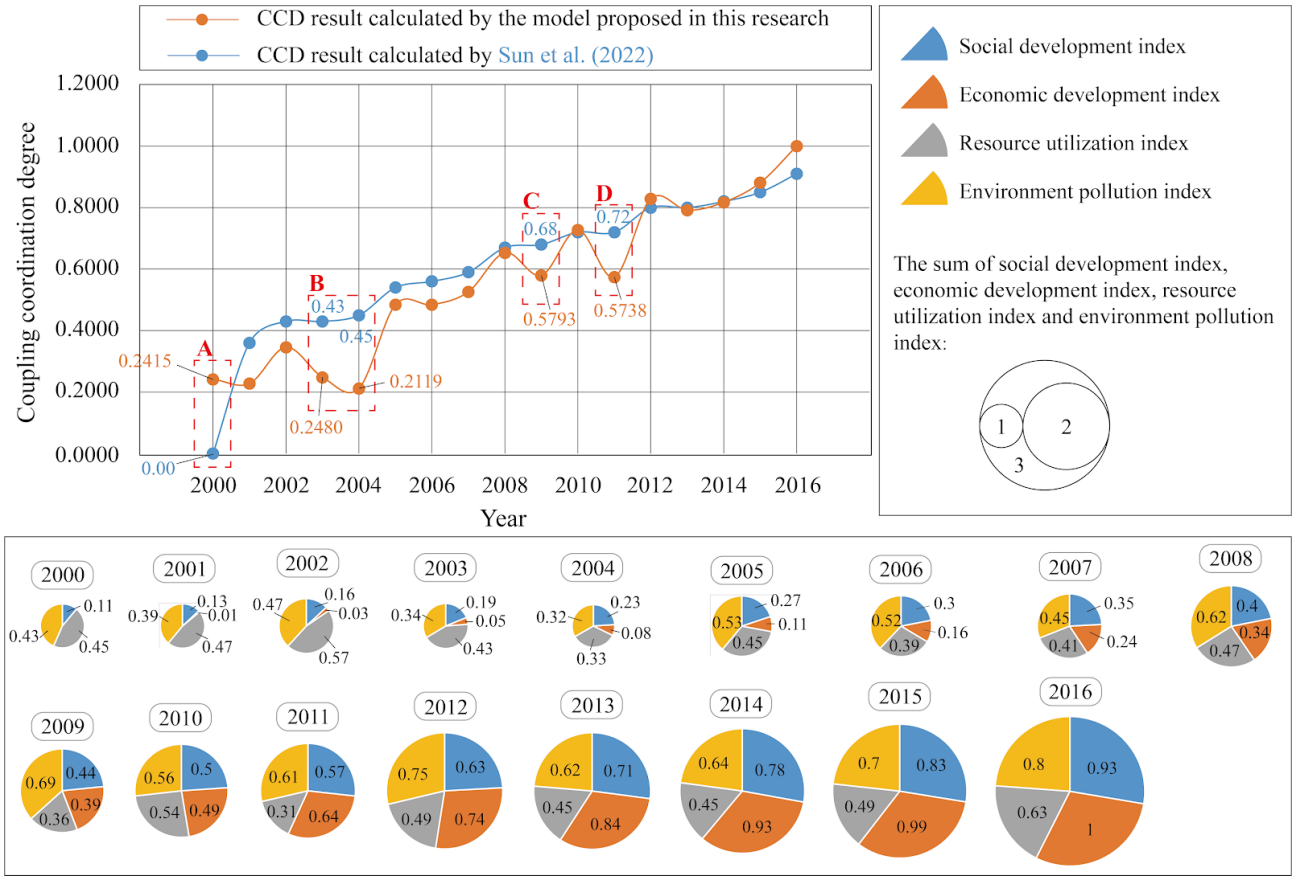

Fig. 6: Comparison of the model proposed in this study with that of Sun et al. (2022)

However, the evaluation results of the two models have slight differences. First, the evaluation model proposed in this research solves the failure problem of the original model (as shown in Fig. 6. Section A). Using the original method, the *CCD* of the social development, economic development, resource utilization and environmental pollution in China in 2000 could not be accurately calculated, thus they are represented by 0. However, using the model proposed in this research, the *CCD* of China's social development, economic development, resource utilization and environmental pollution in 2000 can be

accurately calculated, which is 0.2415. Second, the evaluation results of the *CCD* in 2003, 2004, 2009, and 2011 using the two methods have obvious differences, as shown in Fig. 6. Section B, C, D. When calculating $CD^{(Coup)}$, the model proposed in this research starts from the perspective of a multidimensional space and considers the degree of distance from the ideal state of the different coordinates. Therefore, small differences in a single element may cause huge differences in the results. However, the traditional CCD model is only related to the product and average of each element, and the sensitivity is relatively poor. Therefore, it is difficult to accurately measure the CCD of a system. The model proposed in this research is more sensitive and can accurately perceive the $CD^{(Coup)}$ of different element combinations. From the sum of the social development, economic development, resource utilization, and environment pollution indices for 2003, 2004, 2009, and 2011, the sum of these indices is significantly lower. However, Sun et al. (2022), which uses the traditional CCD calculation model, did not capture this change well in the calculation results. This also confirms the rationality of the CCD calculation model proposed in this research.

The $CD^{(Coup)}$, $CD^{(Coord)}$, and *CCD* values calculated by the previous CCD calculation models often have strong correlations. Therefore, in previous studies, $CD^{(Coup)}$ and $CD^{(Coord)}$ were mostly used as the intermediate process of *CCD*. According to our investigation, no one has conducted separate analyses of the $CD^{(Coup)}$ and $CD^{(Coord)}$ in CCD research. However, since the *CCD* is calculated using $CD^{(Coup)}$ and, $CD^{(Coord)}$, the changes in $CD^{(Coup)}$ and $CD^{(Coord)}$ are very important for understanding the changes in the CCD.

Using the model proposed in this study, we can easily calculate the $CD^{(Coup)}$, $CD^{(Coord)}$, and *CCD* values and can see the trends of the results intuitively as shown in Fig. 7.

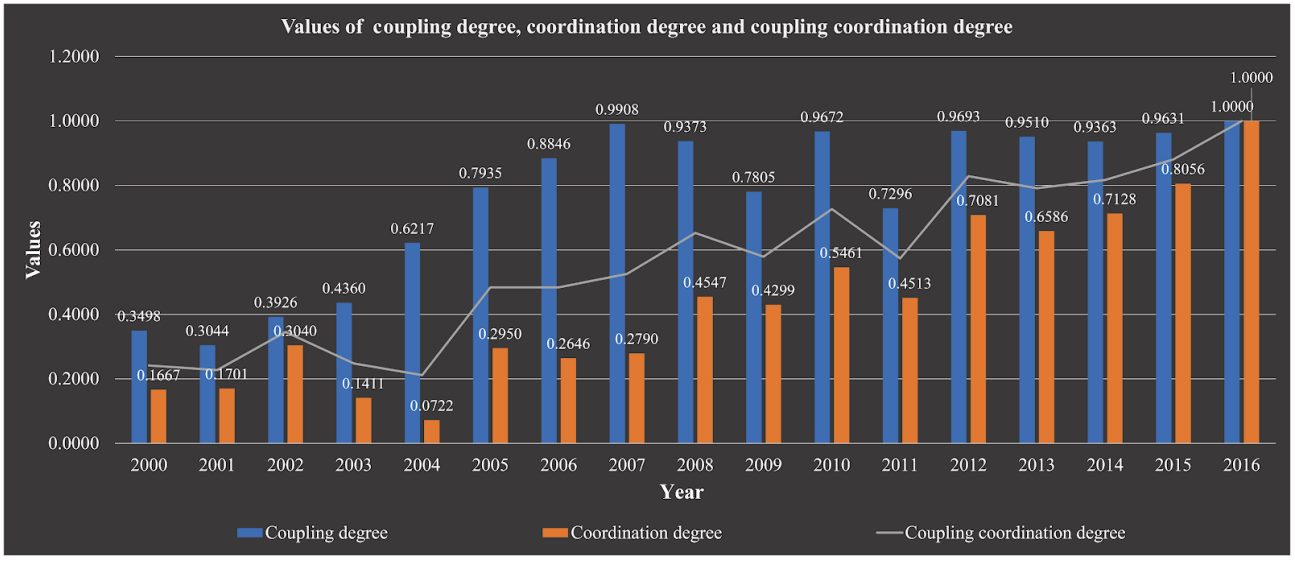

Fig. 7: Visualization of the coupling degree, coordination degree and coupling coordination degree

Fig. 7 shows the $CD^{(Coup)}$ and $CD^{(Coord)}$ values derived from social development, economic development, resource consumption and environmental pollution in China from 2000 to 2016. Through Fig. 7, we can see that there is a huge difference between the trend of $CD^{(Coup)}$ and the trend of $CD^{(Coord)}$. Fig. 7 shows that $CD^{(Coup)}$ showed an upward trend from 2000 to 2007 and then first a declining rising trend from 2007 to 2016. The degree of coordination from 2000 to 2004 showed an upward trend and then a downward trend. The level of coordination in 2004 was the lowest. From 2005 to 2016, the degree of

coordination in China showed an upward trend year by year. The *CCD* also shows a general upward trend year by year. Due to the low $CD^{(Coord)}$ values in 2003 and 2004, the *CCD* in these two years decreased significantly and was at the lowest level of the 2000-2016 period.

Through a two-dimensional Cartesian coordinate system composed of $CD^{(Coup)}$ and, $CD^{(Coord)}$, we can understand the changes in the CCD more clearly. If there is only one year of data, then the different types of coupling coordination in the study area can be obtained. To be more specific, it can be determined which areas have high coupling but low coordination or which areas have high coordination but low coupling. In view of the different types of different regions, more effective countermeasures can be given to improve the CCD. If the data are for multiple years, the evolution of the CCD in different regions with the year can be obtained. Fig. 8 shows the evolution path of the coupling coordination of social development, economic development, resource consumption, and environmental pollution in China from 2000 to 2016.

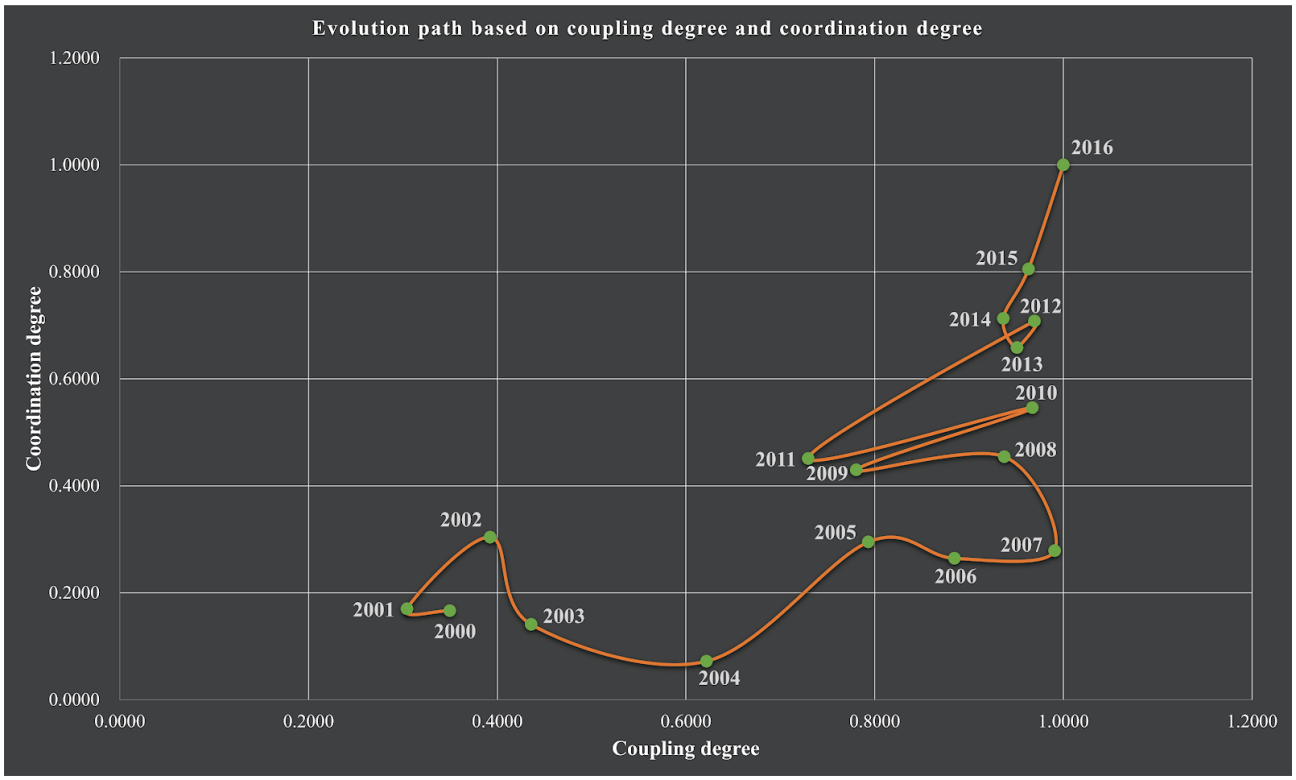

Fig. 8: Evolution path of CCD analysis

It can be seen in Fig. 8 that the evolution trend of the *CCD* of social development, economic development, resource consumption, and environmental pollution in China from 2000 to 2016 is that from a state where the $CD^{(Coup)}$ and $CD^{(Coord)}$ are both low, and evolve to a state with a higher $CD^{(Coup)}$ and $CD^{(Coord)}$ values. The coupling state from 2005 to 2014 is a state of rising volatility, and during this period, the coordination state of the system has been steadily rising.

3.3. Tool effectiveness analysis

The $CD^{(Coup)}$, $CD^{(Coord)}$, and *CCD* values of the 500 virtual areas directly calculated by Excel© are completely consistent with the results calculated by the Ex-CCD tool. This shows that the Ex-CCD tool developed in this research has very good accuracy. The detailed calculation results are shown in the Supplemental Material (S3). It is worth emphasizing that the data type in this research is time series

data. If the data type of the research object belongs to panel data, in order to find out the CCD spatial characteristics, the data calculated by the model proposed in this research needs to be visualized and further analyzed in GIS software.

IV. CONCLUSIONS

The coupling coordination degree (CCD) is a critical yardstick for sustainable development. In recent years, research on the CCD has gradually become a hot spot in the area of sustainable development. CCD can be subdivided into $CD^{(Coup)}$ and $CD^{(Coord)}$. Scholars currently have much controversy about the calculation of $CD^{(Coup)}$, and a variety of improved models have been proposed based on the initial calculation model of $CD^{(Coup)}$. However, these models all have deficiencies that cannot be overcome by themselves, such as the "failure phenomenon", the problem of greater correlation between $CD^{(Coup)}$ and $CD^{(Coord)}$. These problems greatly limit the future development of research on the CCD.

Based on the classification and summary of the existing CCD models and the algorithm decomposition of the initial CCD model, this research proposes a new $CD^{(Coup)}$ calculation method from a brand-new perspective, namely, the cosine of the high-dimensional spatial angle. The CCD is calculated by combining the $CD^{(Coup)}$ calculation method proposed in this research and the well-accepted $CD^{(Coord)}$ calculation method. To facilitate the application of the CCD model proposed in this research, this research has developed an Excel-based tool for CCD calculation named Ex-CCD. This tool not only has the function of calculating the CCD but is also very easy to utilize and has a complete result visualization function. A case study based on the CCD of social development, economic development, resource utilization and environmental pollution in China from 2000 to 2016 confirmed the rationality of the method proposed in this research and verified the effectiveness of the tools developed in this research.

It is hoped that the model proposed and the tool developed for calculating the coupling coordination degree in this research can be widely adopted and studied in the future.

ACKNOWLEDGMENT

The authors would like to extend special thanks to the editor and the anonymous reviewers for their detailed comments and valuable suggestions. All supporting materials could be found at https://doi.org/10.6084/m9.figshare.23997984.v1.

REFERENCES

1. Acutis M, Tadiello T, Perego A, Di Guardo A, Schillaci C, Valkama E (2022) EX-TRACT: An excel tool for the estimation of standard deviations from published articles. ENVIRON MODELL SOFTW 147, 105236. DOI 10.1016/j.envsoft.2021.105236.
2. Ai J, Feng L, Dong X (2016) Exploring coupling coordination between urbanization and ecosystem quality (1985-2010): a case study from Lianyungang City, China. Front. Earth Sci. 10 (3), 527-545. DOI 10.1007/s11707-015-0531-6.
3. Barnum CM (2011) Usability Testing Essentials: Ready, Set, test!. Morgan Kaufmann Publishers, Burlington.
4. Berardi A (2002) ASTROMOD: a computer program integrating vegetation dynamics modelling, environmental modelling and spatial data visualisation in Microsoft Excel. Environmental modelling & software: with environment data news 17, 403-412. DOI 10.1016/S1364-8152(02)00011-7.

5. Bian D, Yang X, Wu F, Babuna P, Luo Y, Wang B, Chen Y (2022) A three-stage hybrid model investigating regional assessment, pattern analysis and obstruction factor analysis for water resource spatial equilibrium in China. J CLEAN PROD 331, 129940. DOI 10.1016/j.jclepro.2021.129940.
6. Cai J, Li X, Liu L, Chen Y, Wang X, Lu S (2021) Coupling and coordinated development of new urbanization and agro-ecological environment in China. SCI TOTAL ENVIRON 776, 145837. DOI 10.1016/j.scitotenv.2021.145837.
7. Chen J, Li Z, Dong Y, Song M, Shahbaz M, Xie Q (2020a) Coupling coordination between carbon emissions and the eco-environment in China. J CLEAN PROD 276, 123848. DOI 10.1016/j.jclepro.2020.123848.
8. Chen N, Qin F, Zhai Y, Cao H, Zhang R, Cao F (2020b) Evaluation of coordinated development of forestry management efficiency and forest ecological security: A spatiotemporal empirical study based on China's provinces. J CLEAN PROD 260, 121042. DOI 10.1016/j.jclepro.2020.121042.
9. Delinom RM, Assegaf A, Abidin HZ, Taniguchi M, Suherman D, Lubis RF, Yulianto E (2009) The contribution of human activities to subsurface environment degradation in Greater Jakarta Area, Indonesia. SCI TOTAL ENVIRON 407, 3129-3141. DOI 10.1016/j.scitotenv.2008.10.003.
10. Ding L, Zhao W, Huang Y, Cheng S, Liu C (2015) Research on the coupling coordination relationship between urbanization and the air environment: a case study of the area of Wuhan. Atmos 6 (10), 1539-1558. DOI 10.3390/atmos6101539.
11. Dong F, Li W (2021) Research on the coupling coordination degree of "upstream-midstream-downstream" of China's wind power industry chain. J CLEAN PROD 283, 124633. DOI 10.1016/j.jclepro.2020.124633.
12. Etherington MK, Gibson J, Higginbotham HF, Penfold TJ, Monkman AP (2016) Revealing the spin-vibronic coupling mechanism of thermally activated delayed fluorescence. Nat. Commun. 7, 13680. DOI 10.1038/ncomms13680.
13. Fan W, Wang H, Liu Y, Liu H (2020) Spatio-temporal variation of the coupling relationship between urbanization and air quality: A case study of Shandong Province. J CLEAN PROD 272, 122812. DOI 10.1016/j.jclepro.2020.122812.
14. Fan YP, Fang CL, Zhang Q (2019) Coupling coordinated development between social economy and ecological environment in Chinese provincial capital cities assessment and policy implications. J. Clean. Prod. 229, 289-298. DOI 10.1016/j.jclepro.2019.05.027.
15. Feng Y, He S, Li G (2021) Interaction between urbanization and the eco-environment in the Pan-Third Pole region. SCI TOTAL ENVIRON 789, 148011. DOI 10.1016/j.scitotenv.2021.148011.
16. Geng Y, Wang R, Wei Z, Zhai Q (2021) Temporal-spatial measurement and prediction between air environment and inbound tourism: Case of China. J CLEAN PROD 287, 125486. DOI 10.1016/j.jclepro.2020.125486.
17. Gorgij AD, Kisi O, Moghaddam AA, Taghipour A (2017) Groundwater quality ranking for drinking purposes, using the entropy method and the spatial autocorrelation index. Environ. Earth Sci. 76. DOI 10.1007/s12665-017-6589-6.
18. Han D, Yu D, Cao Q (2020) Assessment on the features of coupling interaction of the food-energy-water nexus in China. J CLEAN PROD 249, 119379. DOI 10.1016/j.jclepro.2019.119379.
19. Han G, Shi Y, Lu Y, Liu C, Cui H, Zhang M (2021) Coupling relation between urbanization and ecological risk of PAHs on coastal terrestrial ecosystem around the Bohai and Yellow Sea. ENVIRON POLLUT 268, 115680. DOI 10.1016/j.envpol.2020.115680.
20. Huan Y, Liang T, Li H, Zhang C (2021) A systematic method for assessing progress of achieving sustainable development goals: A case study of 15 countries. SCI TOTAL ENVIRON 752, 141875. DOI 10.1016/j.scitotenv.2020.141875.

21. IZAGIRRE O, BERMEJO M, POZO J, ELOSEGI A (2007) RIVERMET©: An Excel-based tool to calculate river metabolism from diel oxygen–concentration curves. ENVIRON MODELL SOFTW 22, 24-32. DOI 10.1016/j.envsoft.2005.10.001.
22. Jones WR, Spence MJ, Bowman AW, Evers L, Molinari DA (2014) A software tool for the spatiotemporal analysis and reporting of groundwater monitoring data. ENVIRON MODELL SOFTW 55, 242-249. DOI 10.1016/j.envsoft.2014.01.020.
23. Kurz-Kim J (2008) Combining forecasts using optimal combination weight and generalized auto regression. J. Forecasting. 27, 419-432. DOI 10.1002/for.1069.
24. Li J, Sun W, Li M, Meng L (2021b) Coupling coordination degree of production, living and ecological spaces and its influencing factors in the Yellow River Basin. J CLEAN PROD 298, 126803. DOI 10.1016/j.jclepro.2021.126803.
25. Li J, Wang X, Miao C, Liu J (2014) The coordination analysis about level and quality of urbanization: a case study of Henan Province. Econ. Geogr. 34, 70-77. (in Chinese)
26. Li W, Wang Y, Xie S, Cheng X (2021a) Coupling coordination analysis and spatiotemporal heterogeneity between urbanization and ecosystem health in Chongqing municipality, China. SCI TOTAL ENVIRON 791, 148311. DOI 10.1016/j.scitotenv.2021.148311.
27. Li W, Yi P (2020) Assessment of city sustainability—Coupling coordinated development among economy, society and environment. J CLEAN PROD 256, 120453. DOI 10.1016/j.jclepro.2020.120453.
28. Li Y, Li Y, Zhou Y, Shi Y, Zhu X (2012) Investigation of a coupling model of coordination between urbanization and the environment. J. Environ. Manag. 98, 127-133. DOI 10.1016/j.jenvman.2011.12.025.
29. Liu H, Huang B, Yang C (2020a) Assessing the coordination between economic growth and urban climate change in China from 2000 to 2015. SCI TOTAL ENVIRON 732, 139283. DOI 10.1016/j.scitotenv.2020.139283.
30. Liu J, Jin X, Xu W, Gu Z, Yang X, Ren J, Fan Y, Zhou Y (2020b) A new framework of land use efficiency for the coordination among food, economy and ecology in regional development. SCI TOTAL ENVIRON 710, 135670. DOI 10.1016/j.scitotenv.2019.135670.
31. Liu W, Jiao F, Ren L, Xu X, Wang J, Wang X (2018) Coupling coordination relationship between urbanization and atmospheric environment security in Jinan City. J CLEAN PROD 204, 1-11. DOI 10.1016/j.jclepro.2018.08.244.
32. Meng F, Guo J, Guo Z, Lee JCK, Liu G, Wang N (2021) Urban ecological transition: The practice of ecological civilization construction in China. SCI TOTAL ENVIRON 755, 142633. DOI 10.1016/j.scitotenv.2020.142633.
33. Peng T, Deng H (2020) Comprehensive evaluation on water resource carrying capacity based on DPESBR framework: A case study in Guiyang, southwest China. J. Clean. Prod. 268, 122235. DOI 10.1016/j.jclepro.2020.122235.
34. Perry GLW (2004) SpPack: spatial point pattern analysis in Excel using Visual Basic for Applications (VBA). ENVIRON MODELL SOFTW 19, 559-569. DOI 10.1016/j.envsoft.2003.07.004.
35. SS Nugroho (2019) After Jokowi's First Term–Moving the Nation's "Keraton": A Javanese Perspective (RSIS Commentaries, No. 174). RSIS Commentaries Nanyang Technological University, Singapore.
36. Shen L, Shu T, Liao X, Yang N, Ren Y, Zhu M, Cheng G, Wang J (2020) A new method to evaluate urban resources environment carrying capacity from the load-and-carrier perspective. RESOUR CONSERV RECY 154, 104616. DOI 10.1016/j.resconrec.2019.104616.
37. Shi T, Yang S, Zhang W, Zhou Q (2020) Coupling coordination degree measurement and spatiotemporal heterogeneity between economic development and ecological environment ----Empirical evidence from tropical and subtropical regions of China. J CLEAN PROD 244, 118739. DOI 10.1016/j.jclepro.2019.118739.

38. Sofowote UM, Allan LM, McCarry BE (2010) Evaluation of PAH diagnostic ratios as source apportionment tools for air particulates collected in an urban industrial environment. J. Environ. Monit. 12 (2), 417-424. DOI 10.1039/b909660d.
39. Sun B, Yang X (2019) Simulation of Water Resources Carrying Capacity in Xiong'an New Area Based on System Dynamics Model. Water 11(5):1085. DOI 10.3390/w11051085.
40. Sun B, Yang X, Zhang Y, Chen X (2019) Evaluation of Water Use Efficiency of 31 Provinces and Municipalities in China Using Multi-Level Entropy Weight Method Synthesized Indexes and Data Envelopment Analysis. Sustain. 2019, 11(17):4556. DOI 10.3390/su11174556.
41. Sun X, Zhu B, Zhang S, Zeng H, Li K, Wang B, Dong Z, Zhou C (2022) New indices system for quantifying the nexus between economic-social development, natural resources consumption, and environmental pollution in China during 1978–2018. SCI TOTAL ENVIRON 804, 150180. DOI 10.1016/j.scitotenv.2021.150180.
42. Sun Y, Chen X, Zhou X, Zhang M (2020) Evaluating the efficiency of China's healthcare service: A weighted DEA-game theory in a competitive environment. J. Clean. Prod. 270, 122431. DOI 10.1016/j.jclepro.2020.122431.
43. United Nations (2018) United Nations World Urbanization Prospects: The 2018 Revision [Key Facts] United Nations, San Francisco, CA, USA (2018). https://www.sciencedirect.com /science/article/pii/S0921344919305221?via%3Dihub#bbib0575.
44. United Nations (2019) The Future is Now: Science for Achieving Sustainable Development. United Nations, San Francisco, CA, USA (2019). https://sustainabledevelopment.un.org /globalsdreport /2019.
45. Uyan M (2014) MSW landfill site selection by combining AHP with GIS for Konya, Turkey. Environ. Earth Sci. 71(4):1629-1639. DOI 10.1007/s12665-013-2567-9.
46. Wang XN, Sun CZ, Zou W (2011) Coupling relation analysis between water poverty and economic poverty. China Soft Science 12, 180-192. (in Chinese).
47. Xiao R, Lin M, Fei X, Li Y, Zhang Z, Meng Q (2020) Exploring the interactive coercing relationship between urbanization and ecosystem service value in the Shanghai–Hangzhou Bay Metropolitan Region. J CLEAN PROD 253, 119803. DOI 10.1016/j.jclepro.2019.119803.
48. Xin R, Skov-Petersen H, Zeng J, Zhou J, Li K, Hu J, Liu X, Kong J, Wang Q (2021) Identifying key areas of imbalanced supply and demand of ecosystem services at the urban agglomeration scale: A case study of the Fujian Delta in China. SCI TOTAL ENVIRON 791, 148173. DOI 10.1016/j.scitotenv.2021.148173.
49. Xu M, Hu W (2020) A research on coordination between economy, society and environment in China: A case study of Jiangsu. J CLEAN PROD 258, 120641. DOI 10.1016/j.jclepro.2020.120641.
50. Yang K, Lv S, Gao J, Pang L (2017) Research on the coupling degree measurement model of urban gas pipeline leakage disaster system. Int. J. Disast. Risk RE 22, 238-245. DOI 10.1016/j.ijdrr.2016.11.013.
51. Zhang L, Nie Q, Chen B, Chai J, Zhao Z (2020) Multi-scale evaluation and multi-scenario simulation analysis of regional energy carrying capacity—Case study: China. SCI TOTAL ENVIRON 734, 139440. DOI 10.1016/j.scitotenv.2020.139440.
52. Zhang R, Ai B, Gu F (2019a) Ecological responses to the coastal exploitation of urban agglomerations along the Pearl River Estuary. ENVIRON RES LETT 14, 124008. DOI 10.1088/1748-9326/ab4d81.
53. Zhang R, Jiang G, Zhang Q (2019b) Does urbanization always lead to rural hollowing? Assessing the spatio-temporal variations in this relationship at the county level in China 2000–2015. J CLEAN PROD 220, 9-22. DOI 10.1016/j.jclepro.2019.02.148.
54. Zhang Z, Li Y (2020) Coupling coordination and spatiotemporal dynamic evolution between urbanization and geological hazards–A case study from China. SCI TOTAL ENVIRON 728, 138825. DOI 10.1016/j.scitotenv.2020.138825.

55. Zhao Y, Wang S, Zhou C (2016) Understanding the relation between urbanization and the eco-environment in China's Yangtze River Delta using an improved EKC model and coupling analysis. SCI TOTAL ENVIRON 571, 862-875. DOI 10.1016/j.scitotenv.2016.07.067.
56. Zhou D, Xu J, Lin Z (2017) Conflict or coordination? Assessing land use multi-functionalization using production-living-ecology analysis. SCI TOTAL ENVIRON 577, 136-147. DOI 10.1016/j.scitotenv.2016.10.143.

Construction and Evolution Analysis of Agricultural Development System based on Multi-party Symbiosis Model

Wang Chen, Feng Rui, Ren Jinlian, Chen Xuedong, Wang Ziyi & Liyongmei

INTRODUCTION

The purpose of the government's rural revitalization is to use flexible market means to guide a large number of farmers (business entities) to participate in rural revitalization. Governments at all levels are the promoters, managers and supervisors of rural revitalization. Enterprises (cooperatives) participate in rural revitalization as organizers of farmers (operating entities), and are participants and organizers of rural revitalization. The government's policies and support, and the number of farmers (operating entities) participating in rural revitalization are the key factors that affect the enthusiasm of enterprises (cooperatives) to participate in rural revitalization.

Keywords: NA

Classification: LCC: S1-972

Language: English

Great Britain Journals Press

LJP Copyright ID: 925651
Print ISSN: 2631-8490
Online ISSN: 2631-8504

London Journal of Research in Science: Natural and Formal

Volume 23 | Issue 15 | Compilation 1.0

Construction and Evolution Analysis of Agricultural Development System based on Multi-party Symbiosis Model

Wang Chen[α], Feng Rui[σ], Ren Jinlian[ρ], Chen Xuedong[Ↄ], Wang Ziyi[¥] & Liyongmei[§]

Author α σ ρ Ↄ ¥ §: Institute of Agricultural Economics and Information Technology, Ningxia Academy of Agriculture and Forestry Sciences.

INTRODUCTION

The purpose of the government's rural revitalization is to use flexible market means to guide a large number of farmers (business entities) to participate in rural revitalization. Governments at all levels are the promoters, managers and supervisors of rural revitalization. Enterprises (cooperatives) participate in rural revitalization as organizers of farmers (operating entities), and are participants and organizers of rural revitalization. The government's policies and support, and the number of farmers (operating entities) participating in rural revitalization are the key factors that affect the enthusiasm of enterprises (cooperatives) to participate in rural revitalization.

According to each subject relationship, the following assumptions are put forward:

Assumption 1, without considering other constraints, the government (g), enterprises (cooperatives) (c) and farmers (operating entities) (u) are regarded as a complete system, the three parties follow the assumption of bounded rationality and incomplete information symmetry. All parties constantly adjust their behavioral strategies to achieve the equilibrium of the evolutionary game.

Assumption 2, the government chooses the strategy of investing and not investing in rural revitalization, and the probability of the corresponding investment strategy is **x** and **1-x** ; The strategy chosen by the enterprise (cooperative) is to organize farmers and not organize farmers to participate in industrialization, and the probability corresponding to the participation strategy is **y** and **1-y;** The strategies chosen by farmers (operating entities) are to participate in and not to participate in industrialization, and the corresponding probability of participating in the strategy is **z** and **1-z**. Among them, x,y,z are functions of time t and satisfy $x,\ y,\ z \in [0,\ 1]$.

Assumption 3, the economic benefit of the government's investment in farmers (operating entities) to join rural revitalization is R_g, the government's credibility is increased to L_g, the subsidies to enterprises are A_c, and the subsidies to farmers are A_u. When the enterprises do not organize farmers (operating entities), the government undertakes additional The cost of establishing an information platform and market transaction behavior is C_g; When the government does not provide subsidies but farmers (operating entities) actively participate, the government benefit is R_{0g}.

Assumption 4, the enterprise (cooperative) provides additional services to farmers (operating entities) to obtain benefits R_c, the sum of labor costs, learning costs and other costs required to provide services C_c, and the government subsidy is A_c, and the potential market value increase due to the provision of services is L_c; The enterprise does not organize farmers (operating entities) and does not suffer losses.

Assumption 5, the income of farmers (business entities) participating in rural revitalization is R_u, the cost of participating in enterprise organizations is C_u, the cost of farmers (business entities) participating alone is C_{0u}, and the government subsidies are A_u; Farmers (business entities) do not participate The loss paid is R_{0u}.

Based on the above assumptions, the income matrix under different strategies of each participant can be obtained.

Table 1: Game income matrix of government, enterprises (cooperatives) and farmers (operating subjects)

The parties and their actions				Farmer (operating entity)	
				participating (z)	not participating $(1\text{-}z)$
government	Input (x)	Enterprise (Cooperative)	organize (y)	$R_g - A_c - A_u + L_g$	$L_g - A_c$
				$R_c - C_c + A_c + L_c$	$L_c - C_c + A_c$
				$R_u - C_u + A_u$	$-R_{0u}$
			not organized $(1\text{-}y)$	$R_g + L_g - A_u - C_g$	$L_g - C_g$
				0	0
				$R_u - C_{0u} + A_u$	$-R_{0u}$
	No input $(1\text{-}x)$		organize (y)	R_{0g}	0
				$R_c - C_c + L_c$	$L_c - C_c$
				$R_u - C_u$	$-R_{0u}$
			Not organized $(1\text{-}y)$	$R_{0g} - C_g$	$-C_g$
				0	0
				$R_u - C_{0u}$	$-R_{0u}$

I. CONSTRUCTION OF THE EVOLUTIONARY GAME MODEL OF THE THREE PARTIES IN RURAL REVITALIZATION

1.1 Government's Replication Dynamic Equation and Equilibrium

The expected benefits of the government choosing not to invest and investing in rural revitalization are E_{0g} and E_{1g}, respectively, then:

$$E_{0g}=yzR_{0g}+(1-y)z\left(R_{0g}-C_g\right)+(1-y)(1-z)\left(-C_g\right)=zR_{0g}-C_g+yC_g\ E_{1g}=$$
$$yz\left(R_g-A_c-A_u+L_g\right)+y(1-z)\left(L_g-A_c\right)+(1-y)z\left(R_g+L_g-A_u-C_g\right)+(1-y)(1-z)\left(L_g-C_g\right)$$

$$=y\left(C_g - A_c\right) + z\left(R_g - A_u\right) + L_g - C_g$$

Then the government's replication dynamic equation is:

$$F_x = \frac{dx}{dt} = x(1 - x)\left(zR_g - zR_{0g} - zR_{0g} + L_g - yA_c\right)$$

Derivating the government's replication dynamic equation gives:

$$F'_x = \frac{dx}{dt} = (1 - 2x)\left(zR_g - zR_{0g} - zR_{0g} + L_g - yA_c\right)$$

According to Friedman's theory, if $F'_x = 0$, $F'_x < 0$ are satisfied, do asymptotic stability analysis on the strategy chosen by the government and its evolution: if $zR_g - zR_{0g} - zR_{0g} + L_g - yA_c = 0$,then $F_{(x)} = 0$, the government can choose to invest or not to invest. If $zR_g - zR_{0g} - zR_{0g} + L_g - yA_c \neq 0$, let $F_{(x)} = 0$, and two equilibrium points of $x = 0$, $x = 1$ are obtained. When $zR_g - zR_{0g} - zR_{0g} + L_g - yA_c < 0$, there are $F'_z(0) < 0$, $F'_z(1) > 0$, at this time $x = 0$ is a stable strategy, and the government chooses not to invest; otherwise , if $zR_g - zR_{0g} - zR_{0g} + L_g - yA_c > 0$, $F'_x(0) > 0$, $F'_x(1) < 0$, then $x = 1$is the stabilization strategy, and the government chooses the strategy of raising investment.

1.2 Replication dynamic equation and equilibrium point of enterprises (cooperatives)

The expected benefits of enterprises (cooperatives) not organizing farmers (operating entities) to participate in rural revitalization and organizing farmers (operating entities) to participate in rural revitalization are E_{0c} and E_{1c} respectively, then:

$$E_{0c} = 0\ E_{1c} =$$
$$xz\left(R_c - C_c + A_c + L_c\right) + x(1 - z)\left(L_c - C_c + A_c\right) + (1 - x)z\left(R_c - C_c + L_c\right) + (1 - x)(1 - z)\left(L_c - C_c\right)$$
$$= zR_c + xA_c - C_c + L_c$$

Then the replication dynamic equation of the enterprise (cooperative) is:

$$F_y = \frac{dy}{dt} = y(1 - y)\left(zR_c + xA_c - C_c + L_c\right)$$

The derivation of the replication dynamic equation of the enterprise (cooperative) can be obtained:

$$F'_y = \frac{dy}{dt} = (1 - 2y)\left(zR_c + xA_c - C_c + L_c\right)$$

1.3 Replication dynamic equation and equilibrium point of farmers (operating entities)

The expected benefits of farmers (operating entities) choosing not to participate in rural revitalization and choosing to participate in rural revitalization are E_{0u} and E_{1u} respectively, then:

$$E_{0g}=xy\left(-R_{0u}\right)+x(1-y)\left(-R_{0u}\right)+(1-x)y\left(-R_{0u}\right)+(1-x)(1-y)\left(-R_{0u}\right)=-R_{0u}$$
$$E_{1u}=xy\left(R_u-C_u+A_u\right)+x(1-y)\left(R_u-C_{0u}+A_u\right)+(1-x)y\left(R_u-C_u\right)+(1-x)(1-y)\left(R_u-C_{0u}\right)$$
$$=xA_u+yC_{0u}-yC_u+R_u-C_{0u}$$

Then the replication dynamic equation of the farmer (manager) is:

$$F_z=\frac{dz}{dt}=z(1-z)\left(xA_u-yC_{0u}-yC_u+R_u-C_{0c}+R_{0u}\right)$$

The derivation of the replication dynamic equation for farmers (operating subjects) is:

$$F'_{(z)}=\frac{dz}{dt}=(1-2z)\left(xA_u-yC_{0u}-yC_u+R_u-C_{0c}+R_{0u}\right)$$

1.4 Analysis of evolutionary stability strategy of tripartite subjects in rural revitalization

From the above analysis, the replication dynamic equations of the government, enterprises (cooperatives) and farmers (operating entities) are obtained:

$$\begin{cases}F_{(x)}=x(1-x)\left(zR_g-zR_{0g}-zR_{0g}+L_g-yA_c\right)\\F_{(y)}=y(1-y)(zR_c+xA_c-C_c+L_c)\\F_{(z)}=z(1-z)(xA_u-yC_{0u}-yC_u+R_u-C_{0c}+R_{0u})\end{cases}$$

This equation system describes the relationship between the government, enterprises (cooperatives) and farmers (operating entities) in rural revitalization. When the correction speed of the equation system is zero, that is, the evolution direction does not change, the system is considered to be in a stable equilibrium state, that is, the nash equilibrium is reached.

Let $F_{(x)}=0$, $F_{(y)}=0$, $F_{(z)}=0$, we can get 8 pure strategy local equilibrium points as $E_1(0,0,0)$、$E_2(0,0,1)$、$E_3(0,1,0)$、$E_4(1,0,0)$、$E_5(1,1,0)$、$E_6(1,0,1)$、$E_7(0,1,1)$、$E_8(1,1,1)$.
According to Lyaounov's first law, the Jacobin matrix of the system can be obtained by derivation of each dynamic replication equation as follows:

$$J=\left[\frac{\partial F_g(x)}{\partial x}\ \frac{\partial F_g(x)}{\partial y}\ \frac{\partial F_g(x)}{\partial z}\ \frac{\partial F_c(y)}{\partial x}\ \frac{\partial F_c(y)}{\partial y}\ \frac{\partial F_c(y)}{\partial z}\ \frac{\partial F_u(z)}{\partial x}\ \frac{\partial F_u(z)}{\partial y}\ \frac{\partial F_u(z)}{\partial z}\right]=$$
$$\left[A_{11}\ A_{12}\ A_{13}\ A_{21}\ A_{22}\ A_{23}\ A_{31}\ A_{32}\ A_{33}\right]$$

Then the stable condition can be obtained:

$A_{11}=(1-2x)\left(zR_g-zR_{0g}-zA_u+L_g-yA_c\right)$ $A_{12}=x(1-x)\left(-A_c\right)$ $A_{13}=x(1-x)\left(R_g-R_{0g}-A_u\right)$
The evolution equilibrium solution and stability conditions can be obtained from the Jacobin matrix at each equilibrium point.

II. ESTABLISH THE SYMBIOTIC MODEL OF THE GOVERNMENT, ENTERPRISES AND FARMERS

According to the rural revitalization of the relevant subject symbiotic logic, put forward the following assumptions: (1) under the background of agricultural modernization strategy, the government whether enterprises (cooperatives) and farmers (operators) to participate in the rural revitalization, will promote the development of rural revitalization, due to enterprises (cooperatives) and farmers (operators), the government for enterprises (cooperatives) and farmers (operators) have a role. (2) Suppose that the amount of investment provided by the government, the income available from enterprises (cooperatives) to farmers (operators) by providing services related to rural revitalization and the income of farmers (operators) from participating in rural revitalization are three different data, and the three initial values of the system are not zero.(3) In the case of limited economic resources and limited market resources, the government unit of time investment resources is limited, namely the government investment amount has a maximum, the same enterprise (cooperatives) can also have a maximum income, farmers (operators) can also have a maximum income, namely the three at the same time each have a maximum environmental capacity. In addition, the government's investment policy is a phased and supportive policy, and the government will consider withdrawing from this investment policy when the rural revitalization development reaches a certain stage.

Combined with the combination of symbiosis theory, the three group symbiosis models of rural revitalization considering both the government, enterprises (cooperatives) and farmers (business entities) are established.

$$\{\frac{dx_g}{dt} = r_g x_g\left[1 - \frac{x_g}{m_g}\right] \frac{dy_c}{dt} = r_c y_c\left[1 - \frac{y_c}{m_c} + \delta_{gc}\frac{x_g}{m_g} + \delta_{uc}\frac{z_u}{m_u}\right] \frac{dz_u}{dt} = r_u z_u\left[1 - \frac{z_u}{m_u} + \delta_{gu}\frac{x_g}{m_g} + \delta_{cu}\frac{y_c}{m_c}\right]$$

Table 2: Model parameters and their implications

symbol	explain	symbol	explain
	The amount of government money invested in rural revitalization	y_c	Profits of enterprises (cooperatives) participating in rural revitalization
z_u	Income from farmers (business entities) participating in rural revitalization	r_g	The self-growth rate of the government input policy
r_c	The self-growth rate of enterprises (cooperatives) participating in rural revitalization	r_u	The self-growth rate of farmers (business entities) participating in rural revitalization
m_g	The maximum amount of government spending	m_c	The maximum profits for enterprises (cooperatives) can participate in rural revitalization
m_u	The biggest benefit of peasant households (business entities) from participating in rural revitalization	δ_{gc}	The function coefficient of government effect on enterprises (cooperatives)
δ_{gu}	The function coefficient of the government on farmers (management subject)	δ_{cu}	The function coefficient of enterprises (cooperatives) on farmers (operating subjects)
δ_{uc}	The function coefficient of farmers (operating subject) on enterprises (cooperatives)		

In the formula: $\frac{1-x_g}{m_g}$, $\frac{1-y_c}{m_c}$, $\frac{1-z_u}{m_u}$ respectively represent the retardation coefficient caused by the consumption of limited resources such as financial resources by the government, enterprises (cooperatives) and farmers (operating entities).

III. ANALYSIS OF THE SYMBIOTIC STABILITY OF THE GOVERNMENT, ENTERPRISES AND FARMERS

The equations are now collated into the standard Lotka-Volterra equations.

$$\{\frac{dx_g}{dt} = x_g\left[r_g - \frac{r_g x_g}{m_g}\right] \frac{dy_c}{dt} = y_c\left[r_c - \frac{r_c y_c}{m_c} + r_c \delta_{gc} \frac{x_g}{m_g} + r_c \delta_{uc} \frac{z_u}{m_u}\right] \frac{dz_u}{dt} = z_u\left[r_u - \frac{r_u z_u}{m_u} + r_u \delta_{gu} \frac{x_g}{m_g} + r_u \delta_{cu} \frac{y_c}{m_c}\right]$$

The internal interaction coefficient matrix between the government and enterprises (cooperatives) and farmers (Operating subjects) is shown in.

$$A = \left[-\frac{r_g}{m_g} 00 \frac{r_c \delta_{gc}}{m_g} \quad -\frac{r_c}{m_c} \frac{r_c \delta_{uc}}{m_u} \frac{r_u \delta_{gu}}{m_g} \frac{r_u \delta_{cu}}{m_c} \quad -\frac{r_u}{m_u}\right]$$

Solve the symbiosis equation to get the symbiosis balance point between the government, enterprises (cooperatives) and farmers (operating subjects).

Table 3: The symbiosis balance point between the government, enterprises (cooperatives) and farmers (operating subjects)

	x_g	y_c	z_u
	0	0	0
N_2	m_g	0	0
N_3	0	m_c	0
N_4	0	0	m_u
N_5	m_g	$\frac{m_c(\delta_{uc}-1)}{\delta_{uc}\delta_{cu}-1}$	0
N_6	m_g	0	$\frac{m_u(\delta_{cu}-1)}{\delta_{uc}\delta_{cu}-1}$
N_7	0	$\frac{m_c(\delta_{uc}-1)}{\delta_{uc}\delta_{cu}-1}$	$\frac{m_u(\delta_{cu}-1)}{\delta_{uc}\delta_{cu}-1}$
N_8	1	$\frac{\delta_{gc}+\delta_{gu}\beta_{uc}-\delta_{cu}\delta_{uc}-1}{1-\delta_{cu}\delta_{uc}}$	$\frac{\delta_{gu}-\delta_{cu}+\delta_{cu}\delta_{gc}+1}{1-\delta_{cu}\delta_{uc}}$

In the table, $N_8\left(x_g^*, y_c^*, z_u^*\right)$ is the equilibrium point of symbiotic stability. According to the symbiotic stability condition, the matrix determinant of the formula should be less than zero, namely:

$$|A| = \frac{r_g r_c r_u}{m_g m_c m_u}\left(\delta_{cg}\delta_{gc} + \delta_{uc}\delta_{cu} - 1\right) < 0$$

At the same time, since $r_g > 0$, $r_c > 0$, $r_u > 0$, $m_g > 0$, $m_c > 0$, $m_u > 0$, and N_8 satisfies $x_g > 0$, $y_c > 0$, $z_u > 0$, N_8 needs to meet the following conditions.

$$\{\delta_{cg}\delta_{gc}+\delta_{uc}\delta_{cu}<1 \quad \delta_{cu}\delta_{uc}+\delta_{cg}-\delta_{cg}\delta_{uc}>1\ \delta_{gc}+\delta_{uc}<1 \quad \delta_{cg}\delta_{gc}+\delta_{cu}-\delta_{gc}\delta_{cu}>1$$

When the interaction coefficient between the government, enterprises (cooperatives) and farmers (operating subjects) in rural revitalization and development satisfies the above formula, the development of rural revitalization can evolve to the point where the government invests in rural revitalization and development, and enterprises (cooperatives) provide support for farmers (operating entities) to participate in rural revitalization, and farmers (operating entities) actively participate in a good situation.

IV. SYMBIOSIS SIMULATION ANALYSIS OF GOVERNMENT, ENTERPRISES AND FARMERS

In order to further study the dynamic development characteristics of the symbiosis between the government, enterprises (cooperatives) and farmers (operating subjects) in rural revitalization and development, MATLAB was used to explore the symbiosis process of the three through simulation. The corresponding relationship and initial value setting of each initial variable in the simulation model and the corresponding variable of the theoretical model.

Table 4: Initial variable initial value setting table of simulation model

Symbol	Initial Value	Symbol	Initial Value
	0.2	m_c	200
r_c	0.35	δ_{gc}	1.4
r_u	0.45	δ_{gu}	0.2
m_g	100	δ_{uc}	0.3
m_u	100	δ_{cu}	1.2

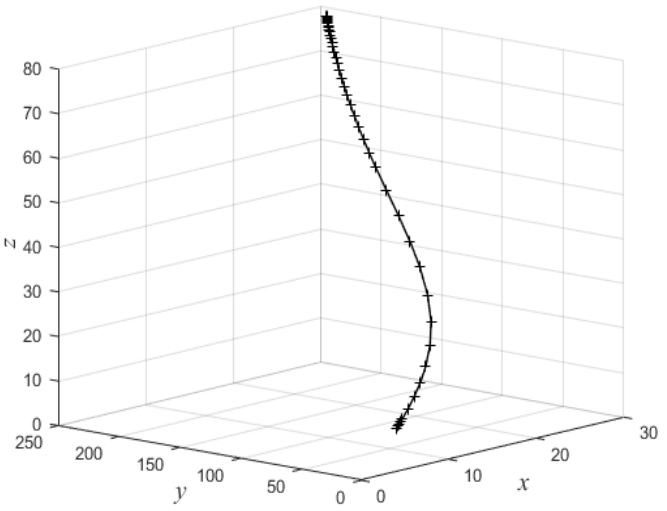

Figure 1: Government-guided Symbiosis Evolution Map of Enterprises (Cooperatives) and Farmers (Business Principals)

From the simulation results:

There is a symbiosis-dependent game evolution relationship between the government, enterprises (cooperatives) and farmers (operating subjects). The evolution of the tripartite symbiosis system to a balanced and stable state in symbiotic development is a long-term process, which promotes each other and evolves and grows.

The growth rate of the three parties' income in rural revitalization is dynamic and different. In the early stage of rural revitalization development, it developed rapidly due to less market restrictions. The enthusiasm of the participants has been improved. Compared with the initial stage of the number of enterprises (cooperatives) and farmers (operating entities) participating in rural revitalization with government investment, the growth rate of the two has gradually decreased to zero.

The growth rate of the three parties' income in rural revitalization is dynamic and different. In the early stage of rural revitalization development, it developed rapidly due to less market restrictions. Under the existing condition (i.e., without considering the government's late adjustment of input Policy), as participation subjects become more active, the number of enterprises (cooperatives) and farmers (operating entities) participating in rural revitalization with government input compared with the initial stage, the growth rate of both gradually decreases to zero.

In the early stage of rural revitalization development, affected by the number of enterprises (cooperatives) participating and market acceptance, the participation of enterprises (cooperatives) and farmers (operating entities) in rural revitalization was relatively slow. With the increasing enthusiasm of participants and market development, the role of rural revitalization can be brought into play, the growth rate of the government's investment in enterprises (cooperatives) and farmers (operating entities) participating in rural revitalization gradually increased to a peak, and then gradually decreased. Constrained by market prices, the marginal rate of return of the government's implementation of the input policy will gradually decrease, and the benefits such as the improvement and the increase of public credibility obtained by the government will gradually approach the maximum value. Similarly, the benefits obtained by the participants will also decrease as the number of participants in rural revitalization increases, and gradually approach the maximum value.

The simulation results show that: (1) There is a symbiotic evolution relationship between enterprises (cooperatives) and farmers (operating subjects), and it is a long-term process for the symbiotic system of enterprises (cooperatives) and farmers (operating subjects) to evolve to a balanced and stable state; (2) Under the current situation (that is, regardless of the government's later adjustment and development of rural revitalization investment policies), in the early stage of rural revitalization and development, limited by the limited number and capacity of participation, enterprises (cooperatives) and farmers (operating entities) have continued to gain benefits. However, as the popularity and participation of poets increase, the growth rate of both parties' income gradually slows down and becomes stable.

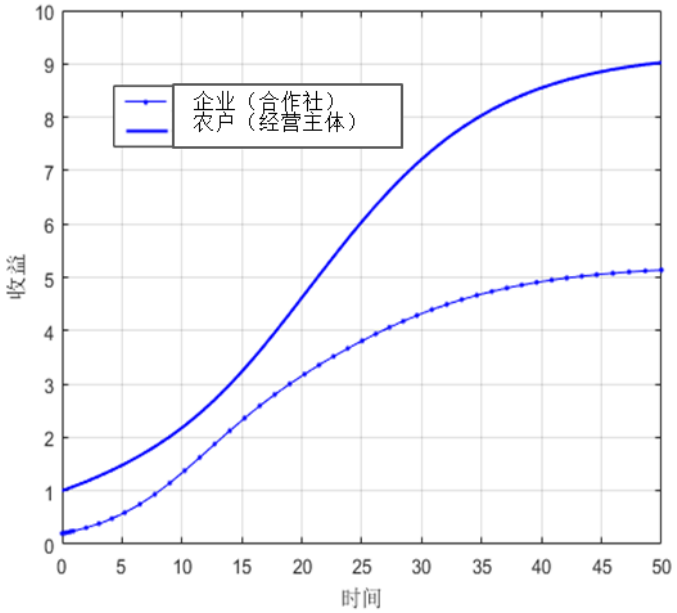

Figure 2: Symbiosis simulation of enterprises (cooperatives) and farmers (operating entities)

V. ANALYSIS OF THE SYMBIOSIS MECHANISM BETWEEN ENTERPRISES AND FARMERS UNDER THE GOVERNMENT'S WITHDRAWAL FROM INVESTMENT

5.1 Construction of symbiosis model under government withdrawal and input

First, enterprises (cooperatives) and farmers (operating entities) can achieve common development through information exchange and resource sharing due to their proximity in space, providing an ideal common "evolution" path for each; Second, the two will act in a cooperative manner for the common good; Third, there is a certain relationship between the subjects of rural revitalization in terms of material and information. and symbiosis will deepen or disappear as this relationship strengthens or fades. The formation of this symbiotic relationship between the subjects of rural revitalization is the result of the mutual game between the participants, and the construction of this symbiotic relationship is the need to promote the development of rural revitalization.

Enterprises (cooperatives) and farmers (operating entities) achieve common development through symbiotic evolution, which is essentially a process in which the distribution of rural revitalization benefits and comprehensive benefits tends to be reasonable. According to the symbiotic logical relationship between the two parties, the following assumptions are put forward: First, enterprises (cooperatives) and farmers (operating subjects) are both bounded rational decision-makers and will adopt a certain symbiotic behavior model in the process of participating in rural revitalization. Second, the change in the income of enterprises (cooperatives) participating in rural revitalization and the change in the per capita income of farmers (operating entities) participating in rural revitalization respectively represent the status of their participation in rural revitalization. The third is that enterprises (cooperatives) and farmers (operating entities) need to consume growth resources (various policy resources and technical resources, etc.) to obtain benefits from participating in rural revitalization. Fourth, the process of enterprises (cooperatives) and farmers (operating subjects) participating in rural revitalization satisfies the growth law of LOGISTIC. The total amount of growth resources limits the growth of the income of enterprises (cooperatives) and farmers (operating subjects). Its income growth rate is not only affected by its own income level, but also related to the income level of the symbiotic subject. At the same time, it is assumed that the benefits of enterprises

(cooperatives) and farmers (operating entities) participating in rural revitalization at time t are x_c and x_u, respectively, and the growth rates of revenue are r_c and r_u, respectively, and the maximum benefits under certain growth resources are m_c and m_u, respectively. ; the symbiotic effect coefficient of farmers (operating subjects) on enterprises (cooperatives) is λ_u, and the symbiotic effect coefficients of enterprises (cooperatives) on farmers (operating subjects) is λ_c, and its absolute value indicates the degree of symbiosis; $r_c x_c$ and $r_u x_u$ respectively Represents the development trend of enterprises (cooperatives) and farmers (operating subjects) participating in rural revitalization, $1-\frac{x_c}{m_c}$ and $1-\frac{x_u}{m_u}$ respectively represent that the enterprises (cooperatives) and farmers (operating subjects) are affected by the consumption of growth resources. Get the retardation effect of revenue growth.

Then the dynamic evolution equation of enterprises (cooperatives) and farmers (operating subjects) participating in rural revitalization can be expressed as:

$$\{\frac{dy_c}{dt}=r_c y_c\left[1-\frac{y_c}{m_c}\right]\frac{dz_u}{dt}=r_u z_u\left[1-\frac{z_u}{m_u}\right]$$

Then the symbiotic dynamic evolution equation of the interaction between the two is:

$$\{\frac{dy_c}{dt}=r_c x_c\left[1-\frac{y_c}{x_{mc}}-\frac{\lambda_u z_u}{m_u}\right]\frac{dz_u}{dt}=r_u x_u\left[1-\frac{z_u}{x_{mu}}-\frac{\lambda_c y_c}{m_c}\right]$$

Let the symbiotic dynamic evolution equation be equal to o, get$E_1(0,\ 0)$,$E_2\left(m_c,\ 0\right)$,$E_3\left(0,\ m_u\right)$, $E_4\left(\frac{m_c\left(1-\lambda_u\right)}{(1-\lambda_u\lambda_c)},\frac{m_u\left(1-\lambda_c\right)}{(1-\lambda_u\lambda_c)}\right)$ four equilibrium points.

5.2 Analysis on the symbiosis stability of enterprises (cooperatives) and farmers (operating entities) under the withdrawal of government investment

According to the stability theory of differential equations, it can be seen that:

$E_1(0,\ 0)$ *is the unstable equilibrium point.*

$E_2\left(m_c,\ 0\right)$ is the stable equilibrium point, then $\lambda_c > 1$. Currently, enterprises (cooperatives) have a blocking effect on farmers (operating entities) participating in rural revitalization. Enterprises (cooperatives) use growth resources to obtain maximum benefits, while farmers (cooperatives) Business entities) choose not to participate in rural revitalization due to insufficient growth resources, which is meaningless.

$E_3\left(0,\ m_u\right)$ is a stable equilibrium point, then $\lambda_u > 1$. Currently, farmers (operating subjects) have a blocking effect on the participation of enterprises (cooperatives) in rural revitalization. Farmers (operating subjects) use growth resources to obtain maximum benefits, while enterprises (Cooperatives) choose not to participate in rural revitalization due to insufficient growth resources, which is also meaningless.

$E_4\left(\frac{m_c\left(1-\lambda_u\right)}{(1-\lambda_c\lambda_u)},\ \frac{m_u\left(1-\lambda_c\right)}{(1-\lambda_c\lambda_u)}\right)$ is the stable equilibrium point, when $\lambda_c < 1$ and $\lambda_u < 1$, the evolution equilibrium results of the equilibrium point E_4 under different λ_c and λ_u values are obtained, indicating that the symbiotic relationship between enterprises (cooperatives) and farmers (operating subjects)

shows different evolutionary equilibrium results with the change of the symbiotic interaction coefficient. Moreover, the symbiotic model of enterprises (cooperatives) and farmers (operating subjects) is not static, and their symbiotic relationship has also undergone a process of evolution from constant development and change to stability. The distribution of benefits between the two tends to be rationalized with the influence of the policy system, the market environment and the increase in the scale of farmers (operating subjects).

Table 5: The symbiotic behavior model of enterprises (cooperatives) and farmers (operating entities)

Symbiosis coefficient value	Equilibrium	Benefit distribution form	Symbiosis mode
$0 < \lambda_u < 1$, $0 < \lambda_c < 1$	P_1	Since rural revitalization is voluntary participation and individual declaration, the two parties are decentralized and independent for limited resource competition.	independent symbiosis
$\lambda_u = 0, \lambda_c = 0$	P_2	Both sides do not affect each other	independent symbiosis
$0 < \lambda_u < 1, \lambda_c < 0$	P_3	Farmers benefit, enterprises (cooperatives) suffer	parasitic symbiosis
$\lambda_u < 0, 0 < \lambda_c < 1$	P_4	Enterprises (cooperatives) benefit, farmers suffer	
$\lambda_u = 0, \lambda_c < 0$	P_5	Enterprises (cooperatives) are harmless, farmers benefit	Symbiosis
$\lambda_u < 0, \lambda_c = 0$	P_6	Enterprises (cooperatives) benefit, farmers suffer no loss	
$\lambda_u < 0, \lambda_c < 0$	P_7	Mutual benefit for both parties to achieve the goal of carbon neutrality in rural revitalization	Mutualism

Take $0 < \lambda_c < 1, 0 < \lambda_u < 1$ as an example for analysis: when $0 < \lambda_c < 1, 0 < \lambda_u < 1$, G_c=0 and G_u=0 divide the phase plane into S1, S2, S3 and S4 four areas. The S1 area is located below G_c=0 and G_u=0. In this area, the growth rates of enterprises (cooperatives) and farmers (operating entities) are both greater than zero, and their incomes will increase with time. If the initial relationship between the enterprise (cooperative) and the farmer (operating subject) is in this area, it will move to the upper right as time goes by, and it may approach the equilibrium point E4, or move to the S2 and S3 areas. If the symbiotic relationship between the enterprise (cooperative) and the farmer (operating subject) is in the S2 area, where the growth rate of the scale of the enterprise (cooperative) is greater than zero, and the growth rate of the farmer (operating subject) is less than zero, over time, the symbiotic relationship between the two will become stronger. Move down to the right and approach the equilibrium point E4 or enter the S4 area. If the initial symbiotic relationship between the enterprise (cooperative) and the farmer (operating subject) is in the S4 area, and the scale growth rate of the two in this area is lower than zero, the phase point will move to the lower left and tend to the equilibrium point E4, or enter S2 or S3 area. If it enters the S2 area, it will eventually tend to the equilibrium point E4 according to the above analysis. If the symbiotic relationship between enterprises (cooperatives) and farmers (operating entities) is in the S3 area, where the growth rate of the scale of enterprises (cooperatives) is less than zero, and the growth rate of farmers (operating entities) is greater than zero, with the increase of time, the symbiosis of the two will occur. The state will move to the upper left, either approaching the equilibrium point E4 or entering the S4 area. As analyzed above, the phase point entering the S4 area will eventually tend to the equilibrium point E4. To sum up, when 0<λ_c<1, 0<λ_u<1, the equilibrium point of the symbiotic evolution of enterprises (cooperatives) and farmers (operating subjects) is E4,

that is, regardless of the initial state of the two, the enterprises (cooperatives) and The symbiotic evolution of farmers (operating subjects) will eventually be stable at the equilibrium point E4. In the same way, the other six situations can reach stability at the equilibrium point (in other cases, the phase plan of the symbiotic evolution of enterprises (cooperatives) and farmers (operating entities) is similar to the above analysis. This shows that the symbiosis coefficient determines the enterprise (cooperative) The symbiotic relationship (symbiotic model) with the farmer (operating subject), different symbiotic relationships will produce different evolutionary equilibrium results.

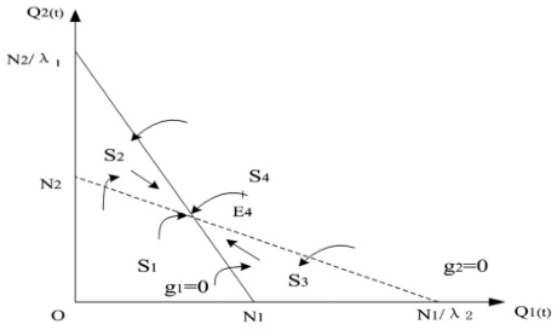

Figure 3: Phase diagram of the symbiotic evolution of enterprises (cooperatives) and farmers (operating entities)

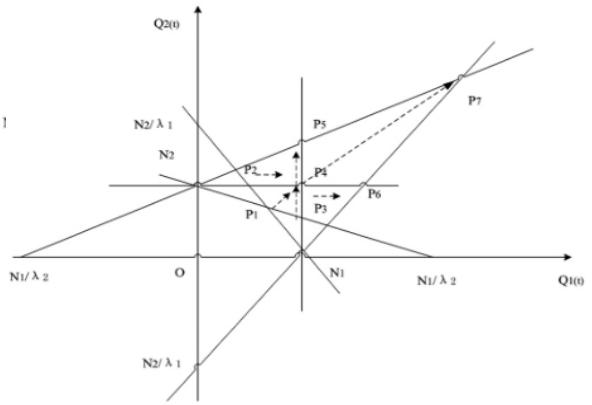

Figure 4: The dynamic path of symbiotic evolution between enterprises (cooperatives) and farmers (operating entities)

VI. CONCLUSION

From a practical point of view, with the development of rural revitalization, enterprises (cooperatives) and farmers (operating subjects) form a symbiotic relationship, which has roughly gone through the following stages: in rural revitalization and development, enterprises (cooperatives) and farmers (operating subjects) in the process of symbiosis evolution, it has experienced different symbiosis stages:

First, the independent symbiosis stage, the two parties have not formed a stable transaction relationship, enterprises (cooperatives) focus on the benefits and market effects in rural revitalization, and farmers (operating entities) focus on participation costs and enterprises. Services, this stage is manifested as the competition between the two parties for limited resources such as government incentives;

The second is the parasitic symbiosis stage. Under the guidance of the government and the promotion of market demand, enterprises (cooperatives) gradually organize and organize farmers' production, and farmers (operators) gradually realize the benefits and begin to participate in large-scale operations. However, there is no clear right and Obligation, which easily breeds speculation and short-term behavior;

The third is the stage of partial benefit symbiosis. Under the condition of stable cost and income, enterprises (cooperatives) pay attention to the number of farmers (operators) involved and business expansion, farmers (operators) focus on information and market services, and farmers (operators) participate in enterprises The number of enterprises (cooperatives) has increased significantly. At this time, the supply side is the mainstay, and enterprises (cooperatives) occupy a dominant position in production and benefit distribution, and there is a situation in which one side benefits and the other loses;

Fourth, in the stage of mutual benefit and symbiosis, both parties pay more attention to the improvement of technical information services and the development of agricultural industrialization. Enterprises (cooperatives) and farmers (operating entities) combine to form a "benefit-sharing and risk-sharing" consortium, and enterprises (cooperatives) return large-scale incremental benefits and government rewards and subsidies to farmers (operating entities), improves the service level and quality, and at the same time, farmers (operating subjects) actively participate in rural revitalization, and make use of the number of farmers (operating subjects) and group effects to expand and strengthen the agricultural industry.

REFERENCES

1. Xie Tiancheng, Zhang Yan, Wang Liexuan, Shi Zulin. Coordinated Development of Rural Revitalization and New Urbanization--Based on Spatial and Temporal Evolution Analysis at Provincial Scale [J]. Economic Issues, 2022, (09): 91-98.
2. Huan Wang and Li Juan. Multi-party education, understanding and empowerment--to promote the new era education of symbiosis, growth and sharing [J]. Chinese Family Education, 2022, (01): 13-19.
3. Ji Yingbo, Zhou Ruichen, Liu Xinnan. Study on multi-party symbiosis model of government, property and users in the development of carbon trading in community buildings [J]. Energy Conservation, 2022, 41 (01): 71-74.
4. Ji Zhijia and Zhang Junyi. Evolution analysis of rural revitalization research hotspots in geography [J]. Yunnan Geographical Environment Research, 2021, 33 (06): 38-45.
5. Shang Hailong, Li Jianfeng, Ming Qingzhong. Dynamic evolution analysis of rural production-life-ecology coupling coordination in Southwest China [J]. Journal of Northwest Normal University (Natural Science Edition), 2020, 56 (04): 90-97.
6. Zhang Fengzhe. Research on Synergistic Symbiosis Mechanism of Internet Public Opinion Based on Multi-party Game [J]. Intelligence Exploration, 2020, (02): 21-27.
7. Wang Yujie. Community ecology: harmonious coexistence under multi-party game [J]. Urban Development, 2010, (07): 41-45.